THESIS

PHYSIOLOGICALLY BASED PHARMACOKINETIC MODELING FOR PREDICTION OF PHARMACOKINETIC PARAMETERS OF CAPREOMYCIN

Submitted by

Catherine Metzler

Department of Chemical and Biological Engineering

In partial fulfillment of the requirements

for the degree of Master of Science

Colorado State University

Fort Collins, CO

Summer 2010

COLORADO STATE UNIVERSITY

June 23, 2010

WE HEREBY RECOMMENED THAT THE THESIS PREPARED UNDER OUR SUPERVISION BY CATHERINE METZLER ENTITLED "PHYSIOLOGICALLY BASED PHARMACOKINETIC MODELING FOR PREDICTION OF PHARMACOKINETIC PARAMETERS OF CAPREOMYCIN" BE ACCEPTED AS FULFILLING IN PART REQUIREMENTS FOR THE DEGREE OF MASTER OF SCIENCE.

Committee on Graduate Work

MaryAnn DeGroote

Ashok Prasad

Advisor: Brad Reisfeld

Department Head (Acting): Ranil Wickramasinghe

ABSTRACT OF THESIS

PHYSIOLOGICALLY BASED PHARMACOKINETIC MODELING FOR PREDICTION OF PHARMACOKINETIC PARAMETERS OF CAPREOMYCIN

Tuberculosis (TB) is a global public health epidemic that is increasingly dangerous and difficult to treat due in large part to drug-resistant strains. New pharmaceutical options must be considered, including capreomycin, an antibiotic discovered in the 1950s but rarely used. Due to more effective, less renal-toxic drugs, capreomycin has not been used as a primary antibiotic in tuberculosis. However, capreomycin has reemerged due to the increase in multi drug resistant TB (MDRTB). Because of its importance in treating drug-resistant strains of TB, improving the understanding of the effective dosages and resulting side effects of capreomycin is necessary. By using a validated model, drugs of interest like capreomycin could be rapidly evaluated for initial recommendations thus reducing drug development time. Using physiologically-based pharmacokinetic (PBPK) models as predictors would be economically and time efficient.

In this study, a PBPK model in combination with experimental concentration profiles in mice was used to predict capreomycin pharmacokinetic parameters. Through scale-up of the model to human physiology, and implementation of the hypothesized

pharmacokinetic parameters, human organ concentration profiles were predicted and compared to literature data to assess the model capabilities. The model and parameters are anticipated to be useful in predicting the disposition of capreomycin in the mouse via various dosing regimens. Although the model is useful in making pharmacokinetic predictions in the mouse, the parameter values will need to be adjusted appropriately to be useful for estimating ADME in humans.

Catherine Metzler
Department of Chemical
And Biological Engineering
Colorado State University
Fort Collins, CO 80521
Summer 2010

Table of Contents

Chapter 1: Introduction

Tuberculosis (TB) is a global public health epidemic that is increasingly dangerous and difficult to treat due in large part to drug-resistant strains. Although drug-sensitive strains of TB are effectively treated with combinations of *first line* antibiotics, resistant strains are conventionally treated with a longer course of combinations of the less effective, and more toxic, *second line* drugs, such as capreomycin. Capreomycin is an antibiotic effective against gram-negative bacteria that was discovered in the 1950s. Unfortunately, there is little experimental information published about this drug, and its pharmacokinetic properties are not well characterized [1]. Because of its importance in treating drug-resistant strains of TB, improving the understanding of the effective dosages and resulting side effects of capreomycin is necessary.

Specifically, development of a realistic model for capreomycin pharmacokinetics in the human body is desirable because of the need for acceptable drug regimens to treat tuberculosis, minimizing toxicity and maximizing efficacy. Tuberculosis requires treatment with multiple drugs over extended periods, usually six to twelve months. In some drug-resistant cases, treatment may take two years or longer [1]. While the drugs used for treatment are already approved for use in humans, the effects of drug combinations and varying dose levels are frequently unknown. As the disease becomes more resistant, new drug regimens are employed. Investigating the numerous possible

regimens, dose levels, and treatment time spans for human treatment would be both time and cost prohibitive. However, a well-developed model could be employed to generate hypotheses of regimens which should be further investigated and those that could be detrimental to the patient's health.

In this study, a physiologically-based pharmacokinetic (PBPK) model in combination with experimental concentration profiles for several tissues and serum in mice following a known dose of capreomycin were used to predict capreomycin pharmacokinetic parameters. Through scale-up of the model to human physiology, and implementation of the hypothesized pharmacokinetic parameters, human organ concentration profiles were predicted and compared to literature data to assess the model capabilities.

Chapter 2: Background

2.1 Tuberculosis

2.1.1 Disease Information

Mycobacterium tuberculosis causes the disease tuberculosis (TB), which most commonly attacks the lungs, although it may affect other parts of the body. Approximately one-third of the world population is affected by TB, and in 2005 it was the cause of about 1.6 million deaths [2].

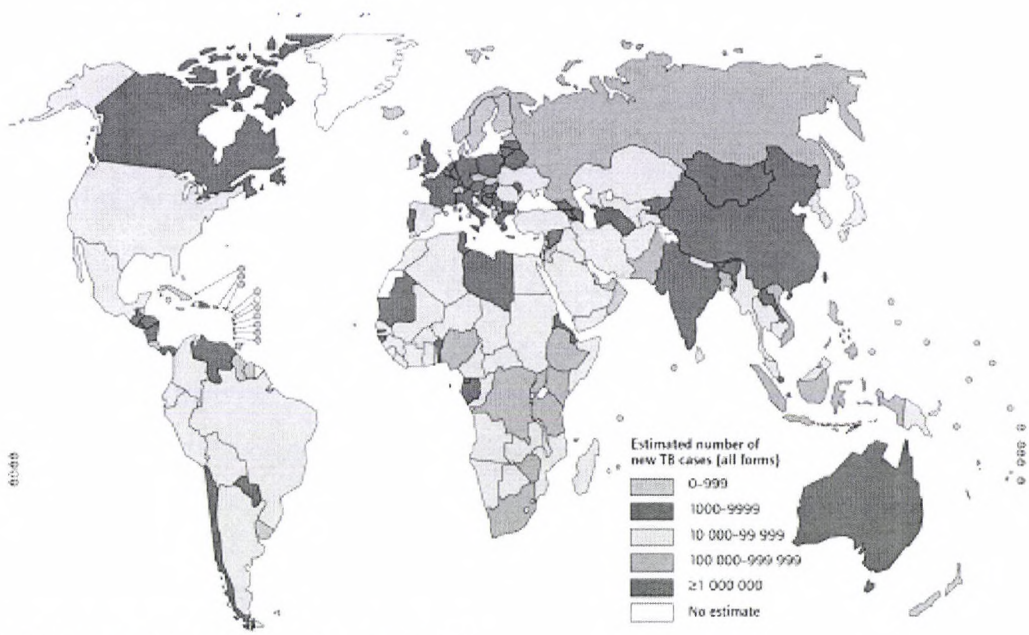

Figure 1: Tuberculosis prevalence by country [2].

The TB bacterium most commonly spreads via airborne droplets exiting the lungs of a person with active disease. Thus it can be spread when an infected person coughs, sneezes, speaks, or sings, but not by sharing food and drink, kissing, or shaking hands.

In the case of an inhalation infection route, alveolar macrophages engulf the inhaled sputum droplets and transport the bacterium to draining lymph nodes. Intracellular bacilli multiply in the macrophages and cause cell lyses, which leads to further infection as more macrophages take up the bacilli. Due to the infection, monocytes also reach the alveolar site and ingest bacilli. However, the monocytes that become immature macrophages cannot destroy the bacilli and thus the bacilli continue to multiply [3].

Macrophages, lymphocytes, fibroblasts, and other immune cells surround the infected macrophages to form a granuloma. A granuloma is a mass of immune cells that walls off a foreign body, and helps prevent further disease dissemination. Within the granuloma, immune cells destroy some of the infected cells, but some remain and become latent as the granuloma essentially contains the infection [4]. Eventually, blood flow to the granuloma is limited and it becomes hypoxic [5]. At this point, the bacteria cannot continue to infect the host; this is referred to as latent tuberculosis infection (LTBI) [6].

While in the latent state, there are no symptoms of the disease, and a skin or blood test is the only method of detection. Fortunately, someone with the latent infection cannot infect others. However, about one-third of the world's population has LTBI, and in about 5-10% of people infected with LTBI, the bacteria eventually become active, especially if their immune system is compromised from a disease such as HIV/AIDS [7].

Active TB can occur upon initial inhalation or when the latent form is released from the walled-off granuloma. Active TB is characterized by bacteria attacking the body and causing symptoms such as coughing up blood.

Treatment of tuberculosis is dependent on the patient's form of TB. A patient with LTBI is treated with the drug isoniazid (INH) for a nine month course of therapy [8] or rifampin (RIF) for four months [1]. For a patient with active drug-sensitive TB, treatment entails chemotherapy with several anti-TB drugs taken over the course of six months. This usually includes first-line drugs such as isoniazid (INH), rifampin (RIF), pyrazinamine (PZA), ethambutol (EMB). As with any antibiotic, the patient must stringently adhere to the drug regimen to prevent drug-resistant strains from evolving. However, due to the unusually extensive treatment periods, adherence is a great challenge in successfully combating TB [9].

2.1.2 Treatment Obstacles

A challenge in the treatment of tuberculosis is discovering and treating the disease while it is still in a latent state. About a third of the world has LTBI, which exhibits no outward symptoms. LTBI can develop into active TB, accounting for a third of the new cases seen per year. It has been found that capreomycin is as effective as metronidazole in vitro, a drug known to be effective against latent TB bacteria in an anaerobic environment, in treating LTBI [6].

A complication in the treatment of TB is the presence of drug-resistant strains. Multi-drug resistant TB (MDR-TB) refers to strains that are resistant to at least isoniazid and rifampicin. In this case, less effective and more toxic second-line drugs must be utilized. This includes viomycin, amikacin, streptomycin, capreomycin, moxifloxacin, and kanamycin [1]. Further complicating treatment is the evolution of extensively drug-resistant TB (XDR-TB), which refers to a TB strain that is resistant to isoniazid and/or rifampin as well as an injectable agent and at least one of the quinolones [2]. Such extensive resistance is a direct result of the compliance difficulties over the long treatment periods for drug-sensitive strains or primary acquisition of a drug-resistant strain. A number of factors contribute to non-compliance: patients feel better and cease taking their antibiotics; drug toxicity leads to side effects and the drug is discontinued; patients are improperly educated with regard to the treatment; drug availability in third-would countries is inconsistent due to a lack of funds to supply drugs in third-world countries; and inaccessibility of rural world populations to healthcare centers.

The major factor that contributed to the rise in TB cases was the HIV/AIDS epidemic. HIV/AIDS greatly compromises the immune system and consequently increases the chances of disease and that a prior infection with TB will cause an active infection [10]. In countries with a high prevalence of HIV, new TB cases have tripled in the past two decades. Over one-third of people with HIV concurrently have TB and those HIV patients that do not already have TB are 20-30 times more likely to contract it [11]. Furthermore, 50% of patients with both diseases have extra pulmonary TB, meaning the

bacterium infects areas other than the lungs, such as the lymph nodes, bones, the nervous system, or the brain [10].

2.2 Capreomycin

Capreomycin is a polypeptide antibiotic composed of four molecular analogs, IA, IIA, IB, and IIB. The pharmacological product capastat sulfate is primarily composed of 80% type IA and 20% IB [12]. It has a molecular weight of 766.786 and it is water soluble, and therefore hydrophilic in the body.

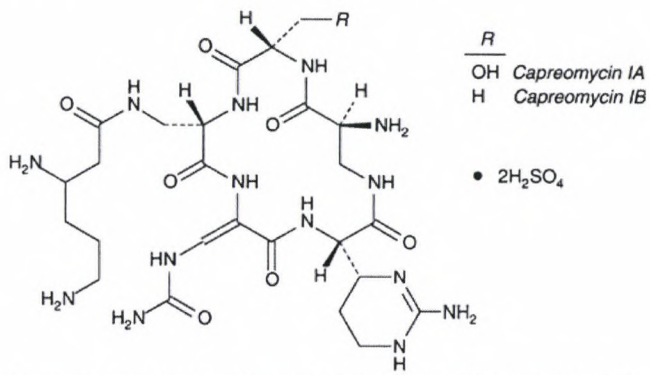

Figure 2: Capreomycin molecule IA and IB isolates [13]

Capreomycin's mode of action involves ribosomal inhibition of protein synthesis [14]. Studies suggest that capreomycin binds to the 16SrRNA molecule of the *M. Tuberculosis* bacterial ribosome, inhibiting up-regulation of a methyl transferase gene and a protein processing gene [15].

Due to similar nomenclature between capreomycin and aminoglycosides like gentamicin or streptomycin, side effects, and mode of action, capreomycin is often compared to and grouped with aminoglycoside antibiotics [1],[14]. Capreomycin was successfully used to

treat tuberculosis starting in the 1960s [16]. The studies by Black, *et al.* noted that approximately 50% of the drug was excreted unchanged (not metabolized) within the first eight hours following intramuscular administration. It was also observed that peak serum concentrations occurred within one to two hours. The collected data compared streptomycin to capreomycin and found similarities in the clearance rates as well as glomerular filtration as the hypothesized primary excretion route. The authors noted that not all administered drug could be accounted for in the urine following a three day collection period, leading to the conclusion that there is a small amount of biliary excretion [17].

Due to more effective, less renal-toxic drugs, capreomycin has not been used as a primary antibiotic in tuberculosis. However, capreomycin has reemerged due to the increase in MDRTB. An advantage of capreomycin is its effectiveness against both the latent and active forms of tuberculosis [2]. Currently, it is administered 5-7 days a week at 15 mg/kg/day in patients with normal renal function [6]. Capreomycin is not administered orally due to poor absorption and is only approved to be administered as an intravenous or intramuscular injection.

Following a one gram dose of capreomycin in a human, approximately 52% of the drug is excreted unchanged in the urine after 12 hours. Because of the kidney's involvement in the clearance process, it experiences significant exposures to capreopmycin, which can often lead to renal toxicity at high doses, A common measure of the negative impact on kidney function is the blood urea nitrogen (BUN) and the creatinine excretion. In the

case of kidney damage, BUN levels are elevated. Of 722 people receiving capreomycin treatment, researchers detected elevated BUN in 36% of patients. There are also known auditory and vestibular toxicity issues [18]. The toxic risks are increased when it is co-administered with vancomycin, cisplatin, or aminoglycoside antibiotics [14]. Capreomycin administration for the treatment of tuberculosis always requires combination with additional drugs. The toxicities are an important risk for health care providers to understand and manage.

2.2.1 Drug Efficacy and Toxicity

While dose concentrations are established in humans, little data are available about capreomycin-specific efficacy and toxicity levels, especially in humans. Toxicity prevention in humans involves establishing the serum creatinine baseline prior to capreomycin administration and subsequent monitoring for increases, which would indicate kidney damage [1].

Drug concentrations in the serum, the lung, and the kidney are of specific interest in determining the therapeutic range. The primary infection site is the lung and understanding the therapeutic range would be useful for dose recommendations. The therapeutic range encompasses the drug concentration minimum for efficacy and maximum before toxicity. The minimum inhibitory concentration (MIC), or the drug concentration required to stop or kill MDRTB bacterium, for capreomycin is known *in vitro*: 2 μg/ml. However, the *in vitro* MIC is unknown. The kidney is the major excretory organ and thus the levels leading to kidney toxicity are also important. In mice,

capreomycin toxic dosage levels were found to result from a 250 mg/kg intravenous dose and 514 mg/kg intramuscular dose [19]. However, the actual dose in the kidneys was unknown.

Capreomycin mode of action and effects on the kidney are similar to those from aminoglycoside antibiotics (AGAs), such as gentamicin, and thus it is often grouped among the AGAs [20]. ; however, it is technically a polypeptide with no glycoside groups [14]. Due to the similarities between gentamicin and capreomycin, it is assumed that the mechanisms for capreomycin absorption, distribution, metabolism, and excretion (ADME) are analogous to gentamicin [20].

2.2.1.1 Lung Interactions

The pathogeneses of tuberculosis in the lung is outlined in Chapter 2.1.1 and for most humans infected, the disease remains in a latent form. Latent tuberculosis infection (LTBI) is difficult to eliminate because the drug regimens take a longer period of time and many of the drugs in the regimen are very toxic over long treatment periods [21]. Furthermore, without any symptoms, patient adherence is a challenge [22]. The efficacy of a drug against tuberculosis depends on the concentration in the lung.

It is documented that aminoglycosides are eliminated more slowly from the lung than the serum, although the mechanism is not specifically known [23], [24]. Aminoglycoside transport into the lungs is suggested to be due to endocytosis, as the polarity of the molecules would prohibit passive diffusion [25]. Reabsorption of antibiotics back into

the blood may also occur, maximized once serum concentrations are lower than the lung concentrations. Keeping serum concentrations at a constant level may minimize reabsorption into the serum, resulting in consistent lung concentrations. Consistent lung concentrations at or above the MIC would likely improve treatment results [26].

Patients suffering from tuberculosis may be more prone to altered antibiotic kinetics due to inflammation [26]. In this study, the mice were not infected with TB and therefore the latter explanation for higher drug concentrations in the lung would not apply.

2.2.1.2 Kidney Interactions

As explained in Chapter 2.2.1, capreomycin-specific information is limited and therefore its effects are assumed to be analogous to those of aminoglycosides like gentamicin. Capreomycin and aminoglycosides are nephrotoxic, with some of the administered dose being retained in the epithelial cells of the kidney proximal tubules [27]. In a study with a tracer-tagged gentamicin injected into mice, the gentamicin was exclusively seen in the proximal tubular cells, concentrated in apical cytoplasm [28]. The accumulation of aminoglycosides is notable as the concentration in the kidney is much greater than serum concentrations [29]. Similarly, kidneys were dissected by Luft *et al.* following dosing with gentamicin, tobramycin, or kanamycin. For all three antibiotics, 85% of the accumulated drug was in the cortex, where the proximal tubule is located (see Figure 3 for an overview of kidney physiology) [30].

There are two causes of necrotic damage and/or death to kidney cells: uptake of the drug into the kidney cells followed by necrotic cellular death accompanied by electrolyte imbalances that can also cause apoptotic death.

Due to the drug retention in proximal cells, damage is concentrated to the proximal tubule portion of the kidney glomeruli [27].

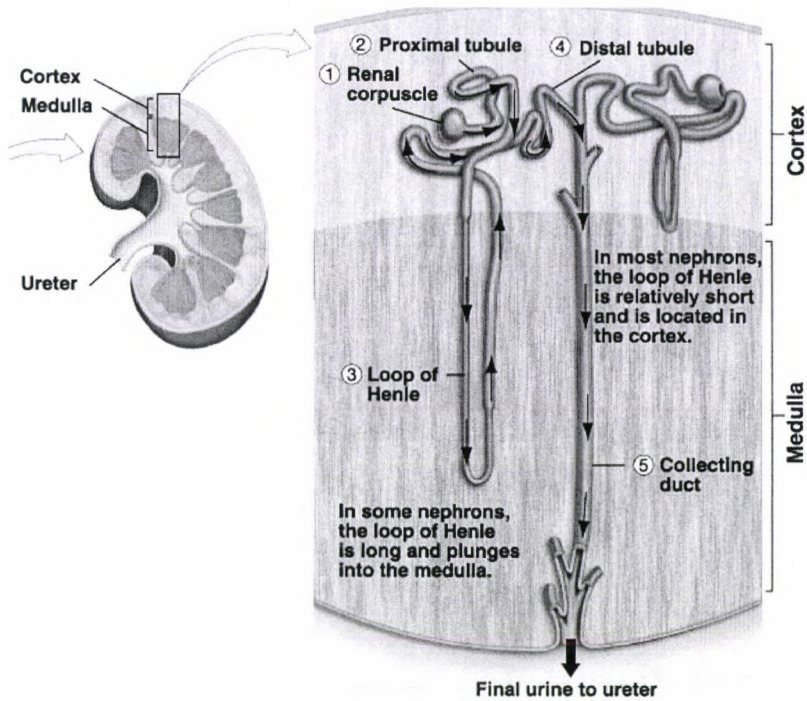

Figure 3: Kidney structure [31]

In the proximal tubule cells, AGAs must enter via apical membrane binding and endocytosis because the charged drug molecule cannot freely cross the cellular membrane. Megalin is the proposed endocytic receptors for such drugs (Figure 4) [29], [32], [33]. Megalin is a glycoprotein expressed in some specialized epithelial cells including in the renal tubule and inner ear epithelium. Capreomycin is known to exert

both renal and ototoxicity, which supports the likelihood that megalin is responsible for uptake [27]. As further evidence that megalin is an important factor in AGA uptake, a study comparing normal and genetically megalin-deficient mice was done by Shmitz *et al.* In this study, gentamicin was tagged with a tracer and administered intraperitoneally or intravenously. The megalin-deficient mice did not have any significant drug accumulation in the kidneys following either route of administration whereas the mice with megalin did exhibit significant accumulation [28].

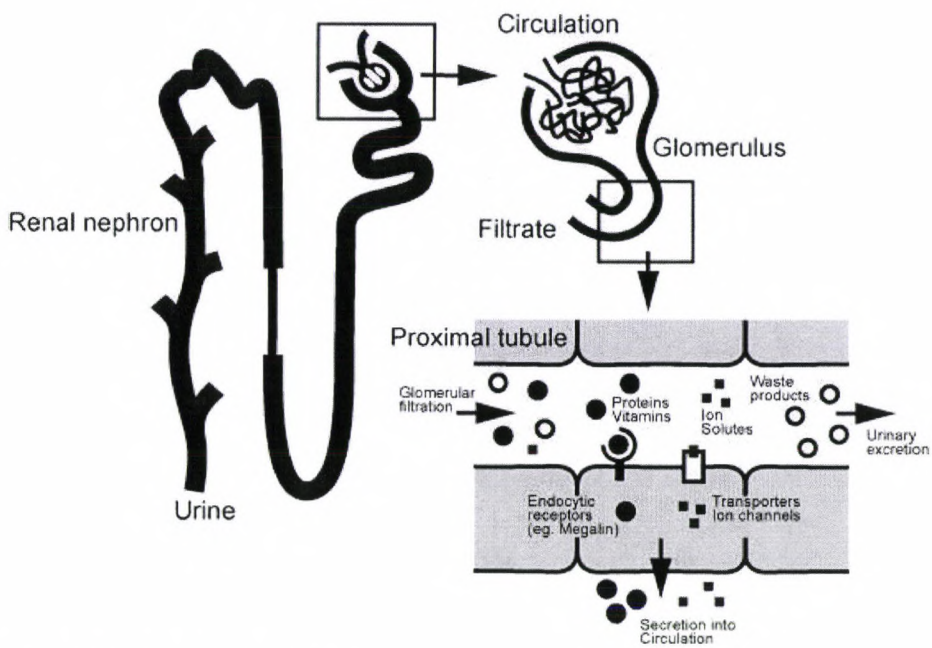

Figure 4: Megalin representation [29]

Megalin is a 600-kDa surface receptor belonging to the low-density lipoprotein receptor family [33]. It nonspecifically binds and uptakes many proteins including hormones, toxins, enzymes, and others ligands [29].

Following endocytosis by megalin, AGAs are sequestered in lysosomes [27], [28]. Drug-induced phospholipidosis occurs, meaning the drugs accumulating and trapped in the

lysosomes form complexes with phospholipids. This unusual level of accumulation causes abnormal levels of myeloid bodies in the tissue [34]. This leads to necrotic cell death once the lysosomes rupture and release acid hydrolases. This is one cause of cellular death in the kidney. It is also proposed that the accumulation of aminoglycosides in the proximal tubule cells inhibits microsomal protein synthesis, inhibits ATP generation, and interferes with the transport of ions [20].

However before the symptoms of necrotic death are apparent, electrolyte imbalances occur and apoptosis is noted [32].

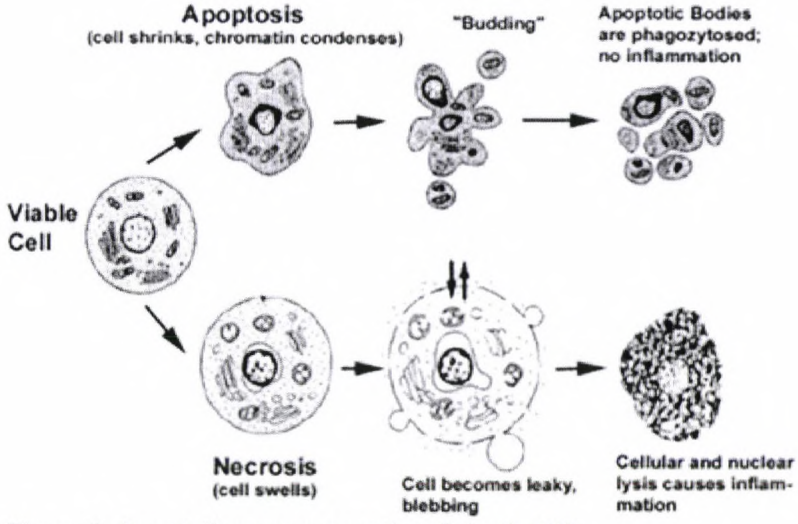

Figure 5: Apoptotic versus necrotic cell death [35]

This apoptotic renal cell death and the aforementioned electrolyte imbalances are due to interactions of AGAs with the calcium-sensing receptor (CaR), especially in the ascending limb of the loop of Henle [20]. This is a G-protein coupled heptahelical receptor with great homology between many mammalian species, including both humans and mice [36].

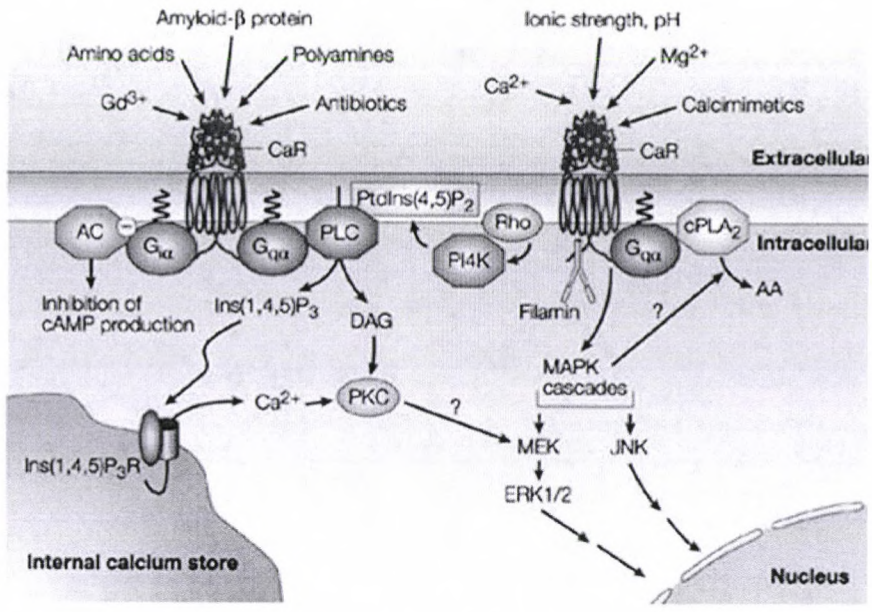

Figure 6: The calcium sensing receptor (CaR) and cascade impact on electrolytes [37]

Elevated levels of extracellular calcium or AGAs all result in intracellular calcium mobilization. The effects of AGAs on CaR include an initial cell proliferation of CaR-containing cells due to several signaling cascades, followed by cell death due to the constant activation of CaR, and thus prolonged elevation of intracellular calcium levels leading to apoptosis [38].

The renal toxicity of a given aminoglycoside drug in relation to the CaR correlates directly to the number of cationic amino groups on the drug [38], [29]. Capreomycin's toxicity is evident as it is compared to similar other drugs in Figures 7-9.

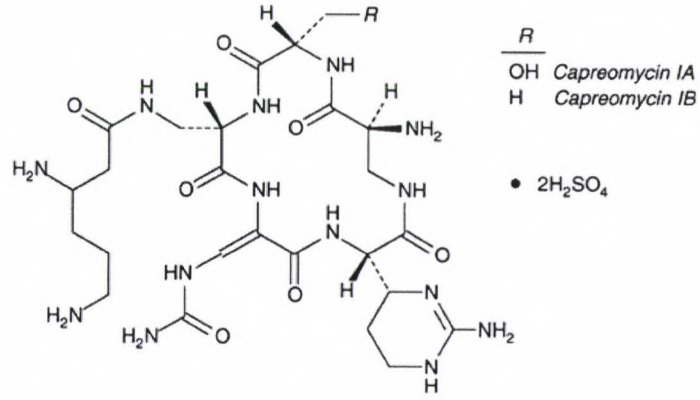

Figure 7: Capreomycin, with 5 amino groups [13]

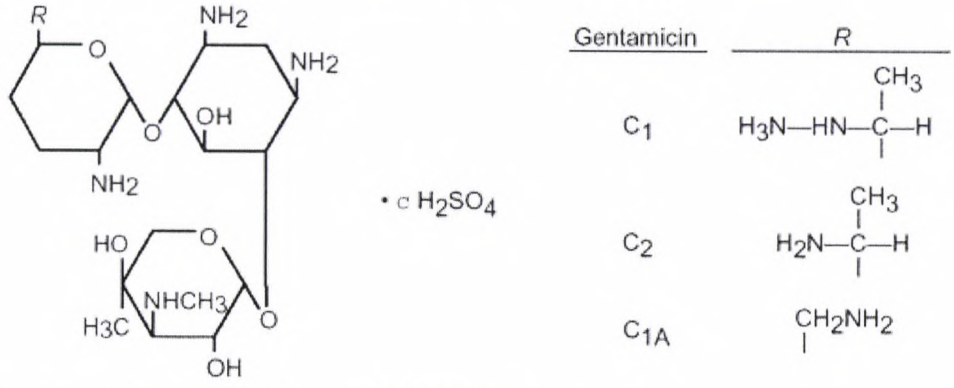

Figure 8: Gentamicin, with 4 amino groups [39]

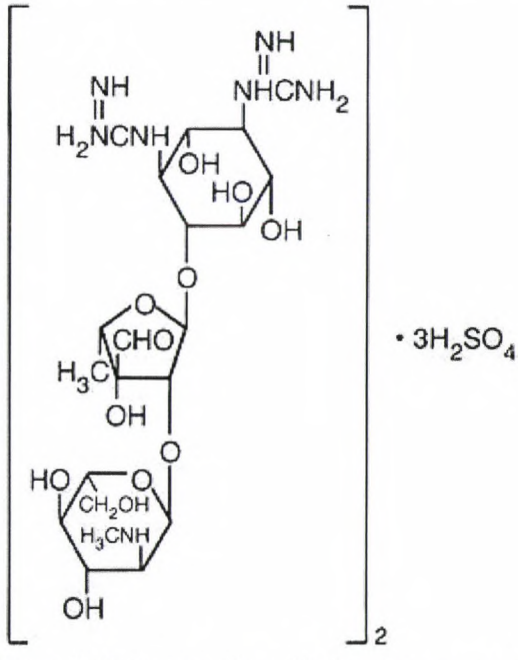

Figure 9: Streptomycin, with 2 amino groups [40]

The main purpose of the CaR is to help maintain normal calcium levels in the body by suppressing parathyroid hormone (PTH) when calcium levels are elevated. Endocrine processes are well-known in the maintenance of calcium homeostasis but the renal sensing is also important [36].

As mentioned, a significant side effect of capreomycin and AGAs is electrolyte disturbances caused by the excretion of the drug through the kidney. The use of capreomycin, especially as part of a multidrug regimen as in tuberculosis treatment, can cause Bartter-like syndrome or Fanconi syndrome. Bartter-like syndrome issues include alkalosis, hypokalemia, hypomagnesaemia, and hypocalcaemia. Fanconi syndrome is the excess excretion of essential compounds like glucose, amino acids, and electrolytes [41]. These issues can be compounded by deficiencies of potassium and magnesium, which are common in tuberculosis patients [42]. Electrolyte imbalances known to occur with the usage of capreomycin can lead to kidney damage or failure [43]. Renal damage is characterized by a resultant plasma creatinine level greater than 45 μmol/L [32]. In addition, the imbalances can lead to heart arrhythmias and muscle problems.

2.3 Pharmacokinetics

2.3.1 Traditional Pharmacokinetic Determinations

Pharmacokinetics involve the interpretation of what effects the body has on a drug in terms of absorption, distribution, metabolism, and excretion (ADME). In the study and characterization of drugs, the determination of pharmacokinetic parameters is based primarily on serum concentrations. Typically, the following values are reported, as they provide insight to the absorption and excretion of pharmaceuticals: the maximum experimentally seen concentration (C_{max}); the time of maximum concentration (t_{max}); the area under the curve (AUC), which provides insight to drug exposure; the minimum effective concentration (MEC); the maximum tolerated concentration as a toxic limit (MTC); the constant of elimination from the serum (slope of the log concentration versus time) (K_{elim}); and the volume of distribution which is the ratio of drug in the body to drug concentration in the plasma ($V_{d.}$).

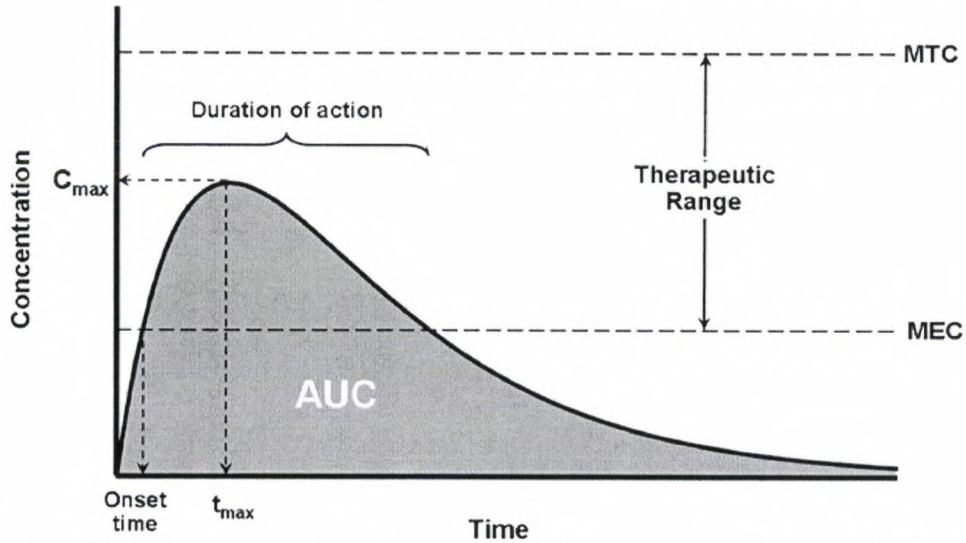

Figure 10: The pharmacokinetic parameters typically reported in literature and to the FDA. These measures are typically based on serum concentration data [44].

For capreomycin, LeConte *et al.* [19] is the primary source cited for pharmacokinetic information. As with the present study, these investigators used mice, but utilized an intravenous dosing method and earlier animal sacrifice time points. The reported parameters from Le Conte et al. are half-life for serum (Table 1) and the area under the curve for multiple compartments (Table 2) following an intravenous dose of 120 mg/kg of free or liposomal-encapsulated capreomycin.

Table 1: LeConte *et al.* half-life for a 120 mg/kg intravenous dose of capreomycin, free and encapsulated (n=5).

	Free	Encapsulated
t1/2 (h)	0.18	0.40

Table 2: LeConte *et al.* area under the curve for a 120 mg/kg intravenous dose of capreomycin, free and encapsulated (n=5).

Organ	AUC for Free	AUC for Encapsulated
Kidney	982.40	1574.00
Serum	34.00	50.40
Spleen	184.00	459.70
Lung	59.70	125.70

To find the half-life, the serum concentration was extrapolated from 0.25 to 2 hours to a hypothesized maximum concentration with exponential regression. The area under the curve was found using the trapezoidal rule [19]. The trapezoidal rule method estimates the integral between each set of data points:

$$\int_a^b f(x)dx \approx (b-a)\cdot\frac{f(a)+f(b)}{2}$$

The variables a and b represent the time and the function of each represent the concentration at the corresponding time point. Figure 11 illustrates the serum data and an example of using the trapezoid rule.

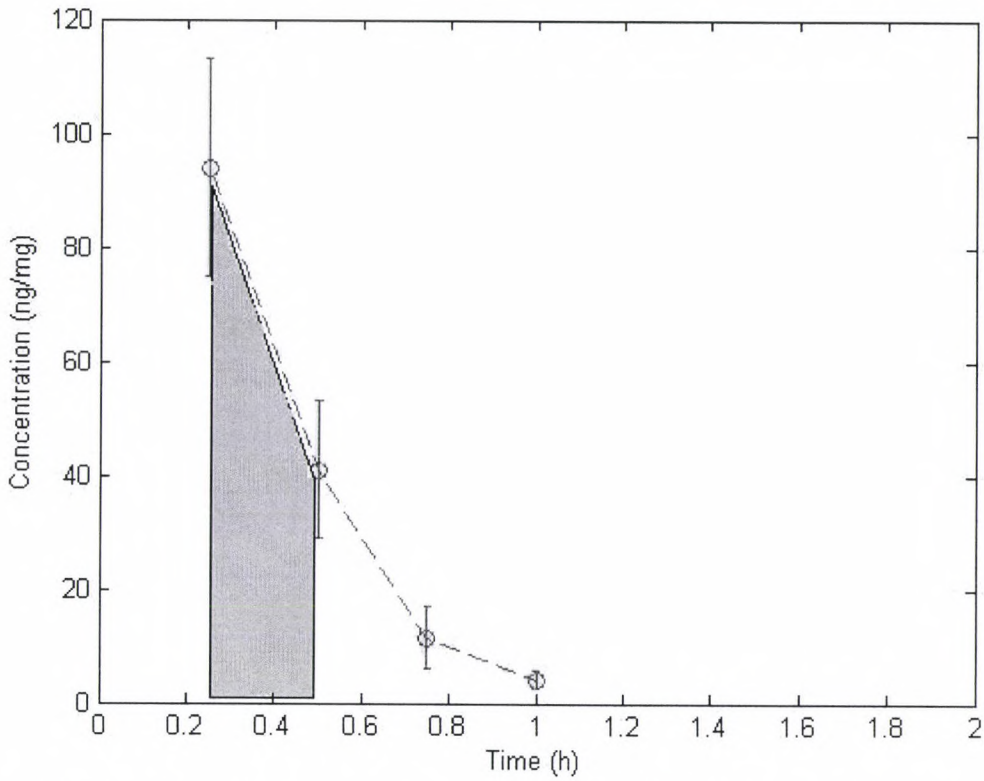

Figure 11: LeConte *et al.* serum concentration data following a 120 mg/kg dose. Example of the trapezoidal AUC method.

A limitation to the traditionally reported parameters is the single homogenous elimination constant to describe drug excretion. While it provides a rate of drug leaving the serum, there is no information on the mechanisms of clearance. Since it is known that capreomycin is renally eliminated and potentially toxic, the specific characterization of the kidney clearance can provide more detail and insight on its function [45].

2.3.2 Pharmacokinetic Models

Pharmacokinetic (PK) models incorporate prior knowledge about drug characteristics and a species' physiology to predict quantitative drug concentrations over time. Drug

characteristics and ADME provide functional information for accurate concentration prediction. In an animal or person, knowledge of the drug concentration in body compartments is useful because 1) low drug concentrations hinder efficacy, and 2) the pharmaceutical could become toxic if levels are too high. Modeling allows rapid predictions about the effects of changing variables such as dose levels, dose frequency, and treatment duration [46].

2.3.3 Physiologically-Based Pharmacokinetic Modeling

The classical PK model assumes the body to be one homogenous, well-mixed vessel. A more sophisticated approach is to divide the body into several physiologically-accurate compartments- organs, blood, tissues- with a mass-balance for each compartment. As ADME information for each compartment is included, the model generally becomes more realistic and the model utility increases. This is the basis for physiologically-based pharmacokinetic (PBPK) modeling.

PBPK models contain separate compartments for relevant organs or tissues for the application of interest [47]. Specifically, in the present model for capreomycin, there are separate compartments for the lung, skin, fat, muscle, kidney, brain, heart, bone, liver, spleen, gut, arterial blood, venous blood, and a carcass compartment that contains all tissues not accounted for in other compartments. The connection between compartments and pathway of blood flow is as follows (see Figure 12).

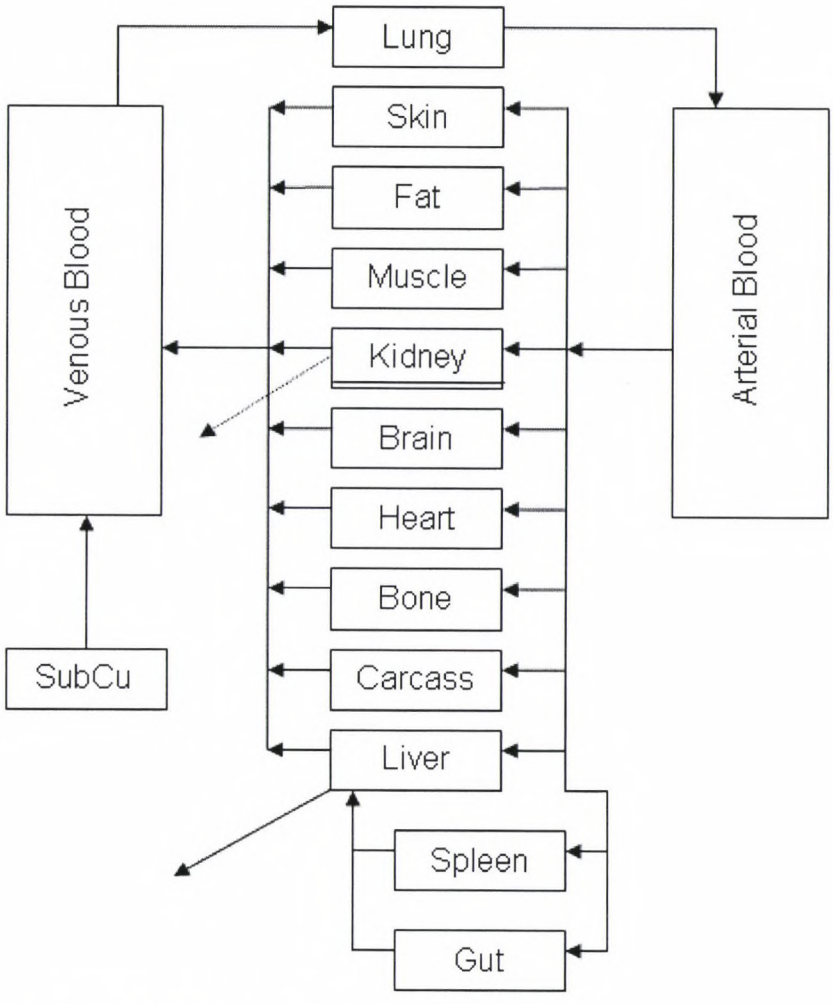

Figure 12: Model compartments and connections.

The general mass balance equation (equation 1) for each compartment assumes flow-limited mass transfer, meaning the blood entering a tissue is quickly in equilibrium with the tissue [48].

Equation 1: PBPK general mass balance

$$\frac{d(M_{organ})}{dt} = Q_{organ} * \left(C_{arterial} - \frac{C_{organ}}{P.C._{organ}} \right)$$

i. M_{organ} is the drug mass in the organ
ii. Q_{organ} is blood flow to organ
iii. $C_{arterial}$ is the drug concentration in the arterial blood flow
iv. C_{organ} is the drug concentration in the organ
v. P.C. is the partition coefficients

Formulating the appropriate form of this mass balance equation for each organ leads to a system of differential equations, and provides the mathematical representation of the PBPK model (Chapter 3.2). The usual application of PBPK models is to predict output concentrations based on known pharmacokinetic information.

In this project, the final capreomycin concentrations in several organs and serum were collected, but no information about the pharmacokinetics were known. Using the known initial doses, experimental physiology, and resulting concentrations, the unknown pharmacokinetic parameters were estimated through an evolving set of model assumptions and simulations. From the determination of these parameters, and assuming that they apply over a range of concentrations, the model could ultimately be used to predict the drug levels following various dosing regimens in the mouse, or potentially in a human model [48].

2.4 Simulation

2.4.1 Simulation Software, MCSim

To predict the unknown pharmacokinetic parameters in the developed PBPK model (Chapter 2.3.3 and 3.2.2), the simulation software *GNU MCSim* [49] was used. MCSim is a software package that is useful in solving statistical and differential equation systems, as in the system of differential equations comprising the PBPK model. The package solves the equations numerically for specific values of parameters, or for specified distributions of parameters using Monte Carlo (MC) analyses [50].

Using *MCSim*, the following steps were taken to predict the unknown parameters:

1. The model (Chapter 3.2) was converted to a .c file
2. The model.c file was compiled and then an executable file is generated
3. The executable file was run with a simple simulation file, which included the unknown parameters, to generate drug concentration profiles for all specified organs (Chapters 2.4.2 and 3.3.1)
4. The executable file was run with a Markov chain Monte Carlo (MCMC) simulation, which updated prior parameter estimations to generate posterior parameter values (Chapter 2.4.3 and 3.3.2).
5. The MCMC posterior values were randomized and run with a "Set Points" simulation to generate possible concentration ranges predicted by the model with the posterior parameter ranges.

2.4.2 Forward Simulations

Due to the unknown pharmacokinetic parameters of capreomycin, "forward" simulations were performed repeatedly to estimate the desired parameters. These simulations generated organ concentration curves, combining the compartment dynamics in the model file and estimated parameters in the simulation file.

The forward simulation inputs such as body weight, organ weight, partition coefficients, and dose size, will override the model file inputs. For this reason, the model file inputs are usually set to an arbitrary place holder, zero or one.

The forward simulation drug concentration output was graphically compared to experimental concentration curves for each organ to determine accuracy. This method provided rough parameter estimations.

2.4.3 Markov Chain Monte Carlo (MCMC) Simulation

Bayesian inference is a method of calculating posterior parameter distributions based on prior parameter values and experimental information.

Equation 2: Bayes' theorem

$$p(\theta \mid y) \propto p(y \mid \theta) \times p(\theta)$$

The unknown parameters, θ, are considered random, and a prior parameter distribution, $p(\theta)$, is formed from any known information. The prior distribution of values uses experimental data, y, to update the values to produce a posterior distribution of the parameters given y, $p(\theta|y)$ [51]. However, for a complex model such as a hierarchical, nonlinear PBPK model, exact analytical Bayesian inference is not possible [52]. A

Markov chain Monte Carlo (MCMC) simulation is one method of computational Bayesian analysis and entails iterative sampling to converge toward posterior parameter values.

MCSim performs a "series of simulations along a Markov chain in the parameter space…" where "…the random choice of a new parameter value is influenced by the current value" [53]. *MCSim* uses Metropolis-Hastings sampling for the MCMC simulation [54]. At the first iteration, each parameter θ is assigned a value from the prior distribution. For the next iteration, the parameter is updated and proposed to be θ' from a proposed distribution. The proposed value is accepted or rejected based on the ratio of the joint posterior density at θ and θ', π and π'. If π'/π is greater than one, θ' is accepted as the updated parameter. This acceptance or rejection is done for all the unknown parameters, completing an iteration of a Markov chain [51]. The result of the MCMC simulation is a Bayesian posterior distribution for the parameters [54].

To initiate a MCMC simulation, MCSim requires the specification of the following: "nRuns," the number of iterations desired; "simTypeFlag" which begins MCMC simulations when set to zero, where parameters are updated by Metropolis-Hastings sampling; "print frequency," which indicates the frequency of iteration outputs; "itersToPrint," the number of final iterations output; and "RandomSeed," a random integer seed to start the iterations [55].

Next, the prior distribution of parameters and variance is characterized. For example, if the prior distribution has a normal distribution, the mean and standard deviation are

required inputs. The probability distribution of the input data is also given in a likelihood statement.

Lastly, the simulation section is used to assign specific values to any input variable in the model. For example, experimentally measured variables are input in the simulation section and the inputs in this section override the model file variable assignments [55].

2.4.4 Set Points Simulation

After the prediction of posterior parameter ranges using the MCMC simulation, a set-point simulation runs multiple forward simulations with randomized parameters to show the range of possible organ concentration predictions with the parameter ranges.

To run a set-point simulation the following must be specified: the output filename, the file containing the parameters to sample from, the number of runs that will be performed, and the names of the parameters to be identified.

Chapter 3: Materials and Methods

3.1 Mouse Study

3.1.1 Dosing and Collection of Concentration Data

In order to parameterize and validate the model, experimental studies were initiated in collaboration with Dr. MaryAnn DeGroote of the Microbiology, Immunology, and Pathology (MIP) Department at Colorado State University. The study examined the capreomycin levels in various organs of treated mice over the time range of 0-20 hours, specifically at the 0.5, 1, 2, 6, and 20 hour time points.

A control group at time zero received an injection containing only 1x phosphate buffer saline (PBS) solution. The mice were six to eight week old C57/B16 female mice from Charles River or Jackson labs and were weighed one day prior to the experiment.

The drug was administered subcutaneously using a 30 gauge ½ inch needle at either a 100 mg/kg or a 250 mg/kg dose. At each of the desired time points for both dose levels, four mice were sacrificed via CO_2 euthanasia followed by cervical dislocation. The mice were immediately bled with a heart stick and the kidneys, lungs, spleen, and liver were harvested. The tissues were weighed and then flash frozen in cryovials at -80 °C. The blood was placed in a serum vial, put on ice for one hour after collection, and spun down to collect the serum.

3.1.2 Analysis of Tissue and Serum

In order to determine the capreomycin levels in each of the harvested organs, an extraction and analysis was performed by the Pharmacology Core Laboratory using LC/MS/MS in the Animal Cancer Center (ACC). The HPLC portion separates the capreomycin from the tissue homogenates. Mass spectrometry quantifies the two major capreomycin species: capreomycin IA (669.3-507.0 amu) and capreomycin IB (653.3-491.3 amu). The transitions for both forms of capreomycin were integrated as one to account for all of the drug in the tissue or serum.

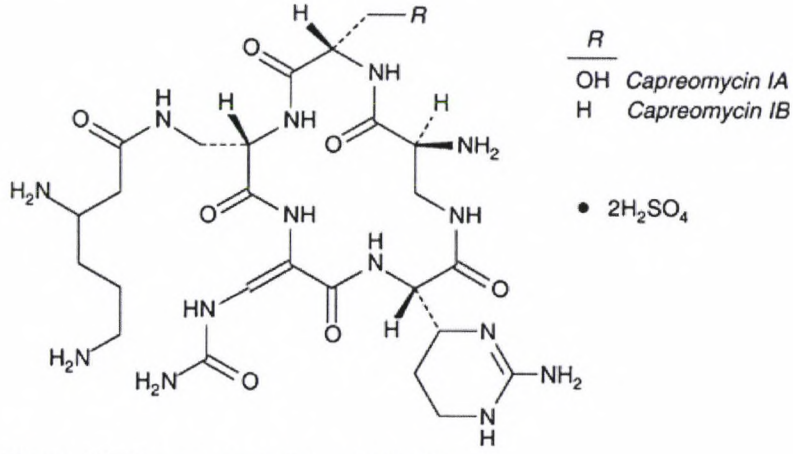

Figure 13: Capreomycin IA and IB [13]

The HPLC column used was a Water Atlantis® HILIC Silica 5 um column with Phenomenex C18. Plastic vials were used as capreomycin exhibits some binding to glass.

Prior to tissue/serum analysis, a standard curve for capreomycin was generated using solutions of 50% acetonitrile (ACN): 50% H_2O with 0.1% acetic acid.

The tissues were prepared for analysis by adding water to make a solution that was 100 mg tissue per ml, and sonicating. The sonication was performed in small bursts while the tissue remained on ice in order to mitigate the effects of heat generated by the sonicater. In some cases, the larger organs were subdivided. The organs were prepared as follows in order to improve homogeneity:

- Spleen- used in entirety due to the small size.
- Kidneys- one kidney was used from each mouse. It was assumed that there was no preferential clearance in one kidney or the other.
- Lung- portions of each lobe of the lung were removed and homogenized together as the organ was too large
- Liver- after removal of the gallbladder, the liver was diced into small pieces, mixed, and a random sample was taken for sonication

Following sonication, 200 µl of the tissue homogenate or 100 µl of serum were added to a microcentrifuge tube containing 10 µl of capreomycin standard or 10 µl of 50% ACN. The ACN disrupts any protein binding; however, capreomycin does not exhibit known protein binding. The mixtures were vortexed briefly. To the tissue homogenate, 150 µl of methanol + 1% formic acid was added; 300 µl of methanol + 1% formic acid was added to the serum samples to induce protein precipitation. Each sample was then vortexed for 10 minutes followed by centrifugation for 10 minutes to remove cell debris and protein from the liquid portion. Supernatant was then transferred to plastic autosampler vials for analysis.

As a control, organs were harvested from mice that received no capreomycin and were sacrificed at the same time points. The concentrations were measured for each of four mice at all time points, for both dosage levels: 100 mg/kg and 250 mg/kg. If the concentration was below the lower limit of quantification (LLOQ), no concentration data were available.

Table 3: Lower limit of quantification for each harvested and analyzed organ

Organ	LLOQ (ng/mg)
Kidney	50.0
Serum	1.0
Liver	10.0
Lung	10.0
Spleen	10.0

Note: The serum concentration is referred to in the same units (ng/mg) as the organs throughout for consistency. This is equivalent to the typical units describing serum concentration, μg/mL when the serum density is approximated to be ≈ 1 g/mL.

$$\frac{\mu g_{drug}}{mL_{serum}} \cdot \left[\rho_{serum} = 1 \frac{mL}{g} \right] = \frac{\mu g_{drug}}{g_{serum}} \cdot \frac{1g}{1000mg} \cdot \frac{1000ng}{1\mu g} = \frac{ng_{drug}}{mg_{serum}}$$

3.1.3 Literature Comparison

Following the same methods used by LeConte *et al.*, the traditional pharmacokinetic parameters such as half-life ($t_{1/2}$) and area under the curve (AUC) were found for the experimentally collected data. The traditional pharmacokinetic calculation measures can be found in Chapter 2.3.1.

3.2 Model Development

3.2.1 Inputs and Assumptions

The PBPK model is divided into different compartments to represent each organ and blood flow. The size of each organ and the blood flow through each organ are essential inputs. From the experimental data, the following inputs were used directly: body weight of the mice, and lung, liver, kidney, and spleen weights. For the remaining organs and for approximate blood flow through each organ, values from Brown *et al.* were used.

A guiding principle in the model development was to reduce complexity while retaining the ability of the model to make useful predictions and generate hypotheses [56]. To this end, a number of plausible, simplifying assumptions were made. The tissue density for all of the organ systems was assumed to be about equal to that of water, or 1 g/ml [57]. This is valid for most compartments with the exception of bone or fat. However, these were not compartments of interest and so the density was assumed to be averaged with all other tissues to water.

There was also no blood protein binding included because capreomycin has limited to no plasma protein binding properties. Capreomycin does not have any known metabolites and it is hydrophilic [58]. Since it is hydrophilic, the partition coefficients for all the compartments except the lung (discussed in Chapter 3.2.5) are assumed equal to one. The partition coefficient is the amount of drug that moves from the blood into an organ as

the blood flows through. Protein binding, organ fat content, drug hydrophilicity, and metabolite breakdown all affect the partition coefficient. When set to one, it means that there are no barriers for drug transfer.

The kidney is also known to accumulate capreomycin similarly to other aminoglycosides but this is accounted for by specific, known mechanisms within the compartment.

3.2.2 General Model Format

The model predicts drug concentration in a number of organs through a series of related mass balance equations for each organ in the model. For most of the compartments (organs), mass transfer is assumed to be flow limited, or that the compartments come to equilibrium with the blood very rapidly [46], [56]. Capreomycin is hydrophilic and does not exhibit protein binding, so equilibrium between the blood and tissues is a reasonable assumption. Refer to Figure 10 for the blood flow through tissues.

a. General organ except lung, blood, kidney, and liver:

$$\frac{d(M_{organ})}{dt} = Q_{organ} * \left(C_{arterial} - \frac{C_{organ}}{P.C._{organ}} \right)$$

   vi. M_{organ} is the drug mass in the organ
   vii. Q_{organ} is blood flow to organ
   viii. $C_{arterial}$ is the drug concentration in the arterial blood flow
   ix. C_{organ} is the drug concentration in the organ
   x. P.C. is the partition coefficient

b. Lung: $\frac{d(M_{lung})}{dt} = Q_{lung} * \left(\frac{C_{lung}}{P.C._{lung}} - C_{arterial} \right)$

c. Venous blood, which is a mixture of blood leaving organs, with the exception of the lung. The dose enters the venous blood flow.

$$\frac{d(M_{venous})}{dt} = \Sigma_{organs}\left(Q_{organ} * \frac{C_{organ}}{P.C._{organ}}\right) - Q_{lung} * C_{venous} - dt(M_{Dose})$$

d. Arterial blood: $\frac{d(M_{arterial})}{dt} = Q_{lung} * \left(\frac{C_{Lung}}{P.C._{lung}} - C_{arterial}\right)$

e. Kidney, divided into a shallow (S) and deep (D) compartment:

$$\frac{d(MKE)}{dt} = CLR * CVKS$$

$$\frac{d(MKA)}{dt} = \frac{(V_{\max} * CVKS)}{K_m + CVKS}$$

$$\frac{d(MKDE)}{dt} = CLRD * CVKD$$

$$\frac{d(MKS)}{dt} = Q_{kidney} * (C_{arterial} - CVKS) - dt(MKA) - dt(MKE) + dt(MKDE)$$

$$\frac{d(MKD)}{dt} = dt(MKA) - dt(MKDE)$$

$$\frac{d(M_{kidney})}{dt} = dt(MKS) + dt(MKD)$$

xi. MKE is the mass of drug excreted from the kidney

xii. MKDE is the mass of drug excreted from the deep compartment and returned to blood flow.

xiii. MKA is the mass of drug accumulating in the deep compartment of the kidney.

xiv. MKS is the mass of drug in the shallow compartment.

xv. CLR is the rate of capreomycin clearance from kidney blood flow; CLRD is the rate of capreomycin clearance from the deep kidney compartment.

xvi. CVKS is the well-mixed blood in the kidney that is then mixed with the venous blood

xvii. V_{max} and K_m are Michaelis-Menten parameters (see chapter 3.2.4) for accumulation

f. Liver:

$$\frac{d(MLE)}{dt} = CLH * CVL$$

$$\frac{d(M_{liver})}{dt} = Q_{hepaticartery} * C_{arterial} + Q_{spleen} * CV_{spleen} + Q_{gut} * CV_{gut} + Q_{Liver} * CV_{sLiver} - dt(MLE)$$

3.2.3 Drug Dosing Representation

The subcutaneous layer is the bottom layer of the skin and includes fat cells, connective tissue, blood vessels, and nerves. The subcutaneous dose was assumed to be an exponential decay function entering the venous blood compartment.

$$N(t) = N_0 e^{-\lambda t}$$

Where N_0 is the initial drug concentration or dose amount, and λ is the decay constant. The decay constant in traditional pharmacokinetics is based on the half-life of the drug. The decay constant in this model is the decay of the drug from the site of injection (subcutaneous) into the venous blood. In the model, the differential equation for the mass balance on the subcutaneous compartment is

$$dt(MSC) = -MSC * SC\_Decay \quad .$$

The assumption to use a decay function for representing subcutaneous transport away from the point of entry is also proposed by Leucke *et al.* [59].

3.2.4 Kidney Representation

Capreomycin can cause renal toxicity, and both literature and experimental results demonstrate an accumulation of drug in the kidney, with levels surpassing the serum amounts. Few specific details about capreomycin uptake or metabolism are known, and thus parallels to similar drugs such as gentamicin were used to make assumptions [20]. Uptake of AGAs is known to be dependent on megalin endocytosis followed by lysosomal sequestration as described in Chapter 2.2.1 [32].

The notable accumulation led to a non-linear uptake representation of capreomycin in the kidney. The non-linear absorption for this compartment was modeled via a Michaelis-Menten relationship, as seen in the literature for similar applications [56], [60], [61]. Specifically, gentamicin and netilmicin were shown by Giuliano *et al.* to follow a Michaelis-Menten accumulation in the kidney [62]. The general Michaelis-Menten equation (equation 2) is traditionally used to describe an enzyme-substrate reaction where $[S]$ is the substrate, v_{max} is the maximum reaction rate and K_m is the Michaelis constant, corresponding to the substrate concentration at half of the maximum reaction rate.

Equation 3: Michaelis-Menten equation

$$v_0 = \frac{v_{max}[S]}{K_M + [S]}$$

In the case of the model development, capreomycin is the substrate $[S]$, the megalin receptor parallels the enzyme, and v_{max} represents the maximum renal accumulation rate.

Following the death of kidney cells, some capreomycin may be released back into the blood flow through the organ. To account for the sequestration of accumulating capreomycin, the kidney was represented as two linked compartments, referred to as the

shallow and *deep* compartments. Physiologically, the shallow compartment would represent the area of the kidney that blood is flowing through and the deep compartment would represent the cells along the walls of the kidney tubules. In the model, the kidney volume was assumed to be about two-thirds blood perfused shallow compartment and one-third deep compartment.

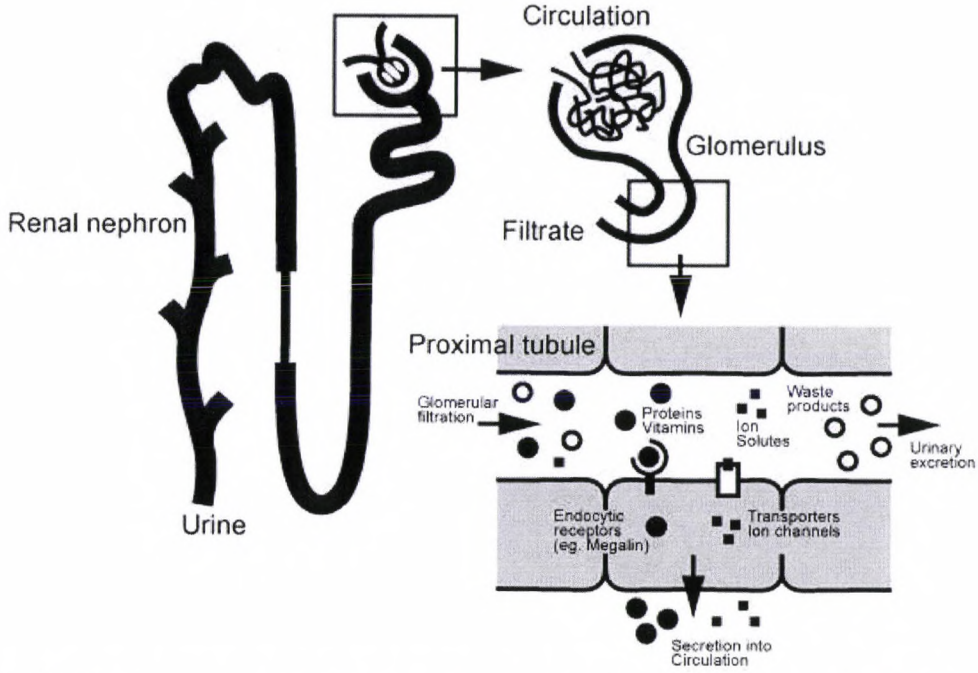

Figure 14: "Shallow" compartment is circulation, or un-shaded area in filtration graphic. "Deep" compartment is the grey shaded cells [29].

The equations in Chapter 3.2.2 describe the mass balance relationship shown in Figure 15.

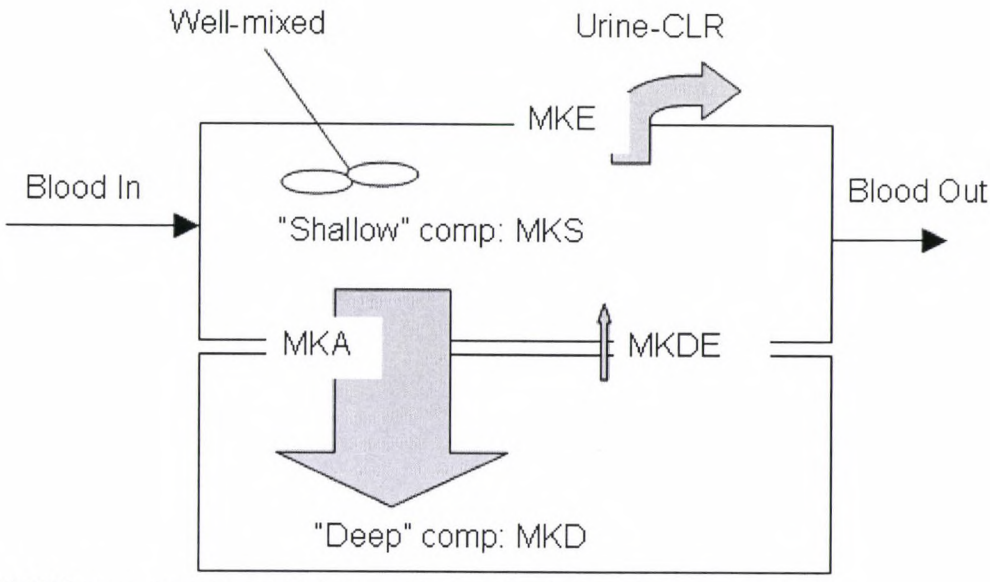

Figure 15: Kidney compartment divisions and excretion/accumulation

3.2.5 Lung Representation

While the kidney is the key organ in excretion of capreomycin, the lung is important because it is the primary site of tuberculosis infection. In Section 2.2.1.1, the clearance of capreomycin accumulation and clearance in the lung is discussed. While there is no conclusive mechanism responsible for lung concentrations, at both the 100 and 250 mg/kg dose level, it was observed that the lung concentration (drug per milligram of organ tissue) was twice as high as the spleen and liver, but less than the kidney and serum. The blood and kidney compartments are expected to be higher because they are receiving and accumulating/excreting the drug, respectively. Based on observed trends in literature and in the experimental data, the lung partition coefficient was assigned a value of two. Even though the mechanisms of capreomycin retention in the lungs are not known, using a partition coefficient about the nominal value of one in the model serves as the simplest means of accounting for these effects.

3.3 Simulation for Parameter Values

Using the experimental physiological data, literature physiology, and experimental concentrations, pharmacokinetic parameters for the entry of the drug into the blood and the accumulation and excretion were predicted.

3.3.1 Forward Simulation for Parameter Estimation

The capreomycin PBPK model development based on known physiological processes resulted in six unknown drug-related parameters to be estimated. By trial-and-error, the six parameters in Table 4 were found for the 100 mg/kg and 250 mg/kg dosages.

Table 4: Unknown pharmacokinetic parameters estimated by simulation

Symbol	Units	Description (relevant compartment)
K_m	ng/kg	Michaelis constant in accumulation (kidney)
V_{max}	ng/h	Michaelis-Menten maximum reaction rate (kidney)
CLR	kg/h	Renal clearance/ urine rate (kidney)
CLRD	kg/h	Deep renal compartment clearance (kidney)
CLHC	L/hr/kg	Hepatic clearance rate (liver)
SC_Decay	h^{-1}	Subcutaneous dose decay rate (subcutaneous)

These parameters were iteratively estimated and assessed. To assess a given set of parameter predictions, the experimental mean concentration values at each time point (n=4 mice) were compared to the forward output concentration for each organ. The experimental data were used in two different ways to predict the parameters:

a) The experimental data was fit assuming the measured maximum to be the definitive maximum drug concentration in each respective organ. This will be repeatedly referred to as the "experimental maximum fit" method.

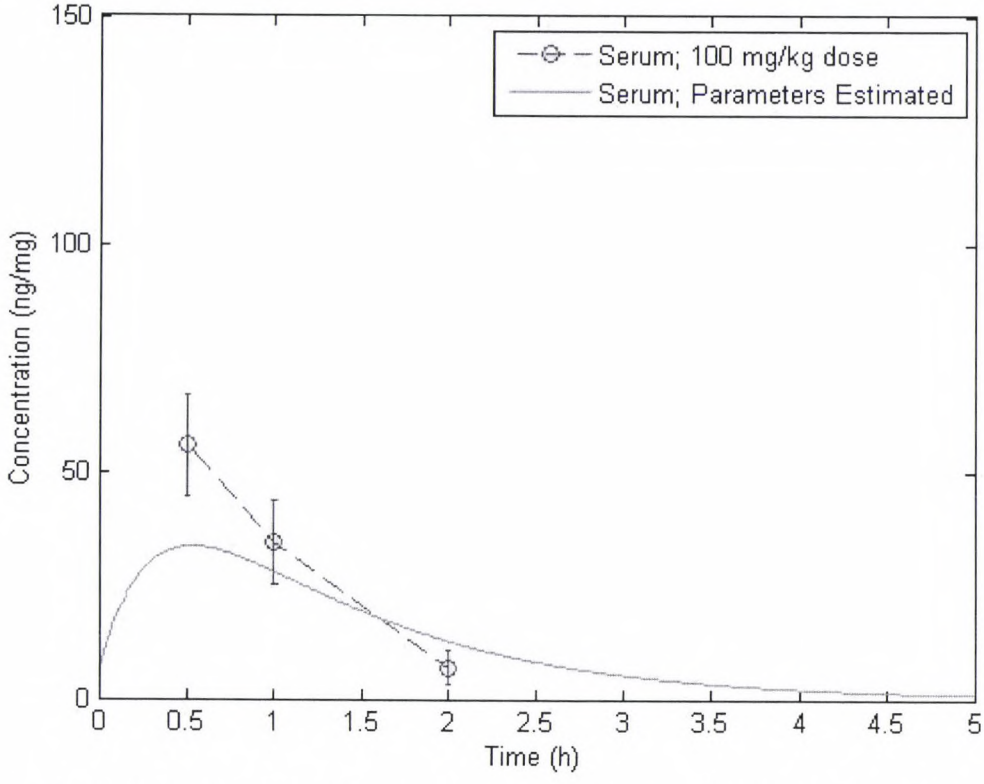

Figure 16: The serum peak concentration is modeled to occur at 0.5 hours, like the data

b) It was assumed that the experimental data did not capture the true maximum in the data from the collected time points. In this case, the maximum is assumed to occur much earlier than shown experimentally (seen in Figure 17). The pharmacokinetic parameters ($t_{1/2}$ and AUC) reported in LeConte *et al.*[19] were estimated using exponential extrapolation and thus the method was considered as a valid interpretation of the data. This will be referred to as the "extrapolated maximum fit" method. The maximum does not occur at $t=0$ because the exponential decay of the dose begins in the subcutaneous compartment and the differential change is subsequently added to the serum.

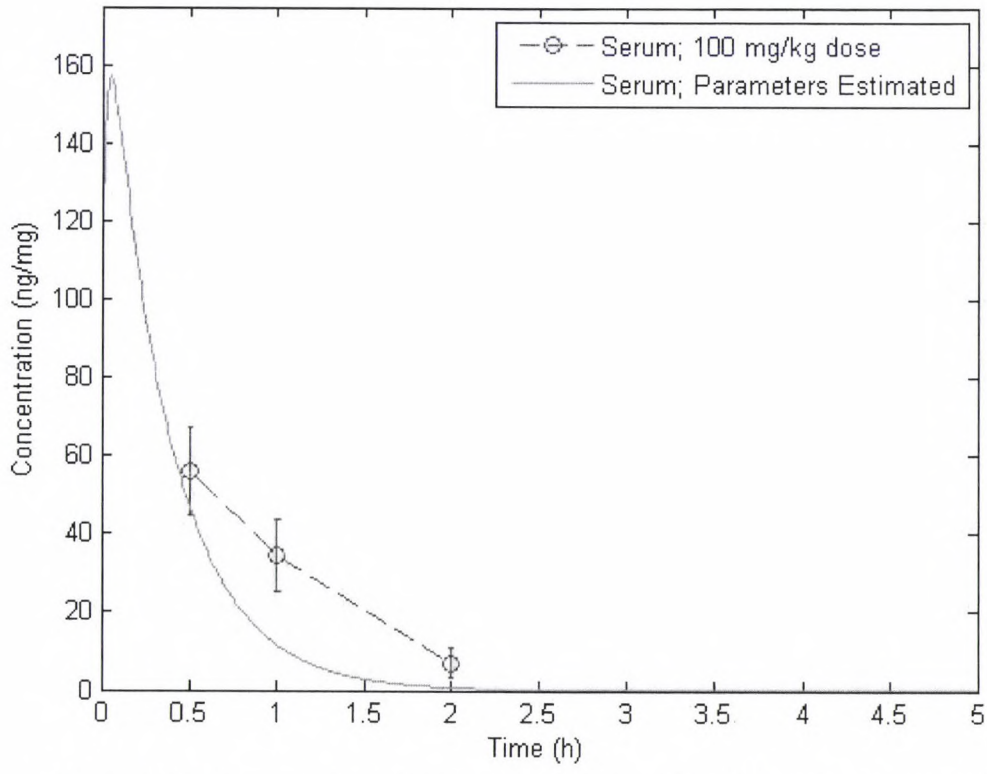

Figure 17: The serum peak concentration is extrapolated based on the available data and the peak concentration is assumed to occur shortly after the dosing.

To see an example of the forward simulation file, please see Appendix VI. From the forward simulation, the effects of each parameter on dose peak time and peak concentration were observed. The relationships of each variable's impact on maximum organ concentration are as follows in Table 5.

Table 5: The arrows indicate the parameter change (increase or decrease) required to increase the maximum concentration in each corresponding organ. Fields left blank indicate little to no noticeable change even with large parameter changes.

	K_m	V_{max}	CLR	CLRD	CLHC	SC_Decay
Kidney	↓	↑	↓	↓	↓	↓
Serum	-	-	↓	-	↓	↑
Liver	-	-	-	-	↓	↑
Lung	-	-	-	-	↑	↓
Spleen	-	-	↓	-	↑	↓

Changing the parameters also influences the time at which the maximum organ concentration is reached. This was useful in determining a balance between parameters that changed maximum organ concentration in opposite directions. For instance, the kidney maximum can be increased by either increasing V_{max} or decreasing K_m. This means that combinations of V_{max} and K_m result in the same maximum kidney concentration (although at different time points). However, decreasing K_m causes the maximum concentration peak time to increase significantly, and increasing V_{max} causes the peak time to increase, though at a lesser degree. Since the maximum time and concentration must match with the data, there is one set of appropriate values.

The kidney, serum, and lung compartments each had experimental concentration values at three or more time points. Therefore, they were primarily used for assessing the model fit. Since the kidney was uniquely sensitive to K_m, V_{max}, and CLRD, those parameters were fit after CLR, CLHC and SC_Decay were assessed.

The simulation output was also used to assess model sensitivity and also to evaluate the structure or assumptions of the model. For example, the effects of changing the kidney clearance rate (CLR) by a factor of ten on kidney and serum can be seen in Figures 18 and 19.

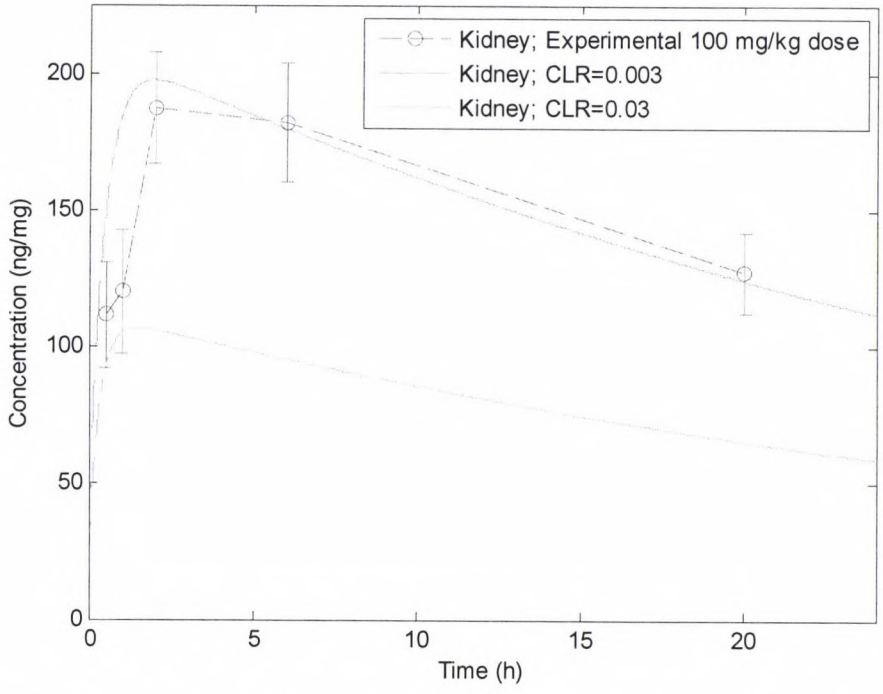

Figure 18: Effect of parameter changes on kidney concentration predictions.

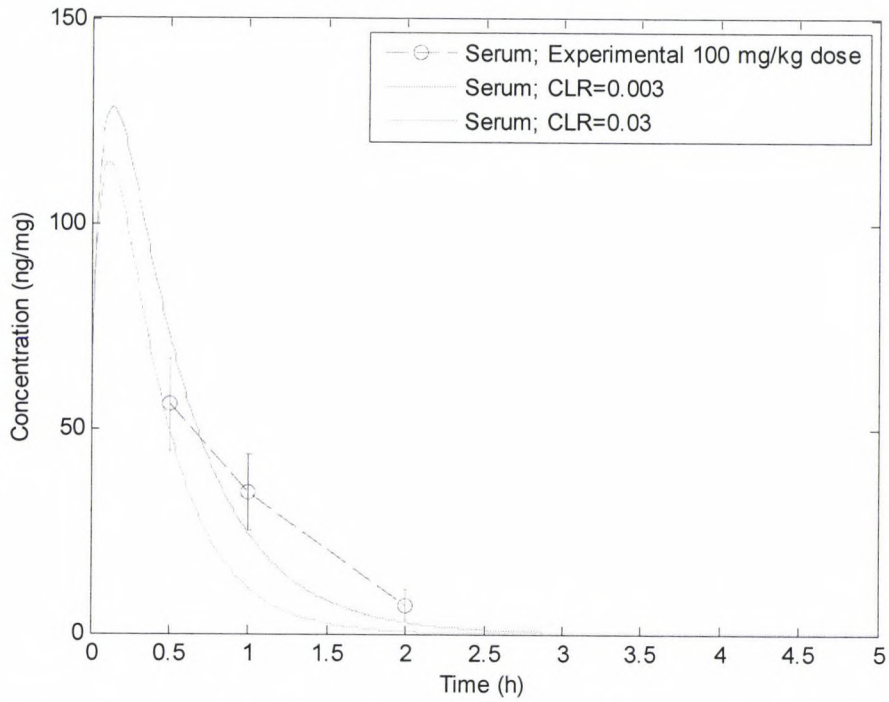

Figure 19: Effect of parameter changes on serum concentration predictions.

The forward model further supported the representation of the kidney as two separate compartments. With just an accumulation term (V_{max} and K_m) and urine clearance (CLR), the predicted shape of the drug concentration function in the kidney never decays, represented in Figure 20.

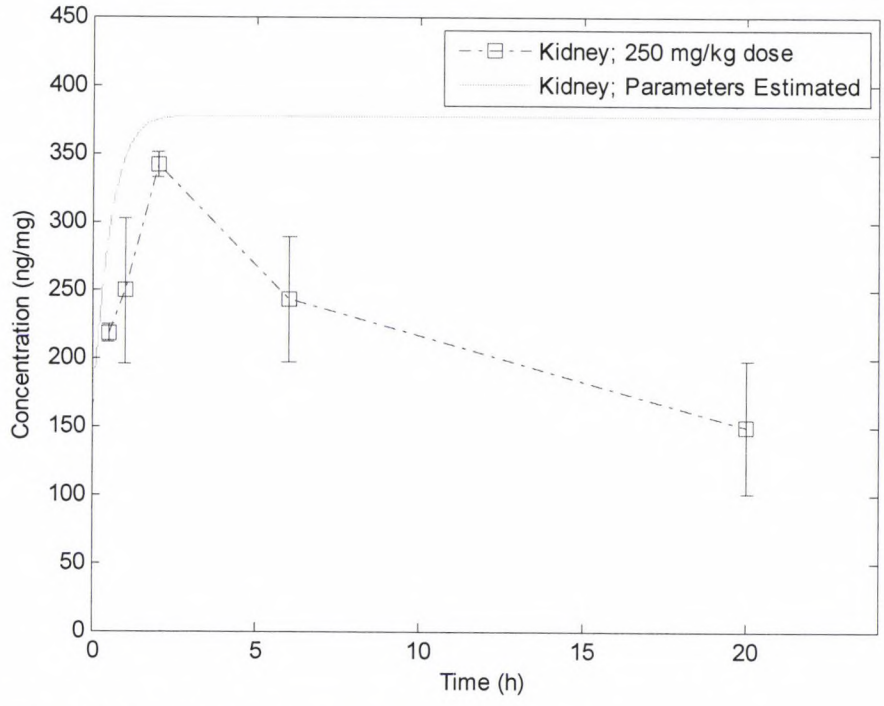

Figure 20: Kidney with one compartment accumulation.

By accounting for the release of capreomycin back into the shallow compartment after cell death (CLRD≠0), the shape of the kidney concentration curve follows the experimentally observed trend in Figure 21.

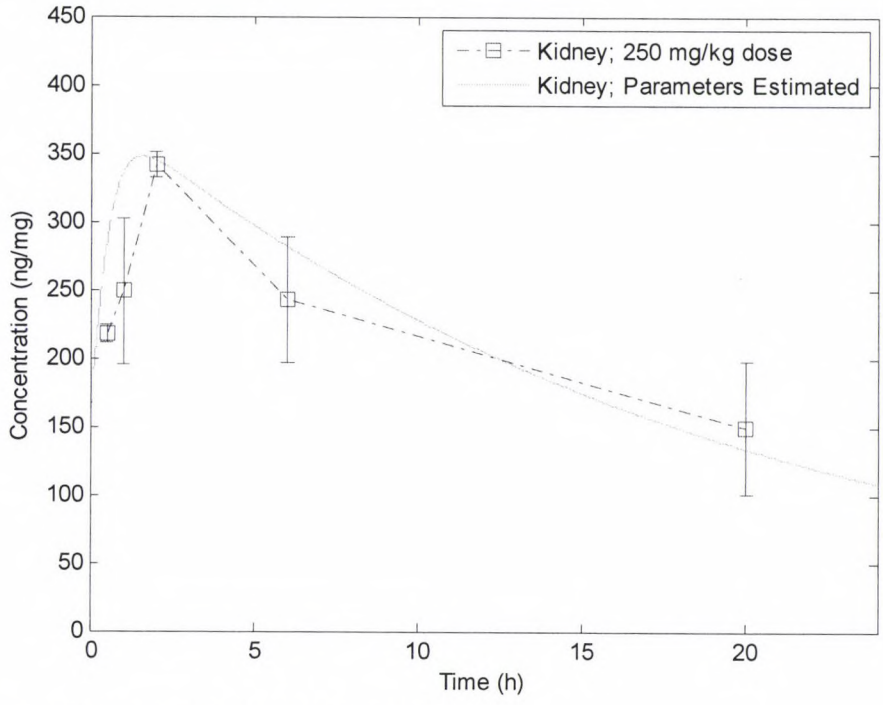

Figure 21: Kidney with CLRD factored in.

After the model parameters were fit to the averaged concentration/time data for the 100 mg/kg dose, the same was done with the 250 mg/kg dose. Ultimately, the desired output was one set of parameters to predict drug concentration profiles for any dosage. Trial-and-error fitting for the 100 and 250 mg/kg dose provided a small range of prior parameter values.

3.3.2 Markov Chain Monte Carlo Simulation for Parameter Prediction

The estimations from the forward simulation were used as the priors in the Markov chain Monte Carlo (MCMC) simulation for the capreomycin PBPK model. The priors were chosen in this way because no comparable data were available about the pharmacokinetics of capreomycin. In traditional pharmacokinetic analysis, the reported values are based solely on serum data and do not differentiate the organs or means of

excretion/absorption. For example, LeConte *et al.* reports the half-life ($t_{1/2}$) and the area under the curve (AUC) to characterize the pharmacokinetics of the drug [19]. While parallels are often made between capreomycin and aminoglycosides, this was not possible for priors due to the disparity between the model parameters and traditional pharmacokinetic parameters.

The distribution chosen for the priors was a truncated normal distribution, which required the following inputs: the mean, standard deviation, minimum, and maximum value. The prior means were estimated as described earlier, while the standard deviation was estimated as ±25% of the respective means. The minimum and maximum values were chosen for truncation were chosen to keep values within biologically-plausible ranges [51].

The two methods of fitting the data, extrapolation-maximum and experimental-maximum (chapter 3.2.2) were based on different priors listed in Tables 6 and 7.

Table 6: Prior values- experimental maximum fitted model

Parameter	Mean	Standard Deviation	Min	Max
K_m (ng/kg)	$6.0*10^8$	$1.5*10^8$	$3.0*10^8$	$9.0*10^8$
V_{max} (ng/h)	$1.0*10^6$	$0.25*10^6$	$0.1*10^6$	$1.75*10^6$
CLR (kg/h)	0.009	0.00225	0.005	0.02
CLRD (kg/h)	$2.75*10^{-6}$	$0.688*10^{-6}$	$1.5*10^{-6}$	$5.0*10^{-6}$
CLHC (L/hr/kg)	3.5	0.875	2.0	5.0
SC_Decay (h^{-1})	1.75	0.44	0.25	3.25

Table 7: Prior values- extrapolated maximum fitted model

Parameter	Mean	Standard Deviation	Min	Max
K_m (ng/kg)	$4.5*10^8$	$1.125*10^8$	$1.0*10^8$	$8.0*10^8$
V_{max} (ng/h)	$0.6*10^6$	$0.15*10^6$	$0.1*10^6$	$1.1*10^6$
CLR (kg/h)	0.004	0.001	0.0009	0.007
CLRD (kg/h)	$3.3*10^{-6}$	$.825*10^{-6}$	$1.0*10^{-6}$	$5.6*10^{-6}$
CLHC (L/hr/kg)	3.0	0.75	1.0	5.0
SC_Decay (h^{-1})	15.0	4.0	8.0	22.0

The prior distributions for the parameters and prior distributions for the variances were separated because the prior knowledge is independent from the variance. The prior distribution for the variance was expressed as an inverse gamma distribution [51], [63], which is defined with a shape parameter and scale parameter in *MCSim*. The shape parameter is equal to three, indicating a large degree of uncertainty, and the scale parameter is equal to the two times the variance, or two times the squared standard deviation.

All of the parameters were simultaneously adjusted for 10,000 iterations in the MCMC simulation, since correlation between the parameters was unknown. Setting one parameter to a single value and then adjusting the other parameters does not allow the simulation to account for potential covariance [51].

Each MCMC simulation has two hierarchical levels: the population level, representing the pool of all the mice, and the individual level, where the unique body weight, organ weights, and concentration data for each mouse are inputs. Using input from each individual mouse is desirable because it takes more variability into account [51]. First, the level containing data for each individual mouse will predict parameters for each

individual. The goal of PBPK modeling is to estimate a parameter distribution to apply to entire population rather than a single individual [64].

The MCMC simulation was run for 10,000 iterations, but only the last 5000 were used in analyses to predict the posterior values; the first 5000 iterations were considered to be the "burn in" period.

A summary of the data posterior mean values and their corresponding standard deviation is as follows in Table 8.

Table 8: MCMC Simulation posterior PK parameter predictions

	Experimental Fit		Extrapolated Fit	
Parameter	**Mean**	**Standard Deviation**	**Mean**	**Standard Deviation**
K_m (ng/kg)	$5.55*10^{8}$	$0.468*10^{8}$	$4.63*10^{8}$	$0.412*10^{8}$
V_{max} (ng/h)	$1.04*10^{6}$	$0.0839*10^{6}$	$5.92*10^{5}$	$0.453*10^{5}$
CLR (kg/h)	0.0120	0.00106	0.00535	0.000456
CLRD (kg/h)	$3.47*10^{-6}$	$0.25*10^{-6}$	$3.25*10^{-6}$	$0.348*10^{-6}$
CLHC (L/hr/kg)	3.97	0.274	4.32	0.262
SC_Decay (h^{-1})	0.902	0.164	19.1	1.22

The major disparity between the two fitting methodologies is the SC_Decay value, which reflects how fast the drug is entering the blood stream and the maximum blood concentration achieved.

To assess the MCMC results, the posterior parameters were input in a forward model to predict organ concentrations and compared to the experimental data. The root mean square deviation was calculated between the experimental data and the forward model concentration values to assess the accuracy of the predictions.

$$RMSD = \sqrt{\frac{\sum_{i=1}^{n}(x_{1,i} - x_{2,i})^2}{n}}$$

$$NRMSD = \frac{RMSD}{x_{\max} - x_{\min}}$$

3.3.3 Set Points Simulation for Concentration Prediction Ranges

Using the final 1000 iterations of the MCMC simulation, the posterior parameter values were randomized and then run in a set points simulation. The simulation runs multiple forward simulations with the randomized parameters to show the range of possible organ concentration predictions.

3.4 Comparison to Human Data

There is little published literature with human clinical data following capreomycin treatment. H.R. Black *et al.* published two papers including human clinical data in 1963 (no standard deviation reported) and 1966 as seen in Table 9 and 10. The serum concentration units as *ng/mg* is equivalent to the units as *μg/mL* as described in Chapter 3.1.2.

Table 9: Human experimental data following a 1 g dose (Black 1963).

Time (h)	Serum Concentration (ng/mg)
0.5	19.2
1.0	28.5
2.0	27.6
4.0	20.2
6.0	8.8
8.0	5.4

Table 10: Human experimental data following a 1 g dose (Black 1966).

Time (h)	Serum Concentration (ng/mg)	Standard Deviation
1.0	29.14	11.99
2.0	32.7	8.27
4.0	19.83	5.97
6.0	12.14	3.91
12.0	3.16	2.76
24.0	0.945	0.14

Based on this limited data, the predicted pharmacokinetic parameters were used in a forward simulation to compare the scaled-to-human model output to human clinical data. The human-scaled model is shown in Appendix XXVI.

Chapter 4: Results

4.1 Experimental Mouse Data

4.1.1 Physiological Parameters from Dosing, Sacrifice, and Organ Collection

Prior to dosing, each mouse was weighed. The average mouse weight was 18.69 ± 0.41 g. After the mouse was sacrificed, organs were removed and placed in pre-weighed vials, then reweighed. The difference was calculated to determine the organ weight. Table 11 summarizes the organ weights. For the organ weight and body weight of each individual mouse, see Appendices I and II, corresponding to the mice for the 100 mg/kg dosing and the 250 mg/kg dosing.

Table 11: Average organ weight for experimental mice.

100 mg/kg mice (mg)			250 mg/kg mice (mg)			All mice (mg)	
	Mean	**S.D**		**Mean**	**S.D.**		**Mean**
Spleen	68.91	8.04	**Spleen**	70.46	8.34	**Spleen**	69.69
Liver	933.54	86.17	**Liver**	970.63	82.24	**Liver**	952.08
Kidneys	261.83	19.93	**Kidneys**	260.29	14.55	**Kidneys**	261.06
Lungs	170.79	17.96	**Lungs**	156.50	16.65	**Lungs**	163.65

4.1.2 Concentration Data from Analysis of Tissues and Serum

The summary data, means and standard deviation for the kidney, serum, lung, liver, and spleen are provided in tabular and graphical form below. For all individual concentration data, refer to Appendix III and IV (100 and 250 mg/kg dosed mice).

Table 12: Mean capreomycin concentration and standard deviation in the kidney

Kidney (ng/mg)				
Time	**100 dose**	**STDEV**	**250 dose**	**STDEV**
0	0	0	0	0
0.5	111.28	19.40	218.00	7.00
1	119.80	22.44	248.75	53.27
2	187.25	20.27	342.00	9.17
6	181.75	21.85	242.25	46.19
20	127.00	14.63	149.50	49.08

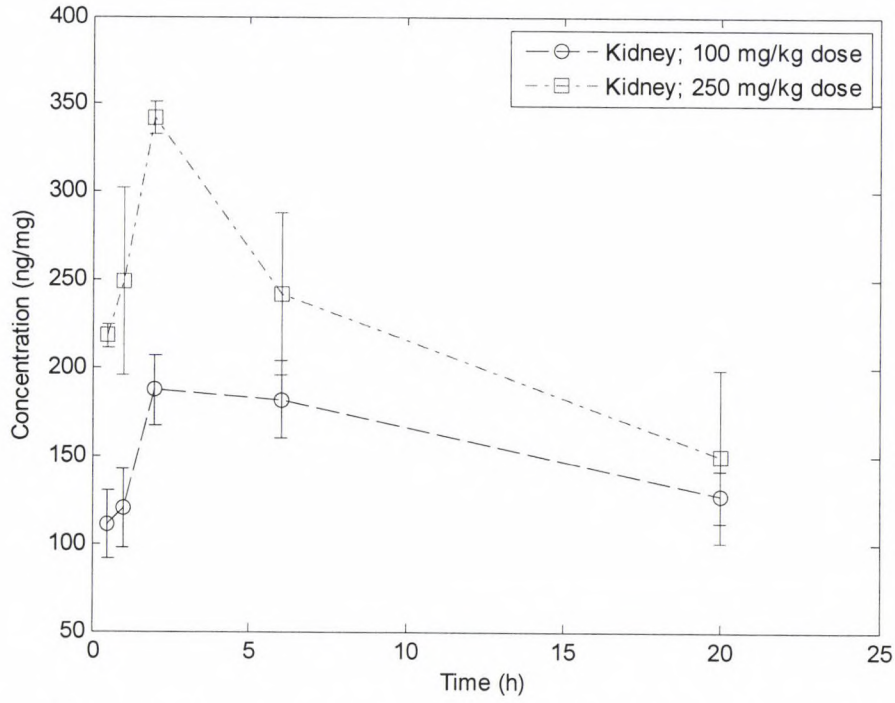

Figure 22: Average capreomycin concentration (with standard deviation) in the mouse kidney following dosing. All data points are based on four mice.

Table 13: Mean capreomycin concentration and standard deviation in the serum

Serum	*(ng/mg)**			
Time	**100 dose**	**STDEV**	**250 dose**	**STDEV**
0	0	0	0	0
0.5	55.87	11.19	168.33	18.50
1	34.35	9.18	86.83	32.11
2	6.94	3.81	12.43	3.96

* The serum concentration units as *ng/mg* is equivalent to the units as $\mu g/mL$ as described in Chapter 3.1.2.

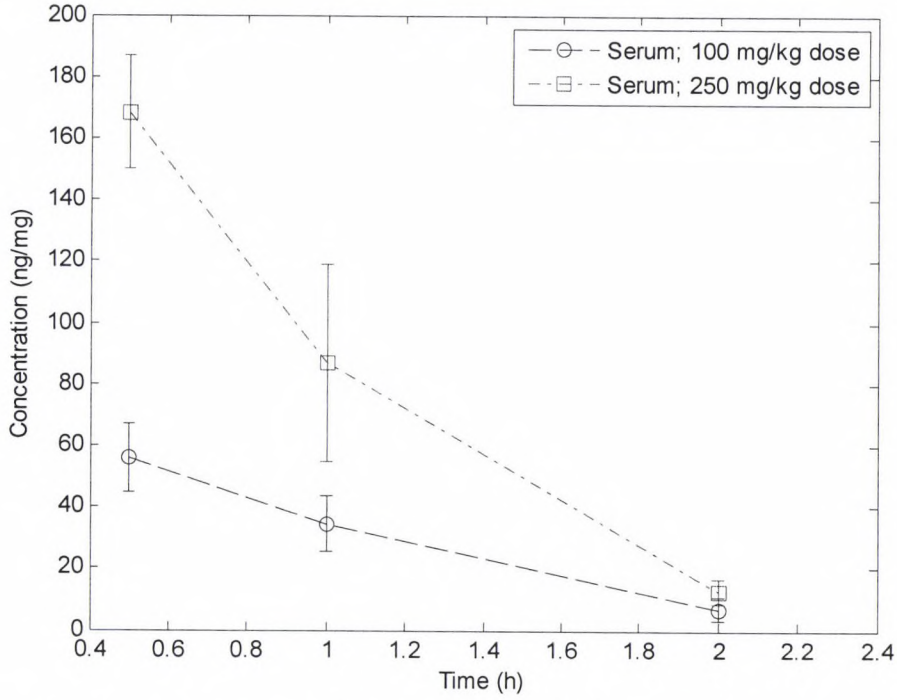

Figure 23: Average capreomycin concentration (with standard deviation) in the mouse serum following dosing. All data points are based on four mice.

Table 14: Mean capreomycin concentration and standard deviation in the lung

Lung	*(ng/mg)*			
Time	**100 dose**	**STDEV**	**250 dose**	**STDEV**
0	0	0	0	0
0.5	46.88	11.30	96.93	5.66
1	21.73	8.37	49.93	8.93
2	11.95	3.08	12.70	2.26
6	10.00*	0.00	10.50*	0.00

*Based on n=1 mouse.

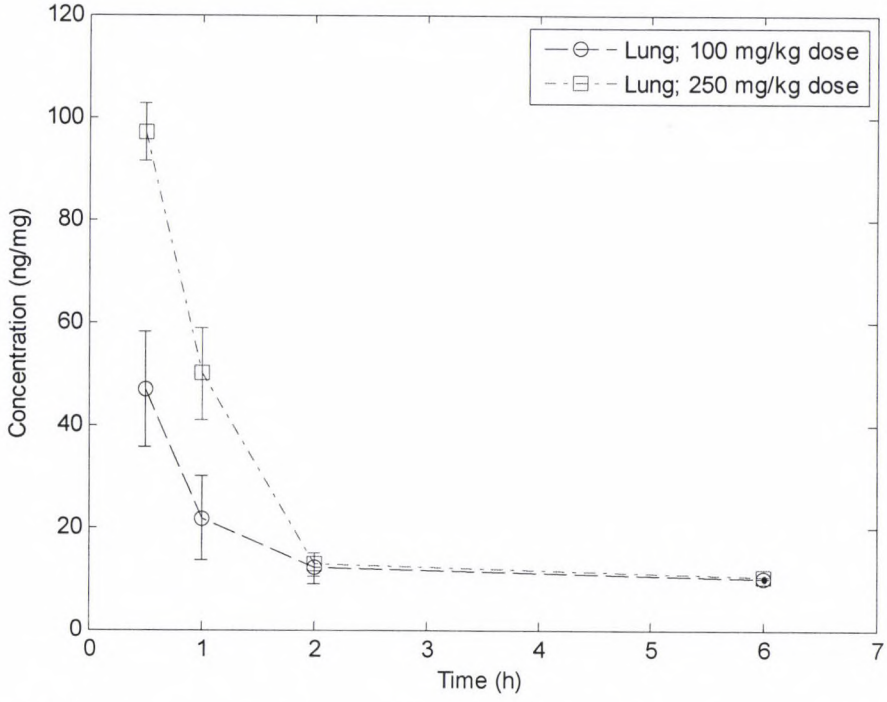

Figure 24: Average capreomycin concentration (with standard deviation) in the mouse lung following dosing. All data points are based on four mice, except both of the 6 hour time points represent data from n=1 mouse subject.

Table 15: Mean capreomycin concentration and standard deviation in the liver

Liver	*(ng/mg)*			
Time	**100 dose**	**STDEV**	**250 dose**	**STDEV**
0	0	0	0	0
0.5	13.95	2.29	26.17	1.40
1	10.40*	0.00	19.10	4.01

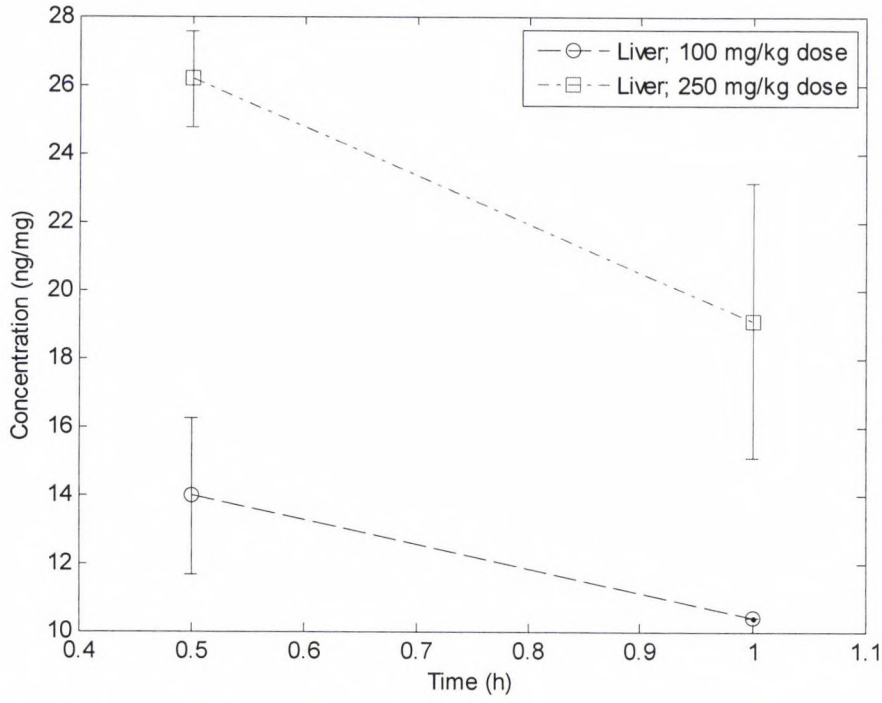

Figure 25: Average capreomycin concentration (with standard deviation) in the mouse liver following dosing. All data points are based on four mice, except the 100mg/kg dose at 1 hour represents data from only one mouse.

Table 16: Mean capreomycin concentration and standard deviation in the spleen

Spleen	*(ng/mg)*			
Time	**100 dose**	**STDEV**	**250 dose**	**STDEV**
0	0	0	0	0
0.5	13.53	2.62	27.10	5.35
1	-	-	15.23	1.99

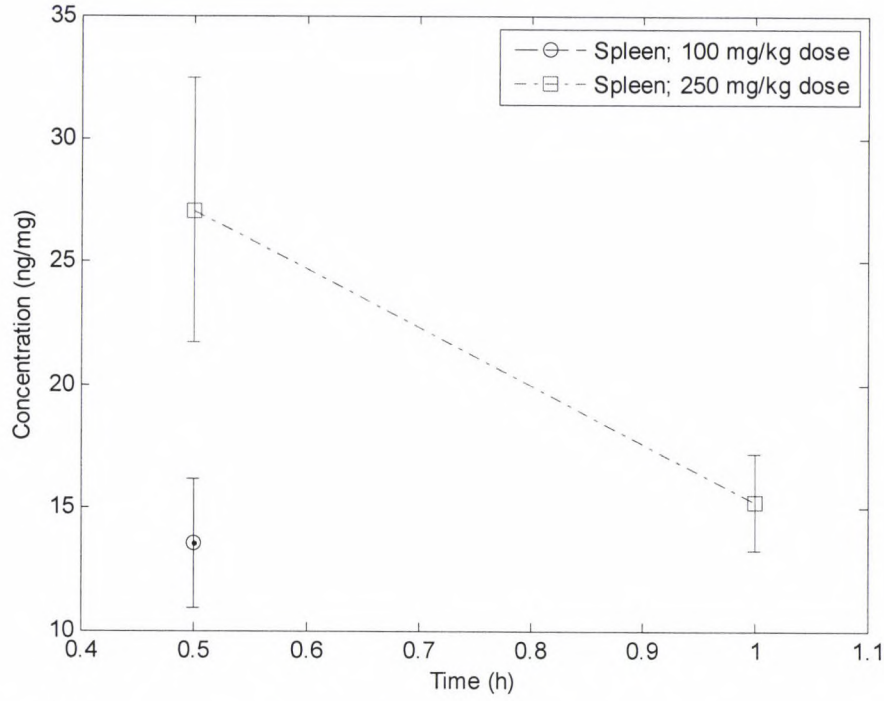

Figure 26: Average capreomycin concentration (with standard deviation) in the mouse spleen following dosing.

4.1.3 Traditional Pharmacokinetic Values

The concentration data results were analyzed to find the serum half-life and the area under the curve (AUC) for each harvested organ. In order to compare the data to literature values, the same methods were implemented that were used in the LeConte *et al.* paper [19].

To find the half-life ($t_{1/2}$), the experimental serum concentration curve was fit to an exponential regression function from 0.5 to 2 hours. The 100 mg/kg dose data exponential fit is seen in equation 4 and the 250 mg/kg dose data fit is seen in equation 5. The variable y represents the concentration and the variable x represents the time.

Equation 4: 100 mg/kg dose serum concentration exponential fit

$$y = 124.3e^{-1.4x}$$

Equation 5: 250 mg/kg dose serum concentration exponential fit

$$y = 444.81e^{-1.8x}$$

The half-life was calculated when y was equal to 0.5, indicating the drug concentration had been reduced by half.

Table 17: Half-life comparison

	Experimental (ng*h/mg)		LeConte Lit. (ng*h/mg)	
	100 mg/kg dose	250 mg/kg dose	120 mg/kg free	120 mg/kg encapsulated
t1/2 (h)	0.49	0.39	0.18	0.40

The trapezoidal rule method was used to find the approximate integral (area under the curve) between each set of data points:

$$\int_a^b f(x)dx \approx (b-a)\cdot\frac{f(a)+f(b)}{2}$$

The variables a and b represent the time and the function of each represent the concentration at the corresponding time point. The sum of the trapezoidal integrals from zero to six hours is the area under the curve.

Table 18: Area under the curve calculated via the trapezoidal rule method from 0-6 hours for all harvested organs compared to LeConte *et al.* literature [19]. All data collected from mice.

	Experimental (ng*h/mg)		LeConte *et al.* (ng*h/mg)	
Organ	100 mg/kg dose	250 mg/kg dose	120 mg/kg free	120 mg/kg encapsulated
Kidney	977.1	1635	982.4	1574
Serum	57.16	155.5	34	50.4
Spleen	6.76	17.36	184	459.7
Lung	69.6	117	59.7	125.7
Liver	9.58	17.86	-	-

The half-life calculated from the experimental data is greater than the selected literature value. This is expected because the LeConte *et al.* data was gathered after an intravenous dose whereas the experimental data was following a subcutaneous dose. An intravenous bolus has a much more rapid entry into the blood supply than the subcutaneous dose.

In evaluating the AUC values, the 100 mg/kg dose experimental results and the 120 mg/kg free capreomycin (non-encapsulated) dose literature results are compared. The kidney and lung AUC values are similar, whereas the serum value is higher in the experimental data and the spleen AUC is higher for the LeConte *et al.* data. The drug enters the serum first and therefore the difference in dosing method might affect the serum AUC. For the spleen, the AUC discrepancy is large and is likely due to the successful collection of only one concentration time point for the experimental data. The LeConte data records the spleen concentration as increasing up until the last collected data point at six hours. Additionally, the mice in the LeConte *et al.* study were infected with *Mycobacterium avium* and infections cause spleen enlargement and thus more blood flow and capreomycin to the organ.

4.2 Forward Simulation

Since there were no data available on the parameter values prior to the simulation, the data were used to find approximate fits through trial and error. This was done via two methods described in Chapter 3.3.1, a fit to the experimental maximum and a fit to an extrapolated maximum based on an exponential regression.

4.2.1 Forward simulation- experimental maximum initial guess priors

Table 19: Prior values- experimental maximum fitted model

Parameter	100 mg/kg	250 mg/kg
K_m (ng/kg)	$7*10^8$	$7*10^8$
V_{max} (ng/h)	$1.2*10^6$	$9*10^5$
CLR (kg/h)	0.006	0.01
CLRD (kg/h)	$2*10^{-6}$	$3.25*10^{-6}$
CLHC (L/hr/kg)	4.0	3.0
SC_Decay (h^{-1})	1.5	2.0

The model prediction with these prior parameters can be seen in Appendix VII and VIII for the 100 mg/kg and 250 mg/kg data. It is a rough estimate and these prior values were used in the MCMC simulation, which updated the parameters with posterior values based on 10,000 iterations.

4.2.2 Forward Simulation- Extrapolated Maximum Initial Guess Priors

Table 20: Prior values- extrapolation fitted model

Parameter	100 mg/kg	250 mg/kg
K_m (ng/kg)	$5*10^8$	$4*10^8$
V_{max} (ng/h)	$0.7*10^6$	$0.5*10^6$
CLR (kg/h)	0.003	0.005
CLRD (kg/h)	$2*10^{-6}$	$4*10^{-6}$
CLHC (L/hr/kg)	3.0	3.0
SC_Decay (h^{-1})	9.7	20.0

The model prediction with these prior parameters can be seen in Appendix IX and X for the 100 mg/kg and 250 mg/kg data. It is a rough estimate and these prior values were used in the MCMC simulation, which updated the parameters with posterior values based on 10,000 iterations.

4.3 MCMC Simulation

4.3.1 Posterior Parameters

The results of the MCMC simulation for the experimental maximum fit are summarized in the table below alongside the posterior parameters for an extrapolated fit. Sample graphs for the K_m prediction of both fit methods are also shown. The converging predictions for the experimental maximum fit can be seen in Appendix XII. The converging predictions for the extrapolated maximum fit can be seen in Appendix XIII.

Table 21: MCMC Simulation posterior PK parameter predictions

	Experimental Fit		Extrapolated Fit	
Parameter	Mean	Standard Deviation	Mean	Standard Deviation
K_m (ng/kg)	$5.55*10^8$	$0.468*10^8$	$4.63*10^8$	$0.412*10^8$
V_{max} (ng/h)	$1.04*10^6$	$0.0839*10^6$	$5.92*10^5$	$0.453*10^5$
CLR (kg/h)	0.0120	0.00106	0.00535	0.000456
CLRD (kg/h)	$3.47*10^{-6}$	$0.25*10^{-6}$	$3.25*10^{-6}$	$0.348*10^{-6}$
CLHC (L/hr/kg)	3.97	0.274	4.32	0.262
SC_Decay (h^{-1})	0.902	0.164	19.1	1.22

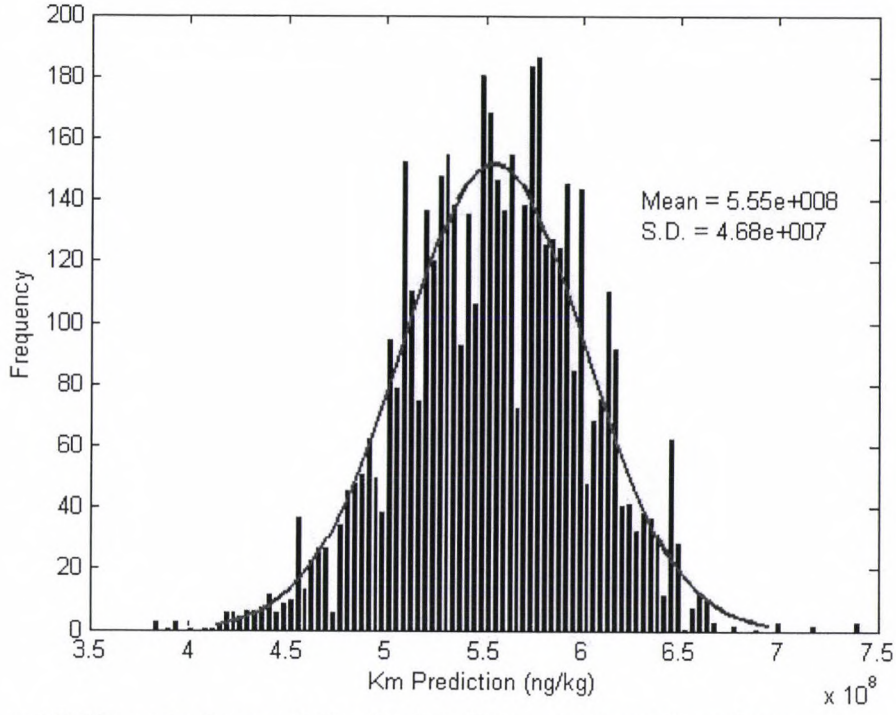

Figure 27: Km posterior prediction for data fit to experimental maximum

The results of the MCMC simulation for the extrapolation method:

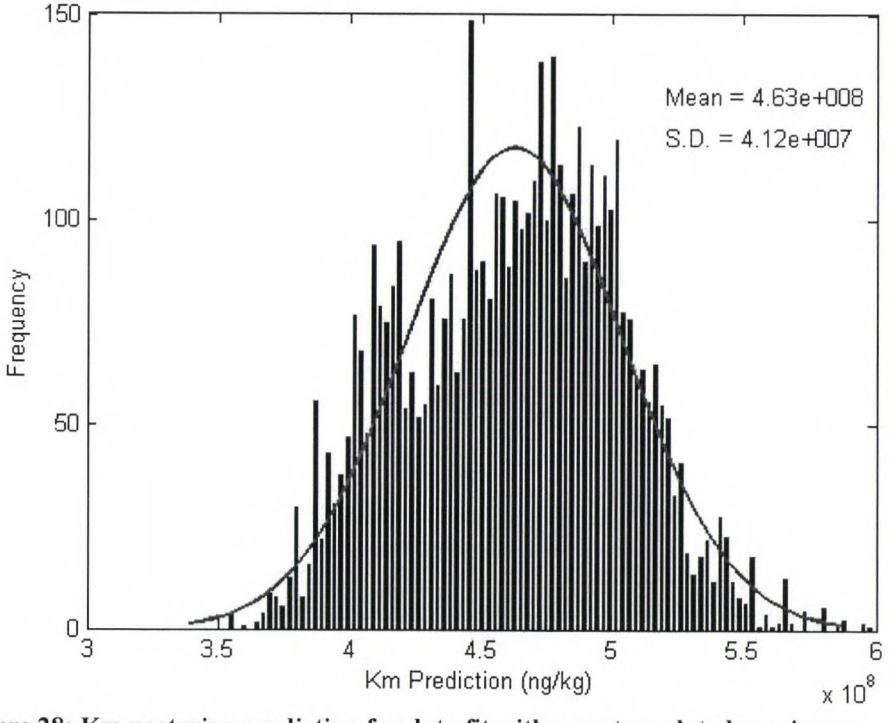

Figure 28: Km posterior prediction for data fit with an extrapolated maximum.

The key disparity is the SC_Decay value, which reflects how fast the drug is entering the blood stream and the maximum blood concentration achieved.

4.3.2 Posterior Parameters in a Forward Simulation

For comparison to the experimental data, the mean posterior value for each parameter was input into a forward simulation and the output, predicted tissue concentration, was plotted against experimental tissue concentrations. The forward simulation file can be found in Appendix VI. For the experimental maximum fit parameters, the comparison to the 100 mg/kg dose can be seen in Appendix XIV and the comparison to the 250 mg/kg dose can be seen in Appendix XV. For the extrapolated maximum parameters, the comparison to the 100 mg/kg dose can be seen in Appendix XVI and the comparison to the 250 mg/kg dose can Appendix XVII.

To assess the model prediction accuracy, the predicted concentrations were compared to the experimental concentrations via root mean square deviation (RMSD) and normalized root mean square deviation (NRMSD).

$$RMSD = \sqrt{\frac{\sum_{i=1}^{n}(x_{1,i} - x_{2,i})^2}{n}}$$

$$NRMSD = \frac{RMSD}{x_{\max} - x_{\min}}$$

For the experimental concentrations following the 100 mg/kg dose, there were five comparable time/concentration points for the kidney, the serum and lung had three

comparable points, the liver had two, and the spleen had just one comparable point. Due to only one experimental time point for the spleen concentration, (other time points had a concentration below the limit of quantification), the NRMSD could not be calculated.

For the experimental concentrations following the 250 mg/kg dose, all of the experimental organ concentrations had the same number of data points except the spleen, which had two comparable experimental data points in this case.

Table 22: RMSD and NRMSD for experimental organ concentration values compared to concentration predictions based on parameters fit to the experimental maximums.

	Experimental Maximum Fit			
	100 mg/kg dose		250 mg/kg dose	
	RMSD	NRMSD	RMSD	NRMSD
Kidney	43.3	56.9%	78.8	40.9%
Serum	33.8	69.0%	97.3	62.4%
Liver	38.0	1071%	102	1450%
Lung	32.0	91.5%	84.8	100.6%
Spleen	53.8	n/a	103.9	875%

* n=1

Table 23: RMSD and NRMSD for experimental organ concentration values compared to concentration predictions based on parameters fit to the extrapolated maximums.

	Extrapolated Maximum Fit			
	100 mg/kg dose		250 mg/kg dose	
	RMSD	NRMSD	RMSD	NRMSD
Kidney	50.6	66.7%	36.0	18.72%
Serum	58.2	119%	45.8	29.4%
Liver	69.3	195%	17.5	247%
Lung	57.0	163%	20.5	24.3%
Spleen	99.3	n/a	27.3	230%

* n=1

For the 100 mg/kg dose, the concentrations predicted using the experimental maximum fit parameters all had lower root mean square deviations and normal root mean square deviations from the complete experimental data than the extrapolated maximum fit. This

indicates less deviation from the experimental mean at all the time points measured. However in the case of the 250 mg/kg dose, the predicted concentrations using the extrapolated maximum fit parameters for all but the liver have a lower RMSD and NRMSD.

4.4 Set Points Simulation for Prediction Scatter

Using the mean posterior parameter values in a forward model is a simplistic way to look at the spread of the posterior prediction ranges. As can be seen in the prediction figures, there is a range of possible inputs. The simulation runs 1000 iterations, selecting a randomized parameter from each of the six posterior parameter distributions (K_m, V_{max}, etc.). Rather than plot all the 1000 iteration outputs, the maximum and minimum boundaries (i.e., the solution *envelope*) are plotted. Using the posterior predicted distributions for all six parameters, it is possible to get an organ concentration profile anywhere within these bounds.

4.4.1 Set Points Simulation with Posterior Prediction (Experimental Maximum Fit)

Figures 29 and 30 show the maximum and minimum possible model predictions for kidney and serum based on the posterior parameter means and standard deviations. The figures are for the 100 mg/kg dose data and the parameters are based on fitting to the experimental maximum. All of the organ concentration plots for the 100 mg/kg dose can be found in Appendix XXI. The serum concentration units as *ng/mg* is equivalent to the units as *μg/mL* as described in Chapter 3.1.2.

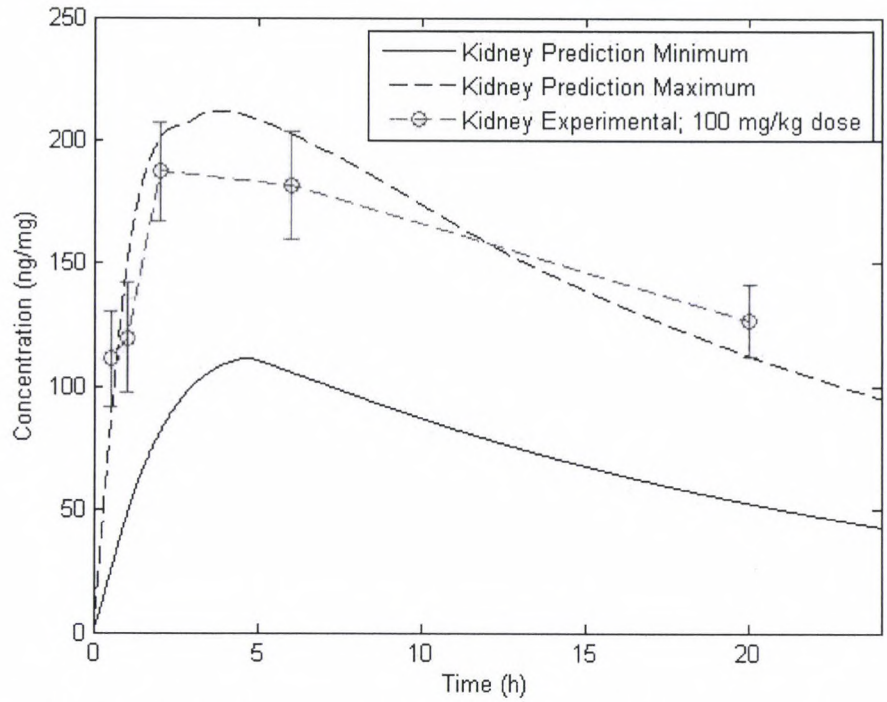

Figure 29: Set Points kidney maximum and minimum model bounds (experimental maximum fit).

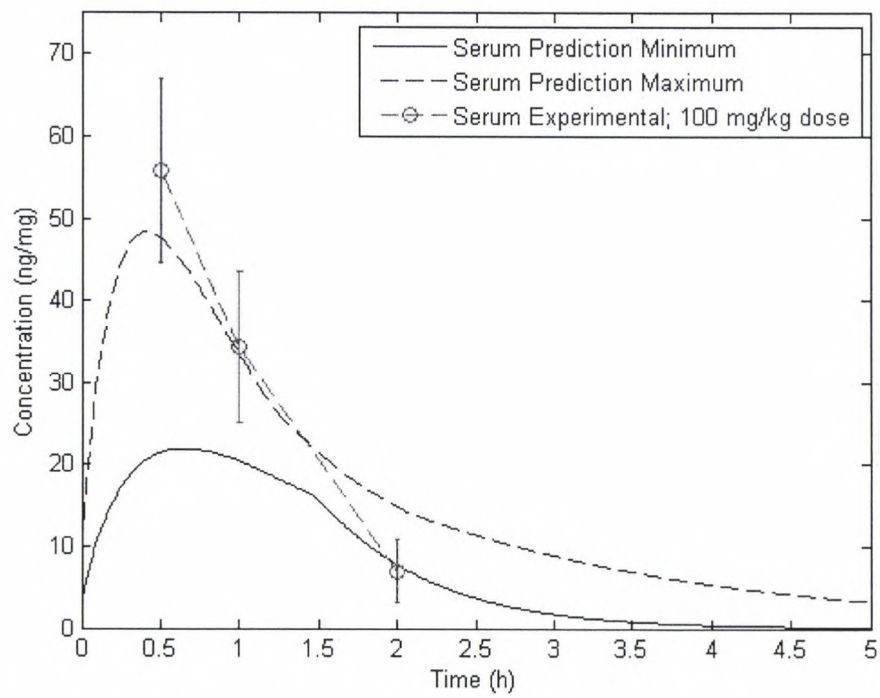

Figure 30: Set points serum maximum and minimum model bounds (experimental maximum fit).

The results for the 250 mg/kg dose data and the parameters based on the experimental maximum can be found in Appendix XXII.

4.4.2 Set Points Simulation with Posterior Prediction (Extrapolated Maximum Fit)

The same set points simulation was done for the data with the extrapolated fit as seen in the following example Figures 31 and 32.

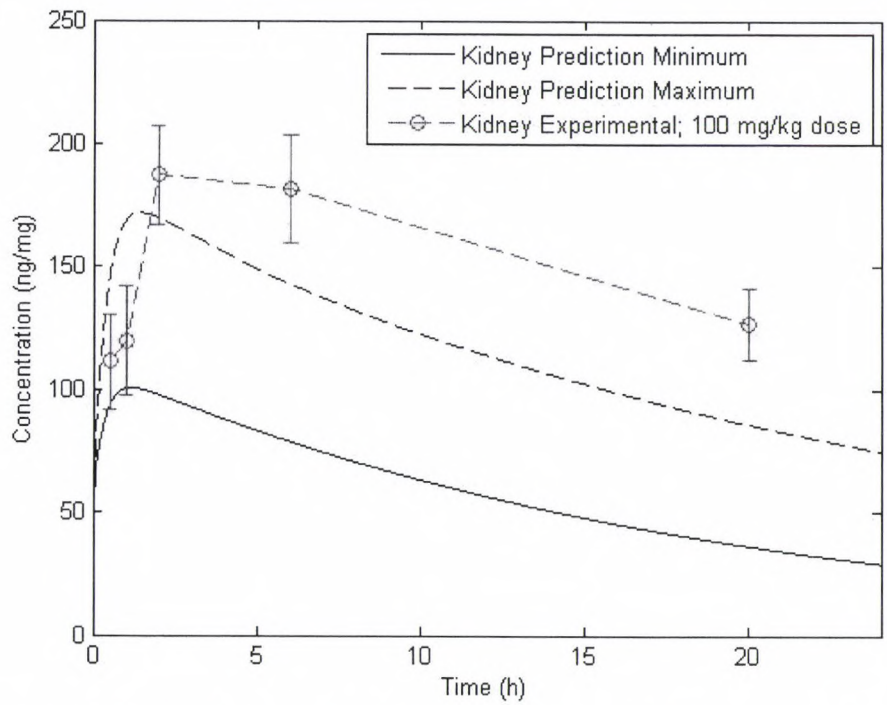

Figure 31: Set points kidney maximum and minimum model bounds (extrapolated maximum fit).

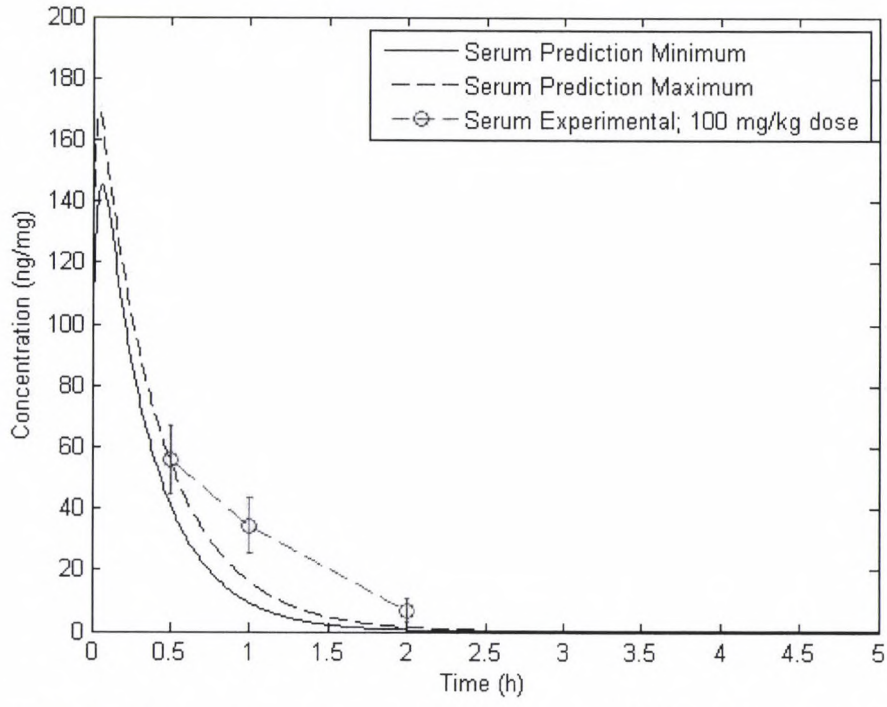

Figure 32: Set points serum maximum and minimum model bounds (extrapolated maximum fit).

The results for all organs following the 100 mg/kg doses and for the 250 mg/kg dose are seen in Appendices XXIII and XXIV.

Visual inspection of the experimental data plotted with the maximum and minimum boundaries shows that the parameters found by fitting the model to the experimental maximum results in wider potential concentration predictions. This is true for both dose levels, and more evident in the serum and all organs but the kidney.

The set points evaluation is in agreement with the lower RMSD and NRMSD between the 100 mg/kg dose data and the concentration predictions from the mean parameters fit to the experimental maximum. When the maximum and minimum bounds are plotted for

predictions based on the experimentally-maximum fit parameters, all of the 100 mg/kg concentration data for every organ lies within the boundaries when the standard deviation is included. In conclusion, the 100 mg/kg concentration data is well represented with the experimental-maximum fit parameters.

Conversely, the RMSD and NRMSD clearly suggest that the organ concentrations following the 250 mg/kg dose show a better fit with the predicted concentrations based on the extrapolated maximum fit *mean* parameters. However, when the parameter prediction ranges are compared to the data, both parameter set's maximum and minimum bounds encompass one to two experimental data points per organ. Neither parameter set shows a clear advantage when the concentration prediction ranges are plotted rather than the concentration based on mean parameter values.

4.5 Comparison to Human Data

Using a model that was scaled-up to average male human physiology [57] the posterior parameter means were used in a forward model to compare the model output to the male human data from Black *et al.*[13], [17]. The renal uptake of gentamicin, an aminoglycoside similar to capreomycin (Chapter 2.2.1) exhibits the same pathway in mice and humans [28].

In Figure 33, the human literature data is compared to the model using posterior parameters fit to the experimental maximum. The 1963 data only provided a mean, with

no standard deviation. This is a specialized population of healthy, average-weight males in the 1960s.

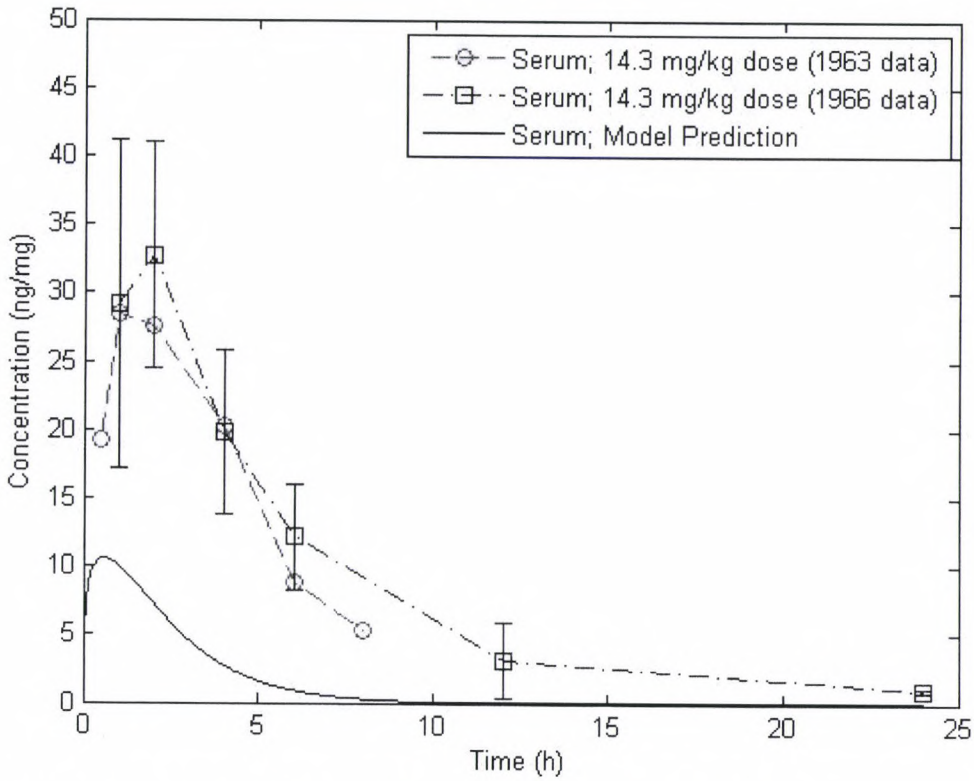

Figure 33: Human clinical data compared to human-scaled model prediction (based on parameters found by fitting to the experimental maximums).

In Figure 34, the human data is compared to the model using posterior parameters fit to the extrapolated maximum.

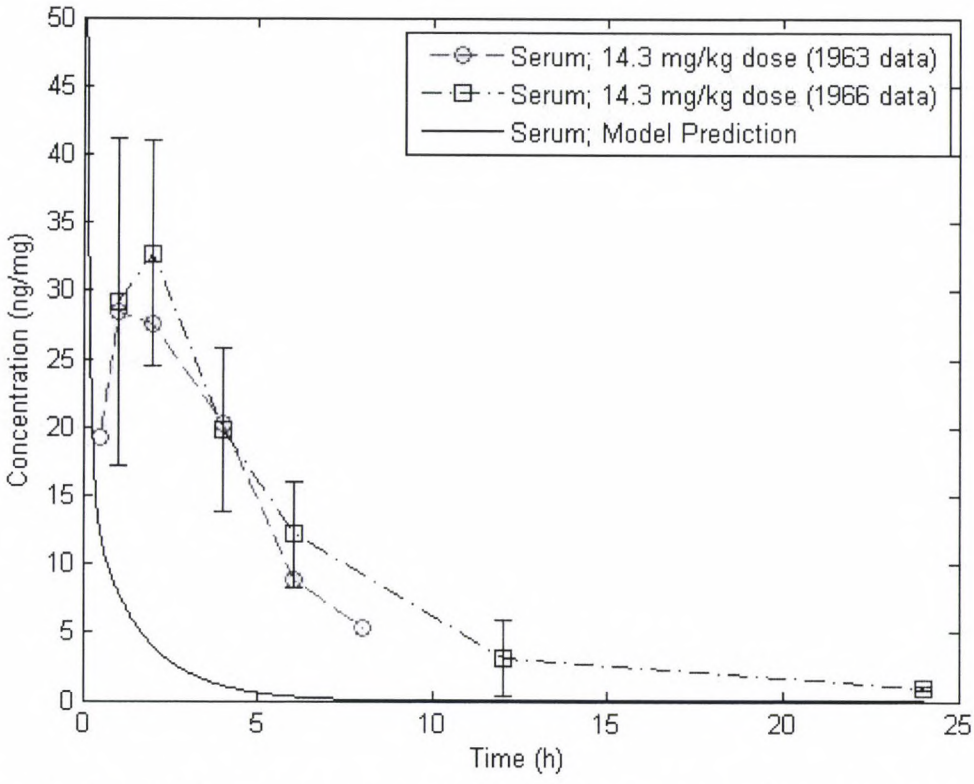

Figure 34: Human clinical data compared to human-scaled model prediction (based on parameters found by fitting to the mouse data extrapolated maximums).

The human-scaled model predictions do not give an accurate indication of the experimental data.

Table 24: RMSD and NRMSD between human clinical data compared to human-scaled model prediction (based on parameters found by fitting to the mouse data experimental maximums).

	Experimental Max Fit Parameters			
Human	Black *et al.* 1963		Black *et al.* 1966	
Measure	RMSD	NRMSD	RMSD	NRMSD
Serum	14.3	61.7%	15.5	48.7%

Table 25: RMSD and NRMSD between human clinical data compared to human-scaled model prediction (based on parameters found by fitting to the mouse data extrapolated maximums).

	Extrapolated Max Fit Parameters			
Human	Black *et al.* 1963		Black *et al.* 1966	
Measure	RMSD	NRMSD	RMSD	NRMSD
Serum	15.8	68.2%	17.2	54.1%

Both sets of parameters result in concentration predictions with large RMSD and NRMSD values, indicating that the model deviates greatly from the experimental data.

To understand potential sources of this discrepancy a basic pharmacokinetic parameter, area under the curve (AUC), of the human serum data versus the experimental data were compared. The AUC was calculated using the trapezoid method (Chapters 2.3.1 and 4.1.3) for zero to two hours because that was the extent of the experimental serum data.

Table 26: Experimental serum AUC compared to Black *et al.* 1966 human serum AUC

	Experimental; mouse (ng*h/mg)		Black *et al.* 1966; human (ng*h/mg)
	100 mg/kg dose	250 mg/kg dose	14.3 mg/kg dose
Serum	57.16	155.5	45.49

The area under the curve for the 100 mg/kg dose for the mouse is similar in magnitude to the AUC for the 14.3 mg/kg dose to the human. The area under the curve is an indication of the drug exposure and the similar values indicate that while the dose concentrations are disparate, they result in the same level of exposure for each respective organism. Ultimately, the mouse clears capreomycin at a faster rate than humans do. Using the parameters developed from the experimental mouse data resulted in much lower serum concentrations due to the difference in clearance rates. In Chapter 3.3.1, the forward model simulations identified the kidney clearance parameter (CLR) as having a major impact on the serum concentration maximum. If CLR is decreased, as would be the case in humans having a slower drug clearance rate than mice, the serum maximum concentration is increased. Furthermore, any hepatic clearance (CLHC) affects the serum

concentration maximum in the same way: a decrease in clearance rate reflects in an increase in serum concentration. Lastly, the decay rate of the drug from the dose site to the bloodstream/serum (SC_Decay) was determined from mice receiving a subcutaneous dose whereas in the Black *et al.* studies, the humans received an intramuscular dose [17]. The intramuscular dose would reach the blood supply more rapidly than the subcutaneous dose and therefore entail a higher drug decay rate. By increasing the SC_Decay parameter, the serum maximum would also be increased.

The kidney is of primary interest because capreomycin can cause renal toxicity at doses of 60 to 120 mg/kg in mice [19]. As capreomycin is administered to humans several days a week for months and no continuous internal drug concentration can be measured for the kidney, the maximum tolerable kidney concentration is not known.

Chapter 5: Model Utility in Improving Drug Regimens

Treatment of tuberculosis faces obstacles such as length of chemotherapy, the number of drugs in a treatment regimen, increased drug resistance, and TB comorbidity with HIV. All of these factors lend to the urgent need to develop shorter, simpler, less toxic, and more effective TB chemotherapy drugs and regimens. Prior to 2000, few pharmaceutical companies were investing in TB research. By 2007, seven drugs led to clinical trials. However, even with a significant effort to make such advances, the length of drug trials is particularly long when treating TB because of a minimum of six months for phase three trials plus a year or more of follow-up [21].

By using a validated model, drugs of interest could be rapidly evaluated for initial recommendations thus reducing drug development time. Furthermore, models for several drugs could be analyzed simultaneously to foresee potential toxicity from drug-drug interaction. Using PBPK models as predictors would be economically and time efficient.

For the PBPK model developed for capreomycin, additional information is needed for an effective prediction. First, more experimental data should be collected from the mice at earlier time points. Additional time points are necessary to establish the true concentration maximums, and would also provide more data to fit the unknown pharmacokinetic parameters. Secondly, there are no published guidelines on toxic concentration levels or minimum effective concentrations (MIC). With known toxic

limits and MIC, a therapeutic range of doses could be predicted via modeling. As seen in Figure 35, while increasing the dose might continue to increase the efficacy of the drug, at some point the effects of nephrotoxicity will be too great a risk for doses. Note that since the limits of efficacy and toxicity are unknown, this is not a to-scale figure.

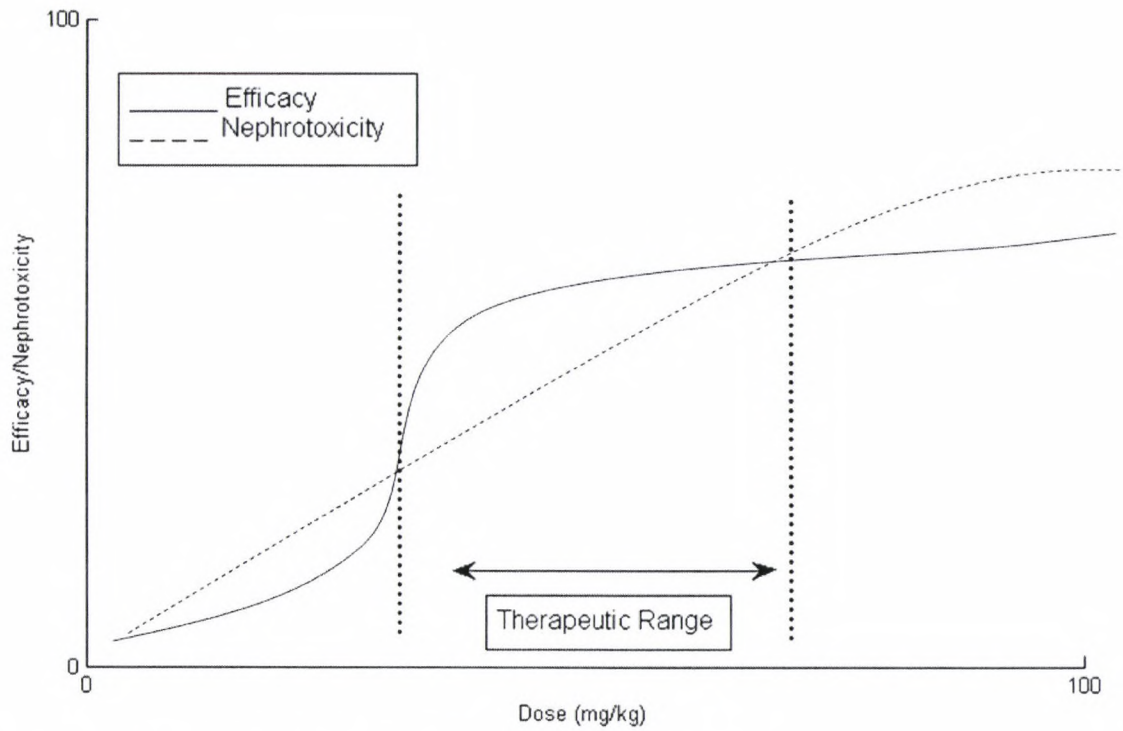

Figure 25: Efficacy of treatment in the lung versus toxic effects in the kidney.

To address issues of efficacy and toxicity, pharmacodynamic information must be included in the analyses. Pharmacodynamics describes what effects the drug has on the host and on the pathogen. These effects include not only the intrinsic mechanisms and modes of action, but also the impacts of physiological differences or changes, due to diseases like HIV, for example.

There are several differences between the human data used for comparison and the model assumptions. First, while the human model accounts for the differences in physiology, there is a great variety in human weight, age, sex, gender, and other factors that would influence the distribution of the drug. For example women are more likely to develop Bartter-like syndrome, which is characterized by increase excretion of essential ions like Na^+, K^+, Ca^{2+}, and Mg^+ [20].

In this human-scaled model, the average weight is assumed to be 70 kg and healthy. However, in the present-day United States many patients are obese, have a metabolic disorder such as diabetes mellitus, or both. These factors complicate treatment and effective dose recommendations [1]. Abroad, the comorbidity of HIV/AIDS greatly compromises the immune system and consequently increases the chances that the TB bacterium will cause an active infection. This is another population that may not be accurately represented in a model of a healthy adult [10]. Children or pregnant women are yet another set of special-case populations that would need different recommendations for treatment.

The utility of a PBPK model applicable to humans would be the ability to develop more individualized dosing [1]. This would ultimately result in safer and effective dosing for various populations.

Chapter 6: Conclusions

A PBPK model for the ADME of capreomycin in the mouse was developed and targeted experimentation was conducted to obtain appropriate concentration-time data. Using the model, a set of pharmacokinetic parameters were estimated based on the experimental data and accounting for variability and uncertainty. The model and parameters are anticipated to be useful in predicting the disposition of capreomycin in the mouse via various dosing regimens.

6.1 Areas for Future Work

The kidney concentration data was the most thorough of all organs collected but could be improved. Separating the kidney into the cortex and medulla prior to concentration analysis would enhance the understanding and prediction of the capreomycin accumulation and excretion. Secondly, since human kidneys cannot be analyzed, a potential experiment would be to collect urine samples from both species to deduce and compare clearance rates. Creatinine levels could also be recorded to determine toxicity limits.

While the kidney must be observed for signs of toxicity, the lung concentration is also important to understand the efficacy of capreomycin at different doses. In this study, the focus was to understand the kidney behavior and accumulation mechanisms. Reasons behind trends for the lung concentration need to be better understood as well because it is

the site of infection. Understanding the mechanisms responsible for lung concentrations could also lead to targeted treatments, which could reduce the TB chemotherapy time.

Since it is unclear where the true concentration maximum occurs, collecting concentration information at time points prior to 0.5 hours is recommended. Furthermore, the additional time points could lead to more accurate fitting and thus predicting.

The established mouse model provides useful insight to the kidney mechanisms and concentrations resulting from doses between 100 and 250 mg/kg. With additional concentration data and understanding of lung ADME, the model could be improved and potentially provide insight for individualized dosing recommendations.

Although the model is useful in making pharmacokinetic predictions in the mouse, the parameter values will need to be adjusted appropriately to be useful for estimating ADME in humans.

Works Cited

1. Hall, R.G., *Treatment of Active Pulmonary Tuberculosis in Adults: Current Standards and Recent Advances: Insights from the Society of Infectious Diseases Pharmacists.* Pharmacotherapy, 2009. **29**(12): p. 1468-1481.
2. *Global tuberculosis control - epidemiology, strategy, financing*. 2009, World Health Organization.
3. Grosset, J., *Mycobacterium tuberculosis in the Extracellular Compartment: an Underestimated Adversary.* Antimicrobial Agents and Chemotherapy, 2003. **47**(3): p. 833-836.
4. Kaufmann, S.H.E., *Protection against tuberculosis: cytokines, T cells, and macrophages.* Annals of the Rheumatic Diseases through the ages, 2002. **61**(Suppl II): p. ii54-ii58.
5. Russell, D.G., *Who puts the tubercle in tuberculosis?* Nat Rev Micro, 2007. **5**(1): p. 39-47.
6. Heifets, L., J. Simon, and V. Pham, *Capreomycin is active against non-replicating M. tuberculosis.* Annals of Clinical Microbiology and Antimicrobials, 2005. **4**(1): p. 6.
7. *Basic TB Facts*. Division of Tuberculosis Elimination 2009; Available from: http://www.cdc.gov/tb/topic/basics/default.htm.
8. *Treatment for Latent TB Infection (LTBI)*. Division of Tuberculosis Elimination 2009; Available from: http://www.cdc.gov/tb/topic/treatment/ltbi.htm.
9. *Treatment for TB Disease*. Division of Tuberculosis Elimination 2009; Available from: http://www.cdc.gov/tb/topic/treatment/tbdisease.htm.
10. Golden, M.P. and H.R. Vikram, *Extrapulmonary Tuberculosis: An Overview.* American Family Physician, 2005. **72**(9): p. 1761-1768.
11. *TB/HIV Facts 2009*, W.H. Organization, Editor. 2009.
12. Holdiness, M.R., *Clinical Pharmacokinetics of Antituberculosis Drugs.* Clinical Pharmacokinetics, 1984. **9**: p. 511-544.
13. *Capastat sulfate (Capreomycin sulfate) injection, powder, for solution* 2008.
14. *Capreomycin.* Tuberculosis, 2008. **88**(2): p. 89-91.
15. Fu, L.M. and T.M. Shinnick, *Genome-wide exploration of the drug action of capreomycin on Mycobacterium tuberculosis using Affymetrix oligonucleotide GeneChips.* Journal of Infection, 2007. **54**(3): p. 277-284.
16. Black, H.R., R.S. Griffith, and J.F. Brickler, *Preliminary Laboratory Studies with Capreomycin.* Antimicrobial Agents and Chemotherapy, 1963. **161**: p. 522-529.

17. Black, H.R., R.S. Griffith, and A.M. Peabody, *Absorption, excretion, and metabolism of capreomycin in normal and diseased states.* Annals New York Academy of Sciences, 1966. **135**(2): p. 974-982.
18. Hesling, C.M., *Treatment with capreomycin, with special reference to toxic effects.* Tubercle, 1969. **50**: p. 39-41.
19. LeConte, P., et al., *Pharmacokinetics, Toxicity, and Efficacy of Liposomal Capreomycin in Disseminated Mycobacterium avium Beige Mouse Model.* Antimicrobial Agents and Chemotherapy, 1994. **38**(12): p. 2695-2701.
20. Zietse, R., R. Zoutendijk, and E.J. Hoorn, *Fluid, electrolyte and acid–base disorders associated with antibiotic therapy.* Nature Reviews Nephrology, 2009. **5**(4): p. 193-202.
21. Ginsberg, A.M. and M. Spigelman, *Challenges in tuberculosis drug research and development.* Nature Medicine, 2007. **13**(3): p. 290-294.
22. CDC, *Update: Fatal and Severe Liver Injuries Associated With Rifampin and Pyrazinamide for Latent Tuberculosis Infection, and Revisions in American Thoracic Society/CDC Recommendations*, N.C.f.H. Division of Tuberculosis Elimination, STD, and TB Prevention, Editor. 2001.
23. Craig, W.A., J. Redington, and S.C. Ebert, *Pharmacodynamics of amikican in vitro and in mouse thigh and lung infections.* Journal of Antimicrobial Chemotherapy, 1991. **27**: p. 29-40.
24. Leggett, J.E., et al., *Comparitive Antibiotic Dose-Effect Relations at Several Dosing Intervals in Murine Pneumonitis and Thigh-Infection Models.* The Journal of Infectious Diseases, 1989. **159**(2): p. 281-292.
25. Honeybourne, D., *Antibiotic penetration into lung tissues.* Thorax, 1994. **49**(2): p. 104-106.
26. Pennington, J.E., *Penetration of Antibiotics into Respiratory Secretions.* Reviews of Infectious Diseases, 1981. **3**(1): p. 67-73.
27. Mingeot-Leclercq, M.-P. and P.M. Tulkens, *Aminoglycosides: Nephrotoxicity.* Antimicrobial Agents and Chemotherapy, 1999. **43**(5): p. 1003-1012.
28. Schmitz, C., *Megalin Deficiency Offers Protection from Renal Aminoglycoside Accumulation.* Journal of Biological Chemistry, 2001. **277**(1): p. 618-622.
29. Nagai, J. and M. Takano, *Molecular Aspects of Renal Handling of Aminoglycosides and Strategies for Preventing the Nephrotoxity.* Drug Metabolism Pharmacokinetics 2004. **19**(3): p. 159-170.
30. Luft, F.C. and S.A. Kleit, *Renal Parenchymal Accumulation of Aminoglycoside Antibiotics in Rats."* The Journal of Infectious Diseases, 1974. **130**(6): p. 656-670.
31. Muller, M.U.o.I.a.C., Department of Biological Sciences." *Bios 100 Lecture 21: The excretory system.* 2004.

32. Ward, D.T., *Aminoglycosides Increase Intracellular Calcium Levels and ERK Activity in Proximal Tubular OK Cells Expressing the Extracellular Calcium-Sensing Receptor.* Journal of the American Society of Nephrology, 2002. **13**(6): p. 1481-1489.
33. Christensen, E.I. and H. Birn, *Megalin and Cubilin: Multifunctional Endocytic Receptors.* Nature Reviews Molecular Cell Biology, 2004. **3**(4): p. 258-268.
34. Reasor, M., H. KL, and R. Ulrich, *Drug-induced phospholipidosis: issues and future directions.* Expert Opinion on Drug Safety, 2006. **5**(4): p. 567-583.
35. Gewies, A., *Introduction to Apoptosis*. 2003.
36. Ward, D. and D. Riccardi, *Renal physiology of the extracellular calcium-sensing receptor.* Pflugers Archiv: European Journal of Physiology, 2002. **445**(2): p. 169-176.
37. Hofer, A.M. and E.M. Brown, *Extracellular calcium sensing and signalling.* Nature Reviews Molecular Cell Biology, 2003. **4**: p. 530-538.
38. Ward, D.T., *Aminoglycosides Induce Acute Cell Signaling and Chronic Cell Death in Renal Cells that Express the Calcium-Sensing Receptor.* Journal of the American Society of Nephrology, 2005. **16**(5): p. 1236-1244.
39. *Gentamicin Sulfate*. 2007; Available from: http://dailymed.nlm.nih.gov/dailymed/fda/fdaDrugXsl.cfm?id=3672&type=display.
40. *Streptomycin injection, powder, lyophilized, for solution* 2006; Available from: http://dailymed.nlm.nih.gov/dailymed/fda/fdaDrugXsl.cfm?id=2187&type=display.
41. *Fanconi Syndrome*. Kidney and Urinary Tract Disorders, Tubular and Cystic Kidney Disorders 2006; Available from: http://www.merck.com/mmhe/sec11/ch146/ch146f.html.
42. Shin, S., *Hypokalemia Among Patients Receiving Treatment for Multidrug-Resistant Tuberculosis.* Chest, 2004. **125**(3): p. 974-980.
43. Holmes, A.M., C.M. Hesling, and T.M. Wilson, *Capreomycin-induced serum electrolyte abormalities.* Thorax 1970. **25**: p. 608-611.
44. Mehrotra, N., et al., *The role of pharmacokinetics and pharmacodynamics in phosphodiesterase-5 inhibitor therapyPharmacokinetics and pharmacodynamics in PD-5 inhibitor therapy.* International Journal of Impotence Research, 2007. **19**: p. 253-263.
45. Muller, M., et al., *Characterization of Peripheral-Compartment Kinetics of Antibiotics by In Vivo Microdialysis in Humans.* Antimicrobial Agents and Chemotherapy, 1996. **40**(12): p. 2703-2709.

46. Gerlowski, L. and R.K. Jain, *Physiologically Based Pharmacokinetic Modeling: Principles and Application.* Journal of Pharmaceutical Sciences, 1993. **72**(10): p. 1103-1125.
47. Theil, F.-P., et al., *Utility of physiologically based pharmacokinetic models to drug development and rational drug discovery candidate selection.* Toxicology Letters 2003. **138**: p. 29-49.
48. Hoang, K.-C.T., *Physiologically based pharmacokinetic models: mathematical fundamentals and simulation implementations.* Toxicology Letters, 1995. **79**(99-106).
49. Bois, F. *MCSim manual, version 5.3.0.* 2009 February 24, 2009 [cited 2009 October]; Available from: http://www.gnu.org/software/mcsim/mcsim.html.
50. Bois, F. *2. Overview* 2009; Available from: http://www.gnu.org/software/mcsim/mcsim.html#SEC4.
51. Bernillon, P. and F.Y. Bois, *Statistical Issues in Toxicokinetic Modeling: A Bayesian Perspective.* Environmental Health Perspectives, 2000. **108**: p. 888-893.
52. Gelman, A. and D.B. Rubin, *"Markov Chain Monte Carlo methods in biostatistics.* Statistical Methods in Medical Research, 1996. **5**(4): p. 339-355.
53. Bois, F. *2.2 Types of simulations* 2009; Available from: http://www.gnu.org/software/mcsim/mcsim.html#SEC4.
54. Yokley, K., et al., *Physiologically-Based Pharmacokinetic Modeling of Benzene in Humans: A Bayesian Approach.* Risk Analysis, 2006. **26**(4): p. 925-943.
55. Bois, F. *6. Running Simulations* 2009; Available from: http://www.gnu.org/software/mcsim/mcsim.html#SEC62.
56. Clewell, R. and H. Clewelliii, *Development and specification of physiologically based pharmacokinetic models for use in risk assessment.* Regulatory Toxicology and Pharmacology, 2008. **50**(1): p. 129-143.
57. Brown, R.P., et al., *Physiological parameter values for physiologically based pharmacokinetic models.* Toxicology and Industrial Health, 1997. **13**(4): p. 407-484.
58. Bastian, I. and R. Colebunders, *Treatment and Prevention of Multidrug-Resistant Tuberculosis.* Drugs, 1999. **58**(4): p. 633-661.
59. Luecke, R., et al., *Windows®® based general PBPK/PD modeling software.* Computers in Biology and Medicine, 2008. **38**(9): p. 962-978.
60. Dewoskin, R. and C. Thompson, *Renal clearance parameters for PBPK model analysis of early lifestage differences in the disposition of environmental toxicants.* Regulatory Toxicology and Pharmacology, 2008. **51**(1): p. 66-86.

61. Alonso, I.G., et al., *Non-linear tissue binding of amikacin in rats: the effect of renal impairment.* European Journal of Drug Metabolism and Pharmacokinetics, 1987. **12**(3): p. 193-201.
62. Giuliano, R.A., et al., *In vivo Uptake Kinetics of Aminoglycosides in the Kidney Cortex of Rats.* The Journal of Pharmacology and Experimental Therapeutics, 1986. **236**(470-475).
63. Lyons, M.A., et al., *Computational Toxicology of Chloroform: Reverse Dosimetry Using Bayesian Inference, Marcov Chain Monte Carlo Simulation, and Human Biomonitoring Data.* Environmental Health Perspectives 2008. **116**(8): p. 1040-1046.
64. Gelman, A., Fredric Bois, and Jiming Jiang. , *Physiological Pharmacokinetic Analysis Using Population Modeling and Inofrmative Prior Distributions.* American Statistical Association 1996. **91**(436): p. 1400-1412.

Appendix 1: Mouse weight and organ weights for 100 mg/kg dosed mice

	Spleen **100 mg/kg day** empty vial	filled vial	difference (organ wt)	**Liver** **100 mg/kg day** empty vial	filled vial	difference (organ wt)	**Kidney** **100 mg/kg day** empty vial	filled vial	difference (organ wt)	**Lungs** **100 mg/kg day** empty vial	filled vial	difference (organ wt)	**Mouse** Weight Total (g)
	Time 0		mg	Time 0		mg	Time 0		mg	Time 0		mg	
A	1915	1977	**62**	1909	2802	**893**	1910	2155	**245**	1903	2050	**147**	**18.4**
B	1908	1983	**75**	1905	2787	**882**	1906	2170	**264**	1884	2060	**176**	**18.1**
C*	1908	2068	**160**	1888	2886	**998**	1913	2093	**180**	1903	2075	**172**	**19.4**
D	1905	1991	**86**	1905	2885	**980**	1901	2170	**269**	1918	2086	**168**	**18.8**
	0.5 hr			0.5 hr			0.5 hr			0.5 hr			
A	1912	1968	**56**	1901	2697	**796**	1904	2169	**265**	1899	2066	**167**	**18.5**
B	1911	1982	**71**	1910	2744	**834**	1915	2158	**243**	1914	2141	**227**	**18.2**
C	1905	1974	**69**	1910	2947	**1037**	1899	2181	**282**	1917	2073	**156**	**18**
D	1906	1974	**68**	1902	2911	**1009**	1924	2229	**305**	1908	2089	**181**	**18.4**
	1 hr			1 hr			1 hr			1 hr			
A	1897	1967	**70**	1897	2969	**1072**	1905	2171	**266**	1921	2088	**167**	**18.2**
B	1910	1986	**76**	1877	2780	**903**	1904	2177	**273**	1888	2073	**185**	**17.9**
C	1906	1967	**61**	1901	2877	**976**	1885	2188	**303**	1901	2077	**176**	**18.3**

D	1907	1985	**78**	1896	2798	**902**	1910	2171	**261**	1894	2060	**166**	**18**
	2 hr			2 hr			2 hr			2 hr			
A	1914	1979	**65**	1908	2803	**895**	1914	2164	**250**	1906	2063	**157**	**18.7**
B	1892	1976	**84**	1905	2829	**924**	1905	2189	**284**	1886	2058	**172**	**18.8**
C	1900	1959	**59**	1905	2786	**881**	1913	2149	**236**	1902	2062	**160**	**17.9**
D	1903	1973	**70**	1908	2747	**839**	1902	2152	**250**	1900	2069	**169**	**17.8**
	6 hr			6 hr			6 hr			6 hr			
A	1876	1938	**62**	1910	2779	**869**	1900	2157	**257**	1907	2066	**159**	**18.5**
B	1910	1978	**68**	1907	2767	**860**	1904	2162	**258**	1919	2075	**156**	**18.9**
C	1902	1971	**69**	1904	2834	**930**	1898	2148	**250**	1908	2076	**168**	**19.1**
D	1893	1954	**61**	1904	2749	**845**	1905	2143	**238**	1910	2053	**143**	**18.9**
	20 hr			20 hr			20 hr			20 hr			
A	1897	1971	**74**	1901	2983	**1082**	1916	2167	**251**	1900	2078	**178**	**18.4**
B	1900	1974	**74**	1904	2782	**878**	1899	2146	**247**	1900	2110	**210**	**18**
C	1906	1962	**56**	1906	3012	**1106**	1900	2189	**289**	1898	2070	**172**	**18.6**
D	1904	1975	**71**	1913	2927	**1014**	1920	2156	**236**	1910	2077	**167**	**17.8**

Appendix II: Mouse weight and organ weights for 250 mg/kg dosed mice

	Spleen 250 mg/kg day empty vial	filled vial	difference (organ wt)	**Liver 250 mg/kg day** empty vial	filled vial	difference (organ wt)	**Kidney 250 mg/kg day** empty vial	filled vial	difference (organ wt)	**Lungs 250 mg/kg day** empty vial	filled vial	difference (organ wt)	
	Time 0		mg	Time 0		mg	Time 0		mg	Time 0		mg	
A	1893	1953	60	1923	2815	892	1914	2152	238	1908	2058	150	17.9
B	1916	1990	74	1911	2896	985	1892	2147	255	1920	2072	152	18.9
C	1911	1992	81	1889	2797	908	1912	2160	248	1916	2065	149	18.5
D	1916	1982	66	1911	2691	780	1908	2169	261	1926	2058	132	18.3
	0.5 hr			0.5 hr			0.5 hr			0.5 hr			
A	1926	1983	57	1923	2897	974	1880	2128	248	1896	2029	133	
B	1916	2007	91	1921	2933	1012	1916	2210	294	1917	2101	184	20.5
C	1899	1963	64	1901	2796	895	1921	2155	234	1916	2057	141	18.9
D	1922	1984	62	1917	2902	985	1910	2167	257	1915	2057	142	18.1
	1 hr			1 hr			1 hr			1 hr			
A	1914	1983	69	1927	2977	1050	1915	2182	267	1911	2067	156	19.7
B	1885	1956	71	1905	2875	970	1903	2177	274	1905	2084	179	19.1
C	1893	1958	65	1905	2812	907	1920	2178	258	1894	2057	163	18.1
D	1923	2000	77	1891	2742	851	1925	2190	265	1881	2028	147	18.8

	2 hr			2 hr			2 hr			2 hr			
A	1892	1954	62	1928	2926	998	1905	2172	267	1901	2094	193	19.5
B	1903	1980	77	1923	3006	1083	1912	2180	268	1912	2074	162	20.1
C	1919	1999	80	1917	3027	1110	1916	2196	280	1882	2045	163	20.6
D	1902	1965	63	1910	2834	924	1868	2115	247	1920	2094	174	19.7
	6 hr			6 hr			6 hr			6 hr			
A	1911	1980	69	1916	2816	900	1895	2130	235	1916	2060	144	18.6
B	1914	1988	74	1923	2886	963	1912	2183	271	1885	2039	154	19.7
C	1913	1977	64	1903	2832	929	1903	2160	257	1918	2059	141	18.3
D	1907	1981	74	1907	2858	951	1902	2175	273	1905	2091	186	19.6
	20 hr			20 hr			20 hr			20 hr			
A	1906	1969	63	1895	2966	1071	1892	2166	274	1919	2084	165	18.2
B	1913	1994	81	1915	3011	1096	1909	2170	261	1814	1960	146	18.3
C	1908	1977	69	1904	2907	1003	1902	2168	266	1907	2055	148	19.1
D	1902	1980	78	1903	2961	1058	1906	2155	249	1894	2046	152	18

Appendix III: Organ/ Serum Concentration Data (100 mg/kg dosed mice)

	Spleen 100 mg/kg day		Liver 100 mg/kg day		Kidney 100 mg/kg day		Lungs 100 mg/kg day		Serum 100 mg/kg day	
	ng/mg	stdev	ng/mg	stdev	ng/mg	stdev	ng/mg	stdev		stdev
A	0 hour									
B	< LLOQ		< LLOQ		< LLOQ		< LLOQ		< LLOQ	
C	< LLOQ		< LLOQ		< LLOQ		< LLOQ		< LLOQ	
D	< LLOQ		< LLOQ		< LLOQ		< LLOQ		< LLOQ	
	< LLOQ		< LLOQ		< LLOQ		< LLOQ		< LLOQ	
A	0.5 hour									
B	16.2		17.2		130		61.4		< LLOQ	
C	12.6		13.8		117		46.6		65.9	
D	15.0		12.8		114		45.7		57.9	
Average	10.3		12.0		84.1		33.8		43.8	
	13.525	2.620	13.950	2.288	111.275	19.402	46.875	11.305	55.867	11.189
A	1 hour									
B	< LLOQ		< LLOQ		96.2		19.1		32.1	
C	< LLOQ		10.4		146		31.1		47.9	
D	< LLOQ		< LLOQ		107		15.0		28.3	
Average	< LLOQ		< LLOQ		130		< LLOQ		29.1	
			10.400		119.800	22.445	21.733	8.367	34.350	9.180
A	2 hour									
B	< LLOQ		< LLOQ		211		10.0		4.55	
C	< LLOQ		< LLOQ		179		< LLOQ		5.73	
D	< LLOQ		< LLOQ		195		15.5		12.6	
Average	< LLOQ		< LLOQ		164		10.4		4.86	
					187.250	20.271	11.950	3.083	6.935	3.810
A	6 hour									
B	< LLOQ		< LLOQ		210		< LLOQ		< LLOQ	
C	< LLOQ		< LLOQ		174		< LLOQ		< LLOQ	
D	< LLOQ		< LLOQ		158		10		< LLOQ	
Average	< LLOQ		< LLOQ		185		< LLOQ		< LLOQ	
					181.750	21.854	10.000			
A	20 hour									
B	< LLOQ		< LLOQ		115		< LLOQ		< LLOQ	
C	< LLOQ		< LLOQ		131		< LLOQ		< LLOQ	
D	< LLOQ		< LLOQ		116		< LLOQ		< LLOQ	
Average	< LLOQ		< LLOQ		146		< LLOQ		< LLOQ	
					127.000	14.629				

Appendix IV: Organ/ Serum Concentration Data (250 mg/kg dosed mice)

	Spleen 250 mg/kg day		Liver 250 mg/kg day		Kidney 250 mg/kg day		Lungs 250 mg/kg day		Serum 250 mg/kg day	
	ng/mg	stdev	ng/mg	stdev	ng/mg	stdev	ng/mg	stdev	ng/mg	stdev
A	0.5 hour									
B	27.0		24.8		221		91.8		178	
C	21.8		27.6		210		103		147	
D	32.5		26.1		223		96.0		180	
Average	< LLOQ		< LLOQ		60.8		20.7		26.8	
	27.100	5.351	26.167	1.401	218.000	7.000	96.933	5.658	168.333	18.502
A	1 hour									
B	18.2		22.4		313		45.4		131	
C	14.2		16.7		244		51.5		61.5	
D	14.0		14.7		183		41.1		64.7	
Average	14.5		22.6		255		61.7		90.1	
	15.225	1.994	19.100	4.011	248.750	53.269	49.925	8.935	86.825	32.109
A	2 hour									
B	< LLOQ		< LLOQ		352		14.3		8.00	
C	< LLOQ		< LLOQ		340		< LLOQ		13.7	
D	< LLOQ		< LLOQ		334		11.1		15.6	
Average	< LLOQ		< LLOQ		30.5		< LLOQ		< LLOQ	
					342.000	9.165	12.700	2.263	12.433	3.955
A	6 hour									
B	< LLOQ		< LLOQ		226		< LLOQ		< LLOQ	
C	< LLOQ		< LLOQ		212		< LLOQ		< LLOQ	
D	< LLOQ		< LLOQ		311		10.5		< LLOQ	
Average	< LLOQ		< LLOQ		220		< LLOQ		< LLOQ	
					242.250	46.191	10.5			
A	20 hour									
B	< LLOQ		< LLOQ		146		< LLOQ		< LLOQ	
C	< LLOQ		< LLOQ		116		< LLOQ		< LLOQ	
D	< LLOQ		< LLOQ		116		< LLOQ		< LLOQ	
Average	< LLOQ		< LLOQ		220		< LLOQ		< LLOQ	
					149.500	49.082				

Appendix V: Mouse Model File

```
# Written for MCSim

# Dimensions/Units:
# mass/kilogram (kg) /gram (g) /milligram (mg) /nanogram (ng).
# volume/liter (L) /milliliter (mL).
# time/hour (hr).

States = { # mass (ng).

  MSC,       # drug in subcutaneous layer.
  MIV,       # drug intravenously injected.
  MV,        # drug in venous blood.
  MLU,       # drug in lung.
  MA,        # drug in arterial blood.
  MBR,       # drug in brain.
  MF,        # drug in fat.
  MH,        # drug in heart.
  MM,        # drug in muscle.
  MB,        # drug in bone.
  MSK,       # drug in skin.
  MK,        # drug in kidney.
  MKE,       # drug eliminated from kidney.
  MKA,       # drug accumulating in kidney.
  MKS,       # drug in shallow kidney.
  MKD,       # drug in deep kidney.
  MKDE,      # drug leaving deep compartment.
  MS,        # drug in spleen.
  ML,        # drug in liver.
  MLE,       # drug eliminated from liver.
  MG,        # drug in gastrointestinal Tract.
  MCR,       # drug in carcass.
};

Inputs = {SC_Dose}
  ;

Outputs = { # Tissue/organ drug concentrations (ng drug/mg
organ).

  CV_ng_mg,  CVP_ng_mg, CV,    # Venous blood, plasma.
  CLU_ng_mg, CLU,              # Lung.
  CA_ng_mg,  CA,               # Arterial blood.
  CSE_ng_mg, CSE,              # Total serum.
  CBR_ng_mg, CBR,              # Brain.
  CF_ng_mg,  CF,               # Fat.
  CH_ng_mg,  CH,               # Heart.
  CM_ng_mg,  CM,               # Muscle.
```

```
CB_ng_mg,  CB,                  # Bone.
  CSK_ng_mg, CSK,               # Skin.
  CK_ng_mg,  CK,                # Kidney.
  CKS_ng_mg, CKS,               # Shallow Kidney.
  CKD_ng_mg, CKD,               # Deep Kidney.
  CS_ng_mg,  CS,                # Spleen.
  CL_ng_mg,  CL,                # Liver.
  CG_ng_mg,  CG,                # Gastrointestinal Tract.
  CCR_ng_mg, CCR,               # Carcass.


# Mass balance checks (total accumulated, net input, balance
error).
  ACC, NetIn, BalErr
};

# Anatomical/physiological parameters for mouse.
  BW  = 0.018;     # Body weight (kg).
  QCC = 16.5;      # Cardiac output (L/hr/kg^0.75).

# Exposure/dose
  SC_Dose   = 1.0;       # Subcutaneous dose (mg drug/kg body
weight).
  SC_Decay  = 1.0;       # Rate of SC dose into blood (1/h).
  IV_Dose   = 1.0;       # Intravenous dose (mg/kg).
  IV_Decay  = 1.0;


# Fractional tissue weights. Davies, et al.
  VLUC = 0.0044;         # Lung (exp).
  VBRC = 0.018;          # Brain.
  VFC  = 0.070;          # Fat.
  VHC  = 0.004;          # Heart.
  VMC  = 0.384;          # Muscle.
  VBC  = 0.107;          # Bone.
  VSKC = 0.165;          # Skin.
  VKC  = 0.014;          # Kidney (exp).
  VKSC = 0.010;          # Shallow Kidney.
  VKDC = 0.004;          # Deep Kidney.
  VSpC  = 0.0037;        # Spleen (exp).
  VGC  = 0.042;          # Gastrointestinal Tract.
  VLC  = 0.05;           # Liver (exp).
  VVC  = 0.0327;         # Venous blood.
  VAC  = 0.0163;         # Arterial blood.
  VCRC                              =                              1-
(VLUC+VBRC+VFC+VHC+VMC+VBC+VSKC+VKC+VSpC+VGC+VLC+VVC+VAC);
                  # Carcass (1 - all others).

# Fractional tissue flows (fraction of cardiac output).
  QLUC = 1.0;            # Lung.
  QBRC = 0.033;          # Brain.
  QFC  = 0.043;          # Fat.
  QHC  = 0.066;          # Heart.
  QMC  = 0.159;          # Muscle.
  QBC  = 0.110;          # Bone.
  QSKC = 0.058;          # Skin.
```

```
  QKSC = 0.091;          # Shallow Kidney.
  QSC  = 0.01;           # Spleen.
  QGC  = 0.13;           # Gastrointestinal Tract.
  QLAC = 0.02;           # Hepatic artery.
  QCRC = 0.28;           # Carcass.

# Partition coefficients.
  BP  = 1.; # Blood:plasma.
  PLU = 1.; # Lung:blood.
  PBR = 1.; # Brain:blood.
  PF  = 1.; # Fat:blood.
  PH  = 1.; # Heart:blood.
  PM  = 1.; # Muscle:blood.
  PB  = 1.; # Bone:blood.
  PSK = 1.; # Skin:blood.
  PKS = 1.; # Shallow kidney:blood.
  PS  = 1.; # Spleen:blood.
  PG  = 1.; # Gastrointestinal Tract:blood.
  PL  = 1.; # Liver:blood.
  PCR = 1.; # Carcass:blood.

# Clearance parameters.
  CLHC = 1.;       # Hepatic clearance (L/h/kg).
  CLR  = 1.;       # Renal clearance (L/h).
  CLRD = 1.;       # Deep renal tissue clearance (L/h).

# Michaelis Menten kidney accumulation parameters.
  Vmax = 1.;       # Max velocity (ng/h).
  Km = 1.;         # MM constant (ng/kg).

# Scaled/calculated parameters.
  CLH; SCR; IVR;
  VLU; VBR; VF; VH; VM; VB; VSK; VKS; VKD; VK; VSp; VG; VL; VV;
VA;  VCR;
  QC; QLU; QBR; QF; QH; QM; QB; QSK; QKS; QS; QG; QLA; QL; QCR;

# Variance of predicted parameters.

  V_CLHC; V_Vmax; V_Km; V_CLR; V_CLRD; V_SC_Decay;

Initialize {

# Dose.
  SCR = (SC_Dose*BW*(1.E6));       # Total dose (ng).
  MSC = SCR;                       #  Initial  drug  mass  in  SubCu
layer.
  IVR = 1.E6*IV_Dose*BW;
  MIV = IVR;

# Compartment weight (kg).
  VTC = VLUC+VBRC+VFC+VHC+VMC+VBC+VSKC+VKC+VGC+VLC+VVC+VAC+VCRC;
  VLU = VLUC*BW/VTC;     # Lung.
  VBR = VBRC*BW/VTC;     # Brain.
  VF  = VFC*BW/VTC;      # Fat.
  VH  = VHC*BW/VTC;      # Heart.
  VM  = VMC*BW/VTC;      # Muscle.
  VB  = VBC*BW/VTC;      # Bone.
```

```
  VSK = VSKC*BW/VTC;     # Skin.
  VKD = VKDC*BW/VTC;     # Deep Kidney.
  VKS = VKSC*BW/VTC;     # Shallow Kidney.
  VK  = VKC*BW/VTC;      # Kidney.
  VSp  = VSpC*BW/VTC;    # Spleen.
  VG  = VGC*BW/VTC;      # Gastrointestinal Tract
  VL  = VLC*BW/VTC;      # Liver.
  VV  = VVC*BW/VTC;      # Venous blood.
  VA  = VAC*BW/VTC;      # Arterial blood.
  VCR = VCRC*BW/VTC;     # Carcass.

# Flow rates (L/hr).
  QC  = QCC*pow(BW, 0.75);     # Cardiac output.
  QTC = QBRC+QFC+QHC+QMC+QBC+QSKC+QKSC+QSC+QLAC+QGC+QCRC;
  QLU = QLUC*QC/QTC;           # Lung.
  QBR = QBRC*QC/QTC;           # Brain.
  QF  = QFC*QC/QTC;            # Fat.
  QH  = QHC*QC/QTC;            # Heart.
  QM  = QMC*QC/QTC;            # Muscle.
  QB  = QBC*QC/QTC;            # Bone.
  QSK = QSKC*QC/QTC;           # Skin.
  QKS = QKSC*QC/QTC;           # Shallow kidney.
  QS  = QSC*QC/QTC;            # Spleen.
  QG  = QGC*QC/QTC;            # Gastrointestinal Tract.
  QLA = QLAC*QC/QTC;           # Hepatic artery.
  QL  = QS+QG+QLA;             # Total liver flow.
  QCR = QCRC*QC/QTC;           # Carcass.

# Clearance (L/hr).
  CLH = CLHC*BW;
}

Dynamics {
# Subcutaneous dose (ng/h).

  dt(MSC) = -MSC*SC_Decay;                # Drug moving from SC
to blood.

# Intravenous dose.

  dt(MIV) = -MIV*IV_Decay;

# Drug Tissue/organ concentrations (ng/kg).
  CV  = MV/VV;                                # Venous blood.
  CA  = MA/VA;                                # Arterial blood.
  CLU = MLU/VLU;   CVLU = CLU/PLU;            # Lung.
  CBR = MBR/VBR;   CVBR = CBR/PBR;            # Brain.
  CF  = MF/VF;     CVF  = CF/PF;              # Fat.
  CH  = MH/VH;     CVH  = CH/PH;              # Heart.
  CM  = MM/VM;     CVM  = CM/PM;              # Muscle.
  CB  = MB/VB;     CVB  = CB/PB;              # Bone.
  CSK = MSK/VSK;   CVSK = CSK/PSK;            # Skin.
  CKS = MKS/VKS;   CVKS = CKS/PKS;            # Shallow kidney.
  CKD = MKD/VKD;   CVKD = CKD;                # Deep kidney.
  CK  = MK/VK;     CVK  = CK/PKS;             # Kidney.
  CS  = MS/VSp;    CVS  = CS/PS;              # Spleen.
```

```
  CG  = MG/VG;      CVG  = CG/PG;          #       Gastrointestinal
Tract.
  CL  = ML/VL;      CVL  = CL/PL;          # Liver.
  CCR = MCR/VCR;    CVCR = CCR/PCR;        # Carcass.



# Tissue/organ dynamics (ng/h).
# Venous blood
  dt(MV) =    QBR*CVBR + QF*CVF + QH*CVH + QM*CVM + QB*CVB +
QSK*CVSK
            + QKS*CVKS + QL*CVL + QCR*CVCR- dt(MSC)-dt(MIV)-
QLU*CV;

# Lung
  dt(MLU) = QLU*(CV - CVLU);

# Arterial blood.
  dt(MA)  = QLU*(CVLU - CA);

# Brain.
  dt(MBR) = QBR*(CA - CVBR);

# Fat.
  dt(MF) = QF*(CA - CVF);

# Heart.
  dt(MH) = QH*(CA - CVH);

# Muscle.
  dt(MM) = QM*(CA - CVM);

# Bone.
  dt(MB) = QB*(CA - CVB);

# Skin.
  dt(MSK) = QSK*(CA - CVSK);

# Kidney.
  dt(MKE) = CLR*CVKS;
  dt(MKA) = (Vmax*CVKS)/(Km+CVKS);
  dt(MKDE)= CLRD*CVKD;
  dt(MKS) = QKS*(CA - CVKS)-dt(MKA)- dt(MKE)+dt(MKDE);
  dt(MKD) = dt(MKA)-dt(MKDE);
  dt(MK)  = dt(MKS) + dt(MKD);

# Spleen.
  dt(MS) = QS*(CA - CVS);

# Gastrointestinal Tract.
   dt(MG) = QG*(CA - CVG);

# Liver.
  dt(MLE) = CLH*CVL;
  dt(ML)  = QLA*CA + QS*CVS + QG*CVG - QL*CVL - dt(MLE);

# Rest of body.
```

```
  dt(MCR) = QCR*(CA - CVCR);

# Mass balance calculations.
 ACC = MA + MV + MLU + MBR + MF + MH + MM + MB + MSK + MK
         + MS + MG + ML + MCR + MSC + MIV;

 NetIn = IVR + SCR - (MLE + MKE);
}

CalcOutputs {
# Tissue/organ drug concentrations (ng/mg).
  CV_ng_mg   = CV/(1.E6);                    # Venous blood.
  CVP_ng_mg  = (CV/BP)/(1.E6);               # Plasma.
  CLU_ng_mg  = CLU/(1.E6);                   # Lung.
  CA_ng_mg   = CA/(1.E6);                    # Arterial blood.
  CSE_ng_mg  = (CA+CV)/(1.E6);               # Total Serum.
  CBR_ng_mg  = CBR/(1.E6);                   # Brain.
  CF_ng_mg   = CF/(1.E6);                    # Fat.
  CH_ng_mg   = CH/(1.E6);                    # Heart.
  CM_ng_mg   = CM/(1.E6);                    # Muscle.
  CB_ng_mg   = CB/(1.E6);                    # Bone.
  CSK_ng_mg  = CSK/(1.E6);                   # Skin.
  CK_ng_mg   = CK/(1.E6);                    # Kidney.
  CS_ng_mg   = CS/(1.E6);                    # Spleen.
  CL_ng_mg   = CL/(1.E6);                    # Liver.
  CG_ng_mg   = CG/(1.E6);                    #    Gastrointestinal
Tract.
  CCR_ng_mg  = CCR/(1.E6);

# Mass balance error.
 BalErr = NetIn - ACC;
}
```

Appendix VI: Sample Forward Simulation File for the Mouse Model

```
# capreo5_SC.sim

 OutputFile("forwardcapsim250_b.out");

# Body and drug parameters.
  BW = 0.018;            # (kg).
  SC_Dose = 250.;        # (mg/kg).
  IV_Dose = 0;           # (mg/kg).

# Capreomycin specific parameters.
  CLHC = 3.97;           # Hepatic clearance (L/h/kg).
  CLR  = 0.012;          # Renal clearance (L/h).
  CLRD = 3.47e-6;        # Deep renal tissue clearance (L/h).
  Vmax = 1.04e6;         # Max velocity (ng/h).
  Km   = 5.55e8;         # MM constant (ng/kg).
  SC_Decay  = 0.902;     # Rate of SC dose into blood (1/h).
  IV_Decay = 42.;        # Rate of IV dose into blood (1/h).

# Partition coefficients.
  BP  = 1.; # Blood:plasma.
  PLU = 2.; # Lung:blood.
  PBR = 1.; # Brain:blood.
  PF  = 1.; # Fat:blood.
  PH  = 1.; # Heart:blood.
  PM  = 1.; # Muscle:blood.
  PB  = 1.; # Bone:blood.
  PSK = 1.; # Skin:blood.
  PKS = 1.; # Shallow kidney:blood.
  PS  = 1.; # Spleen:blood.
  PG  = 1.; # Gut:blood.
  PL  = 1.; # Liver:blood.
  PCR = 1.; # Carcass:blood.

Simulation {

  PrintStep(CV_ng_mg, 0, 24, 0.01);   # Venous.
  PrintStep(CLU_ng_mg, 0, 24, 0.01);  # Lung.
  PrintStep(CA_ng_mg, 0, 24, 0.01);   # Arterial.
  PrintStep(CSE_ng_mg, 0, 24, 0.01);  # Serum.
  PrintStep(CK_ng_mg,  0, 24, 0.01);  # Kidney.
  PrintStep(CS_ng_mg,  0, 24, 0.01);  # Spleen.
  PrintStep(CL_ng_mg,  0, 24, 0.01);  # Liver.
  PrintStep(BalErr,    0, 24, 0.01);  # mass balance error.

}
End.
```

Appendix VII: Parameter estimation (experimental maximum fit) by forward simulation. Fit to the 100 mg/kg dose data

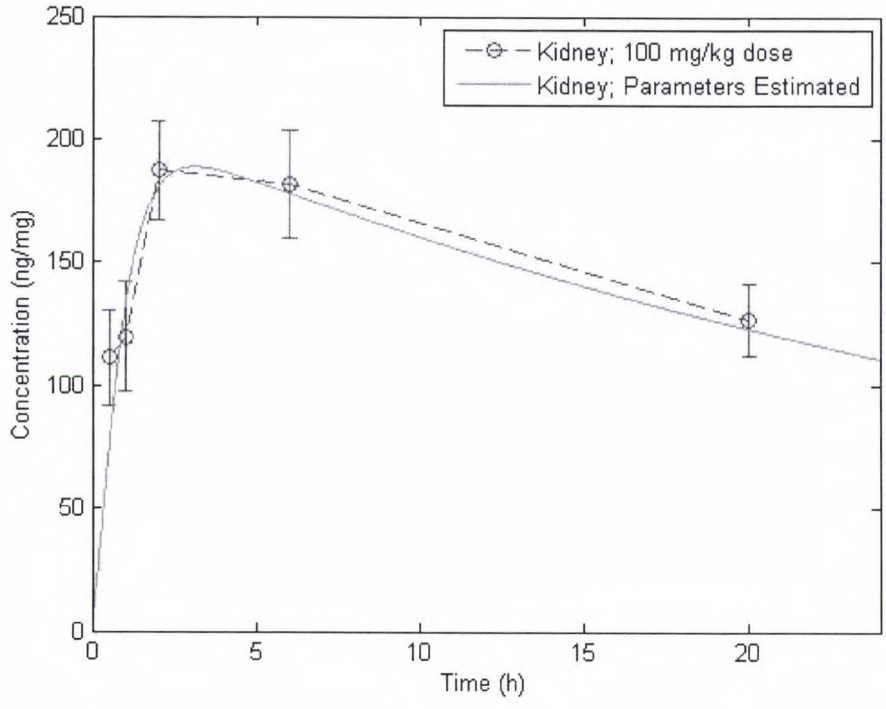

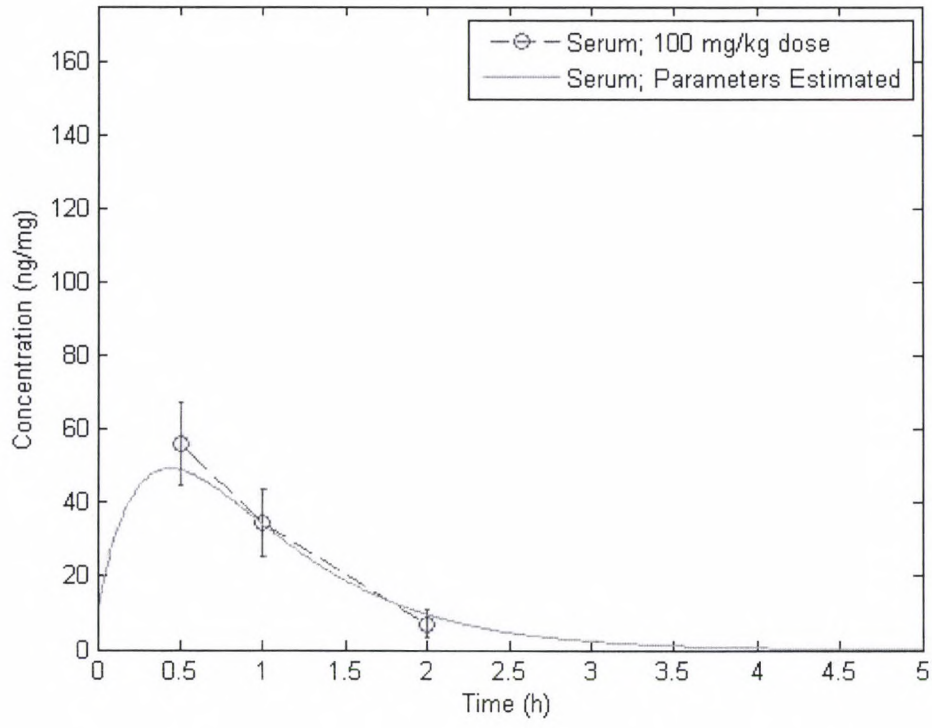
Serum; 100 mg/kg dose
Serum; Parameters Estimated
Concentration (ng/mg)
Time (h)
0
20
40
60
80
100
120
140
160
0
0.5
1
1.5
2
2.5
3
3.5
4
4.5
5

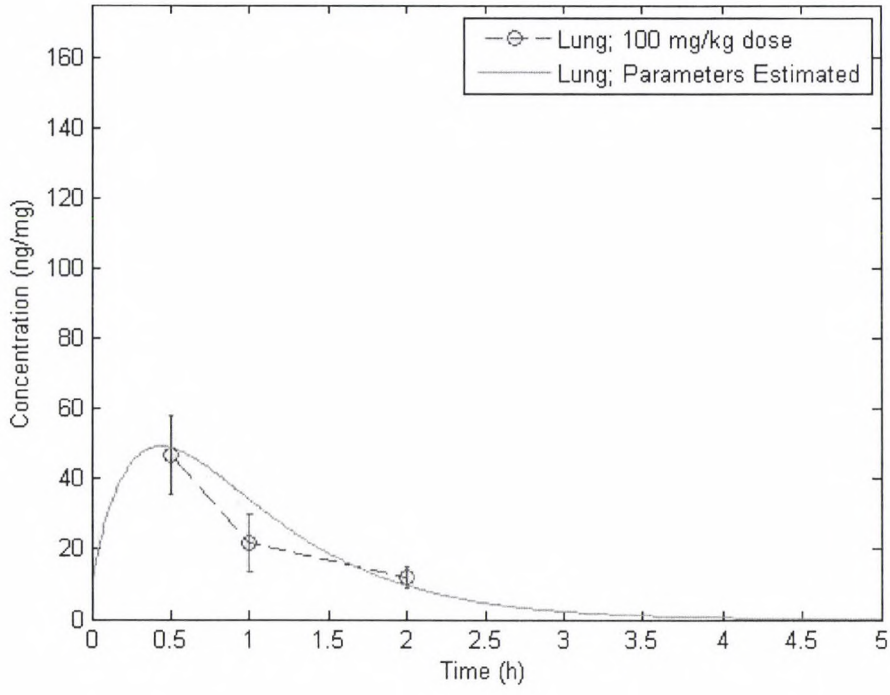
Lung; 100 mg/kg dose
Lung; Parameters Estimated
Concentration (ng/mg)
Time (h)
0
20
40
60
80
100
120
140
160
0
0.5
1
1.5
2
2.5
3
3.5
4
4.5
5

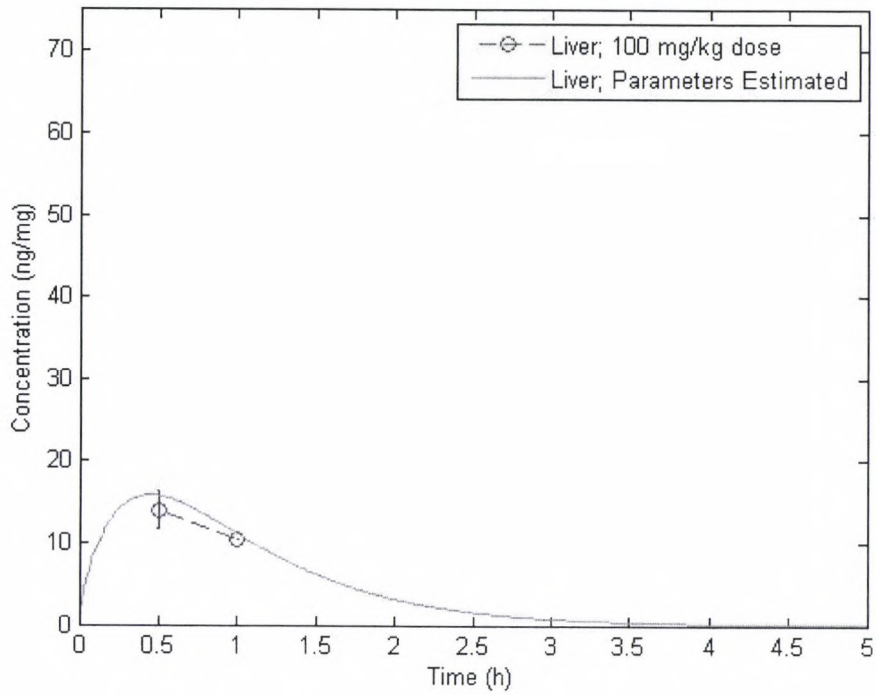
Liver; 100 mg/kg dose
Liver; Parameters Estimated
Concentration (ng/mg)
Time (h)
0
10
20
30
40
50
60
70
0
0.5
1
1.5
2
2.5
3
3.5
4
4.5
5

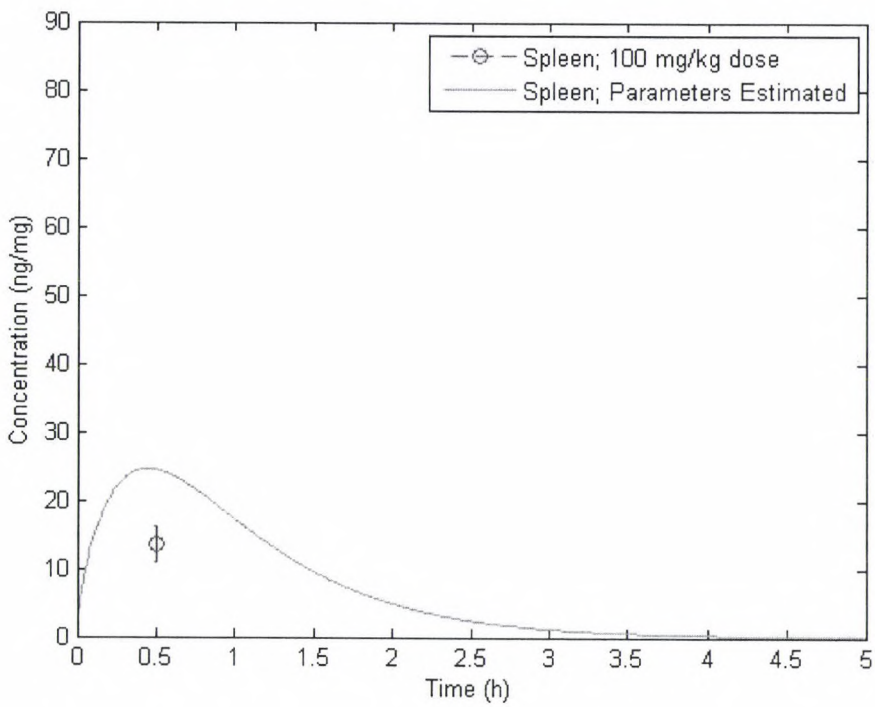
Spleen; 100 mg/kg dose
Spleen; Parameters Estimated
Concentration (ng/mg)
Time (h)
0
10
20
30
40
50
60
70
80
90
0
0.5
1
1.5
2
2.5
3
3.5
4
4.5
5

Appendix VII: Parameter estimation (experimental maximum fit) by forward simulation. Fit to the 250 mg/kg dose data

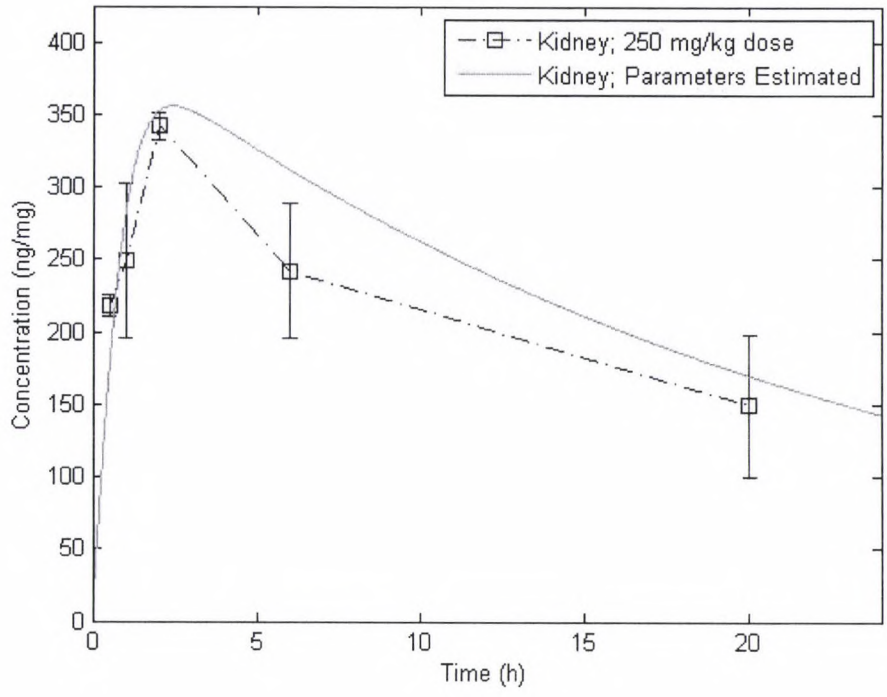

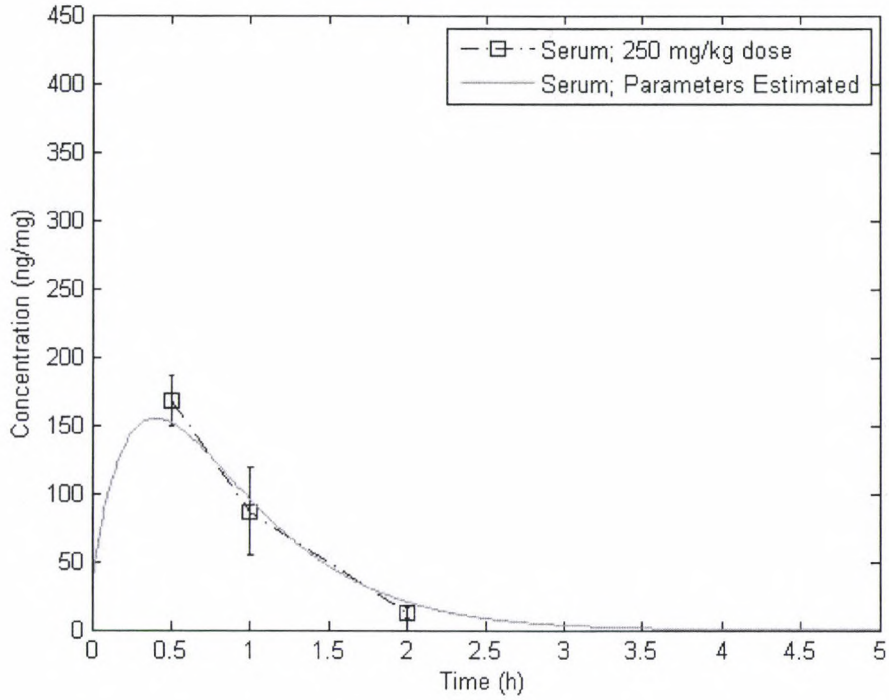
Serum; 250 mg/kg dose
Serum; Parameters Estimated
Concentration (ng/mg)
Time (h)
0
50
100
150
200
250
300
350
400
450
0
0.5
1
1.5
2
2.5
3
3.5
4
4.5
5

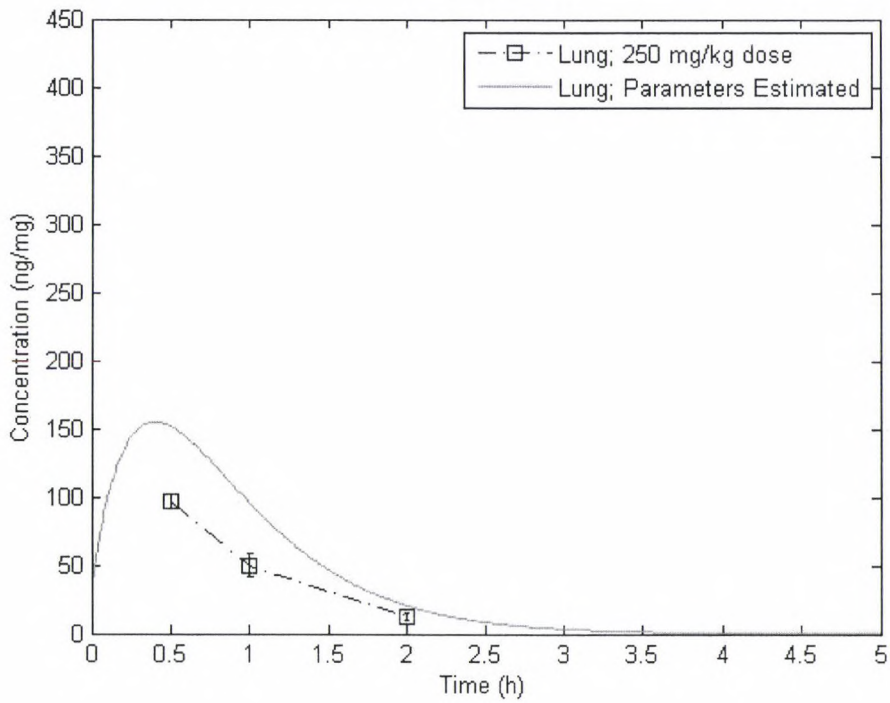
Lung; 250 mg/kg dose
Lung; Parameters Estimated
Concentration (ng/mg)
Time (h)
0
50
100
150
200
250
300
350
400
450
0
0.5
1
1.5
2
2.5
3
3.5
4
4.5
5

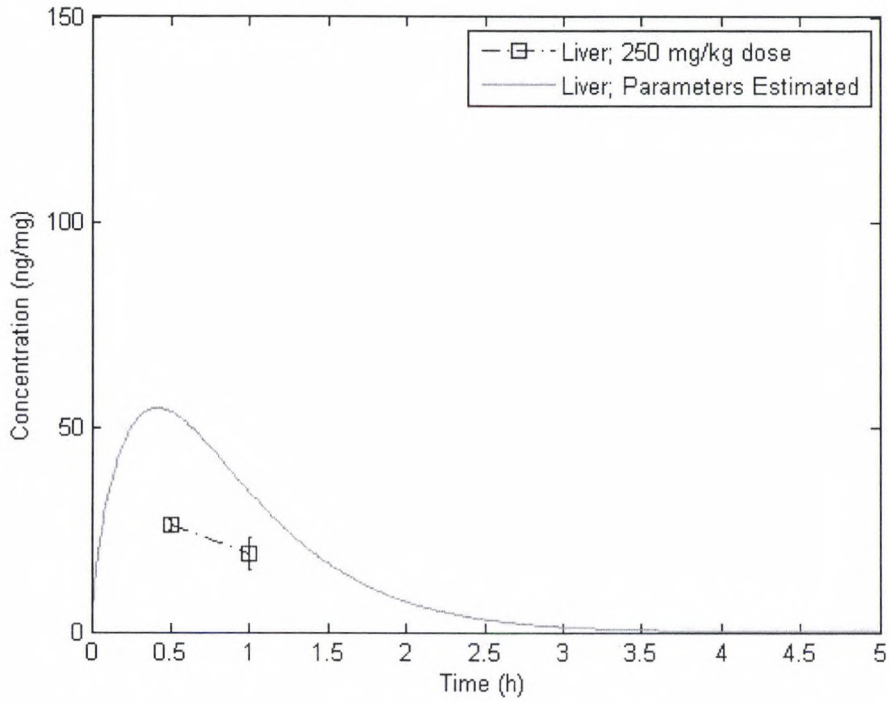
Liver; 250 mg/kg dose
Liver; Parameters Estimated
Concentration (ng/mg)
Time (h)
0
50
100
150
0
0.5
1
1.5
2
2.5
3
3.5
4
4.5
5

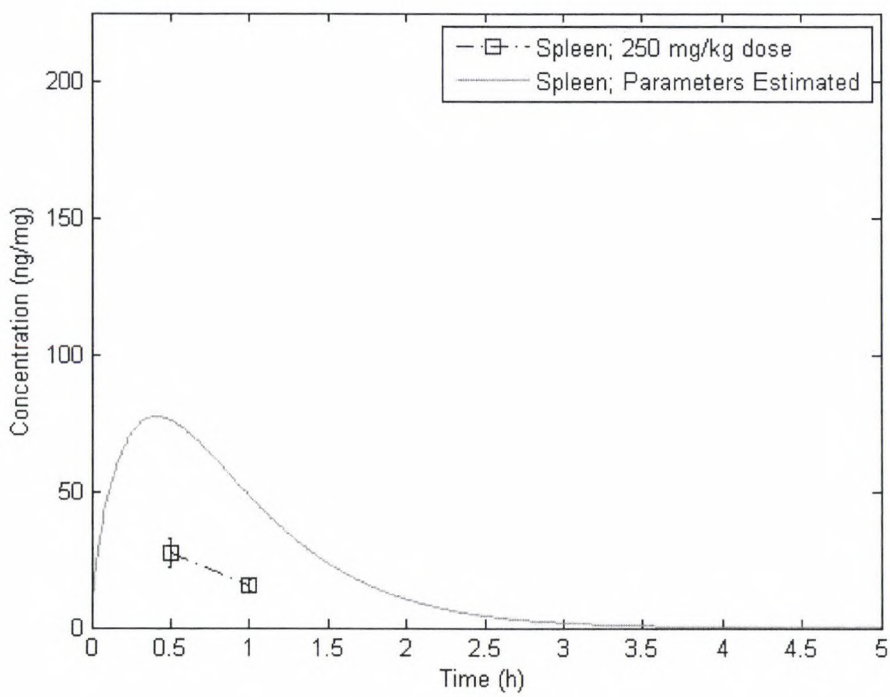
Spleen; 250 mg/kg dose
Spleen; Parameters Estimated
Concentration (ng/mg)
Time (h)
0
50
100
150
200
0
0.5
1
1.5
2
2.5
3
3.5
4
4.5
5

Appendix IX: Parameter estimation (extrapolated fit) by forward simulation. Fit to the 100 mg/kg dose data

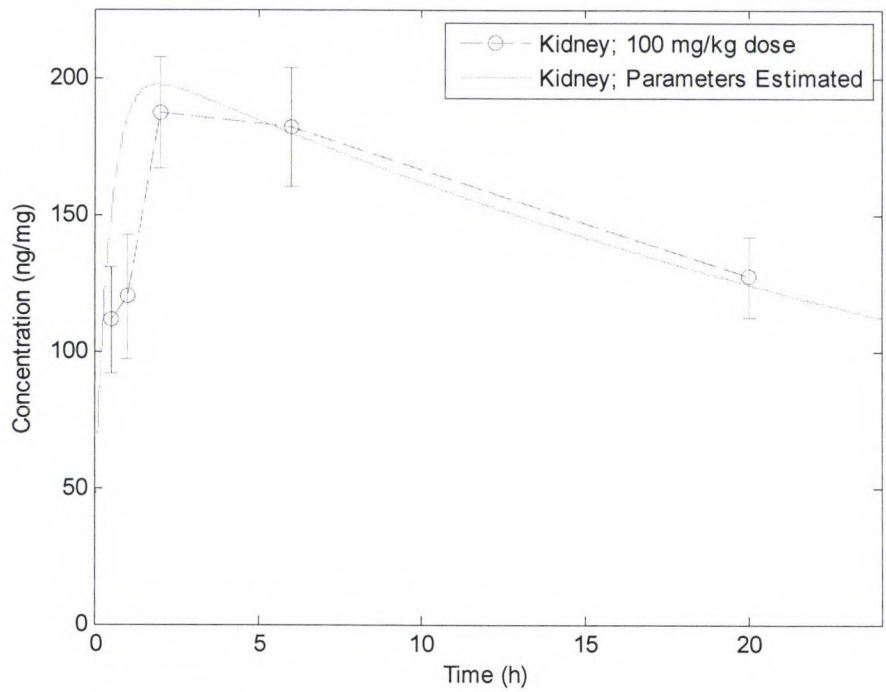

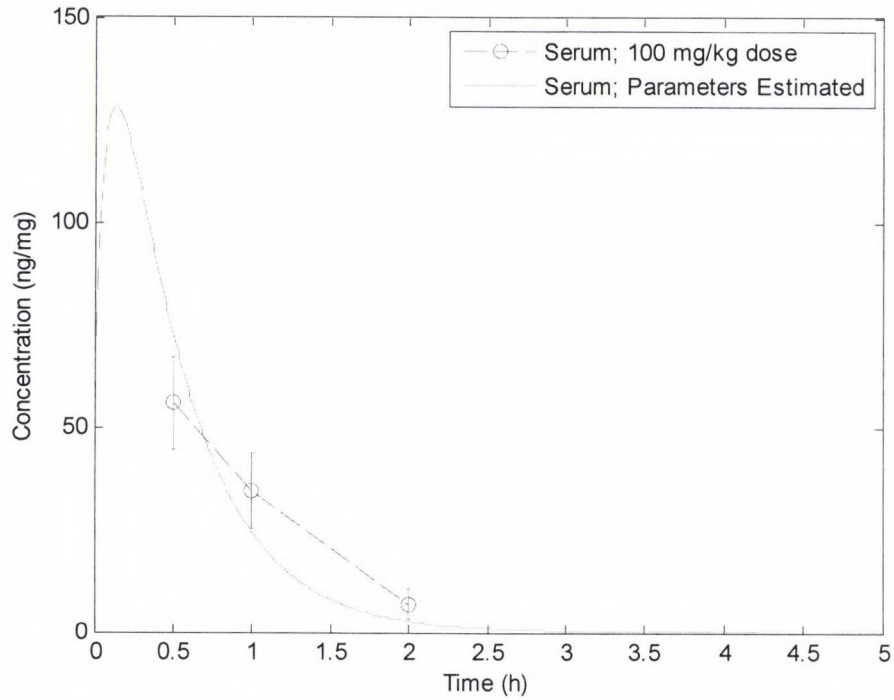
Serum; 100 mg/kg dose
Serum; Parameters Estimated
Concentration (ng/mg)
Time (h)
150
100
50
0
0
0.5
1
1.5
2
2.5
3
3.5
4
4.5
5

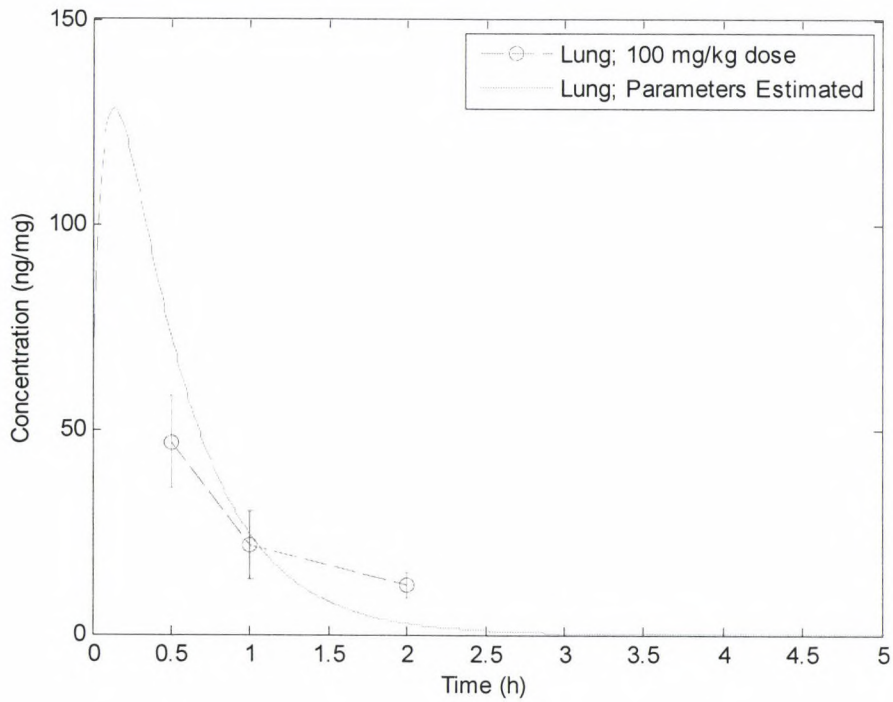
Lung; 100 mg/kg dose
Lung; Parameters Estimated
Concentration (ng/mg)
Time (h)
150
100
50
0
0
0.5
1
1.5
2
2.5
3
3.5
4
4.5
5

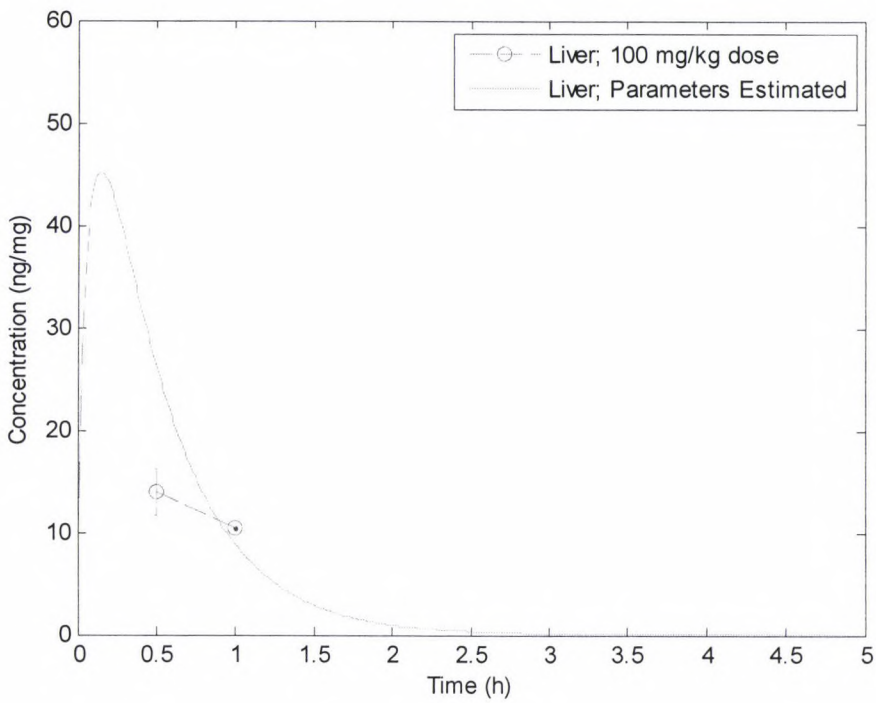
Liver; 100 mg/kg dose
Liver; Parameters Estimated
Concentration (ng/mg)
Time (h)
0
10
20
30
40
50
60
0
0.5
1
1.5
2
2.5
3
3.5
4
4.5
5

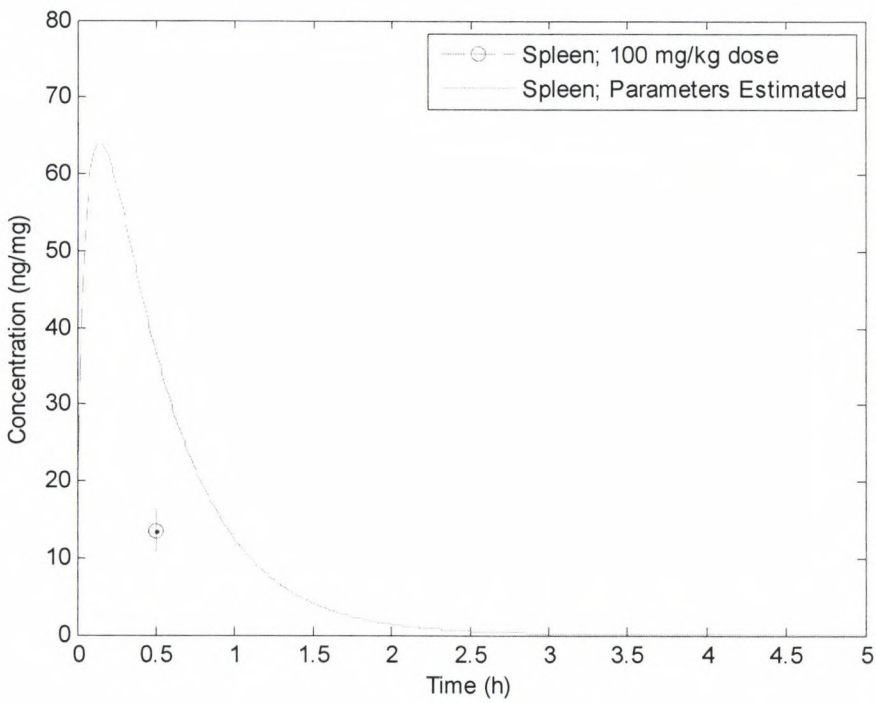
Spleen; 100 mg/kg dose
Spleen; Parameters Estimated
Concentration (ng/mg)
Time (h)
0
10
20
30
40
50
60
70
80
0
0.5
1
1.5
2
2.5
3
3.5
4
4.5
5

Appendix X: Parameter estimation (extrapolated fit) by forward simulation. Fit to the 250 mg/kg dose

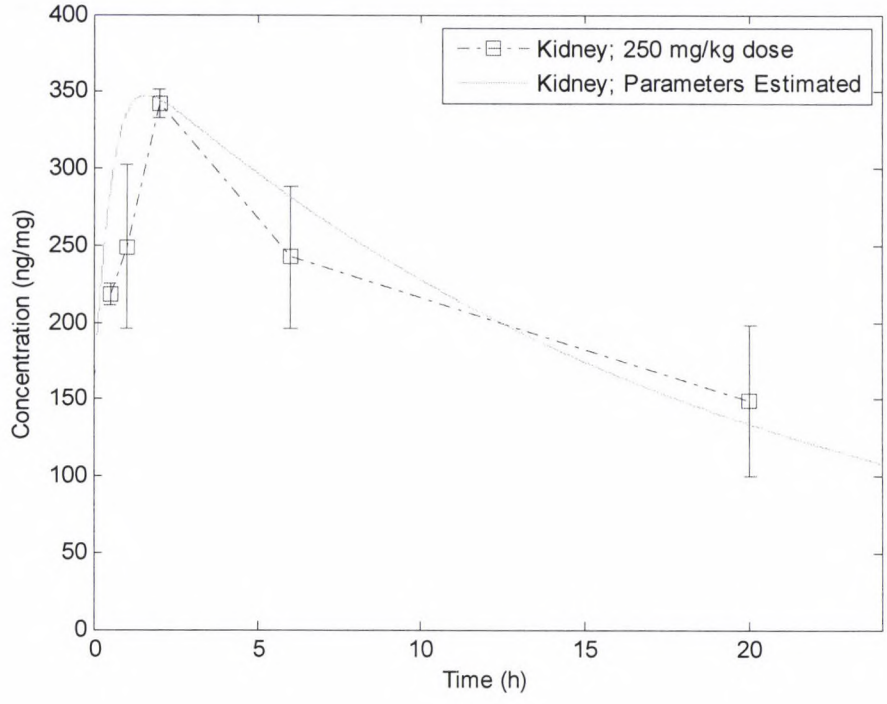

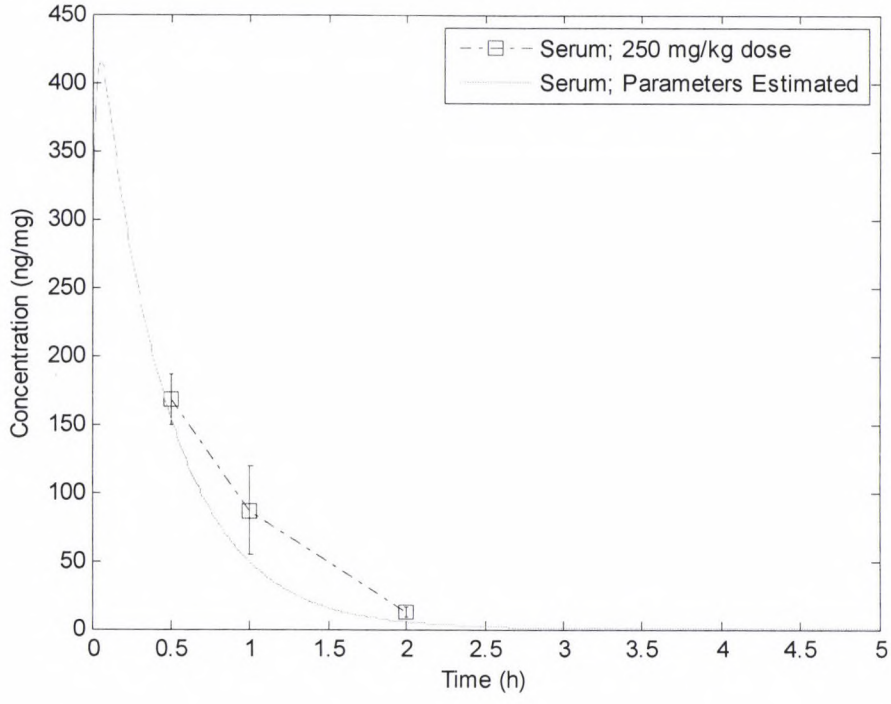
Serum; 250 mg/kg dose
Serum; Parameters Estimated
Concentration (ng/mg)
Time (h)
0
50
100
150
200
250
300
350
400
450
0
0.5
1
1.5
2
2.5
3
3.5
4
4.5
5

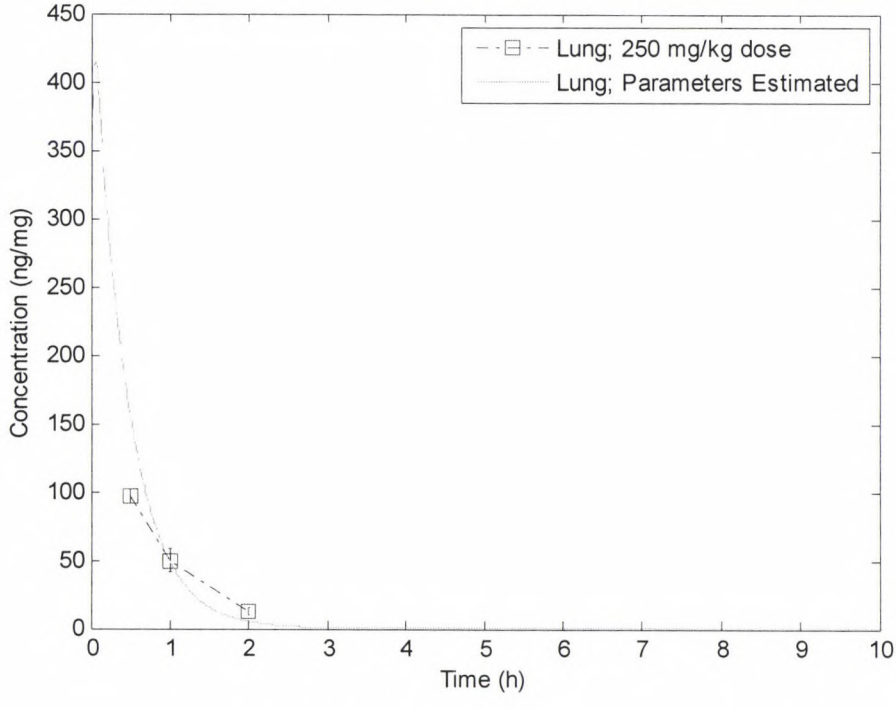
Lung; 250 mg/kg dose
Lung; Parameters Estimated
Concentration (ng/mg)
Time (h)
0
50
100
150
200
250
300
350
400
450
0
1
2
3
4
5
6
7
8
9
10

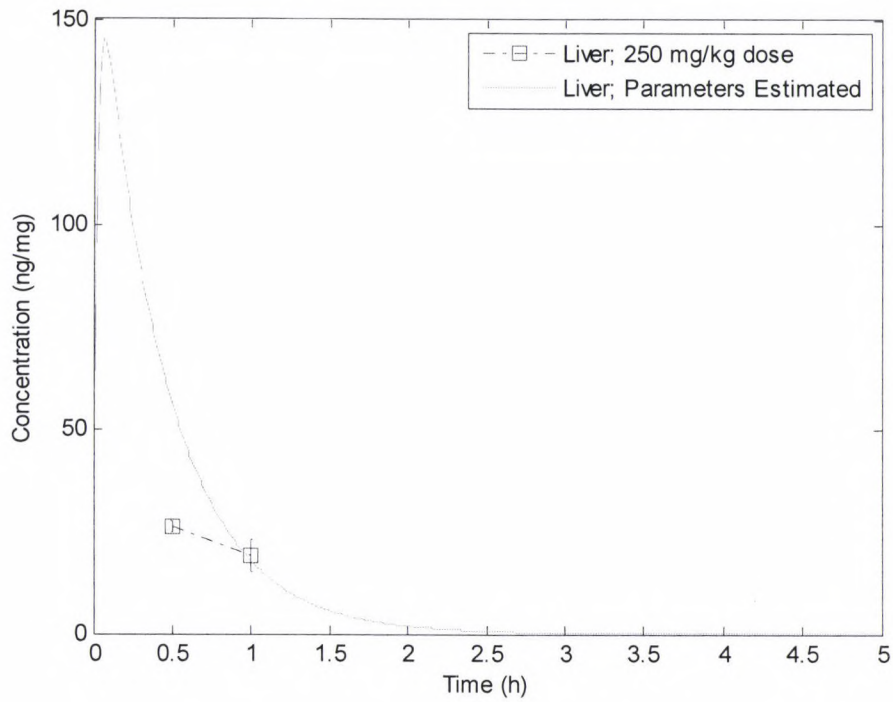
Liver; 250 mg/kg dose
Liver; Parameters Estimated
Concentration (ng/mg)
Time (h)
0
50
100
150
0
0.5
1
1.5
2
2.5
3
3.5
4
4.5
5

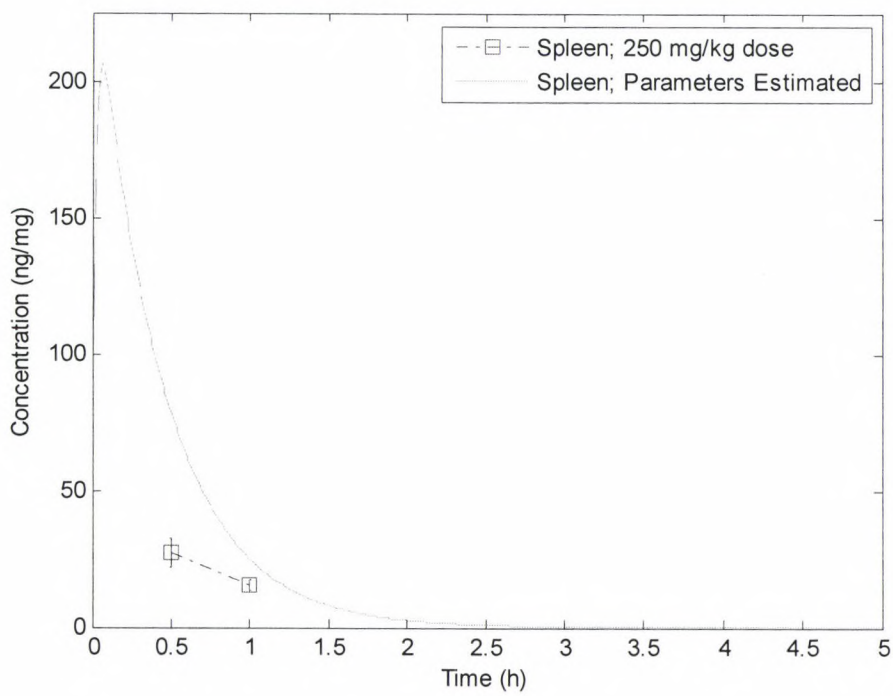
Spleen; 250 mg/kg dose
Spleen; Parameters Estimated
Concentration (ng/mg)
Time (h)
0
50
100
150
200
0
0.5
1
1.5
2
2.5
3
3.5
4
4.5
5

Appendix XI: MCMC Simulation, All Individual Mouse Data Points

```
# capreo_mcmc_individual.sim

 SimType(MCMC);
 MCMC("capreo_mcmc_individual.out", "", "", 10000, 0, 1, 5000,
3.1415);

Level {

# Partition Coefficients
  BP  = 1.; # Blood:plasma.
  PLU = 2.; # Lung:blood.
  PBR = 1.; # Brain:blood.
  PF  = 1.; # Fat:blood.
  PH  = 1.; # Heart:blood.
  PM  = 1.; # Muscle:blood.
  PB  = 1.; # Bone:blood.
  PSK = 1.; # Skin:blood.
  PKS = 1.; # Shallow kidney:blood.
  PS  = 1.; # Spleen:blood.
  PG  = 1.; # Gut:blood.
  PL  = 1.; # Liver:blood.
  PCR = 1.; # Carcass:blood.

  Distrib(CLHC, TruncNormal, 3., 0.75, 1., 5.);
  Distrib(Vmax, TruncNormal, 0.6E6, 0.15E6, .1E6, 1.1E6);
  Distrib(Km, TruncNormal, 4.5E8, 1.125E8, 1.E8, 8.E8);
  Distrib(CLR, TruncNormal, 0.004, 0.001, 0.0009, 0.007);
  Distrib(CLRD, TruncNormal, 3.3E-6, 8.25E-7, 1.E-6, 5.6E-6);
  Distrib(SC_Decay, TruncNormal, 15., 4., 8., 22.);

  Distrib(V_CLHC, InvGamma, 3, 1.12);
  Distrib(V_Vmax, InvGamma, 3, 0.045E12);
  Distrib(V_Km, InvGamma, 3, 2.54E16);
  Distrib(V_CLR, InvGamma, 3, 2.E-6);
  Distrib(V_CLRD, InvGamma, 3, 136.125E-14);
  Distrib(V_SC_Decay, InvGamma, 3, 32.);


Likelihood (Data(CK_ng_mg),  Normal, Prediction(CK_ng_mg), 53.);
  Likelihood (Data(CS_ng_mg),  Normal, Prediction(CS_ng_mg), 3.);
  Likelihood (Data(CL_ng_mg),  Normal, Prediction(CL_ng_mg),
4.5);
  Likelihood (Data(CLU_ng_mg), Normal, Prediction(CLU_ng_mg),
12.);
  Likelihood (Data(CSE_ng_mg), Normal, Prediction(CSE_ng_mg),
33.);

Level  {
```

```
  Distrib(CLHC, TruncNormal_v, CLHC, V_CLHC, 1., 5.);
  Distrib(Vmax, TruncNormal_v, Vmax, V_Vmax, .1E6, 1.1E6);
  Distrib(Km, TruncNormal_v, Km, V_Km, 1.E8, 8.E8);
  Distrib(CLR, TruncNormal_v, CLR, V_CLR, 0.0009, 0.007);
  Distrib(CLRD, TruncNormal_v, CLRD, V_CLRD, 1.E-6, 5.6E-6);
  Distrib(SC_Decay, TruncNormal_v, SC_Decay, V_SC_Decay, 8.,
22.);
```

```
Simulation { # Mouse A,  0. hour

  SC_Dose=100.0;

  BW = 0.0184;  #kg
  VSp = 0.000062; #kg
  VL = 0.000893;
  VK = 0.000245;
  VLU = 0.000147;

  Print(CK_ng_mg, 0., .5, 1., 2., 6., 20.);
  Data(CK_ng_mg, -1, -1, -1, -1, -1, -1);
  Print(CS_ng_mg, 0., .5, 1., 2., 6., 20.);
  Data(CS_ng_mg, -1, -1, -1, -1, -1, -1);
  Print(CL_ng_mg, 0., .5, 1., 2., 6., 20.);
  Data(CL_ng_mg, -1, -1, -1, -1, -1, -1);
  Print(CLU_ng_mg, 0., .5, 1., 2., 6., 20.);
  Data(CLU_ng_mg, -1, -1, -1, -1, -1, -1);
  Print(CSE_ng_mg, 0., .5, 1., 2., 6., 20.);
  Data(CSE_ng_mg, -1, -1, -1, -1, -1, -1);
  }

Simulation { # Mouse B,  0. hour

  SC_Dose=100.0;

  BW = 0.0181;
  VSp = 0.000075; #kg
  VL = 0.000882;
  VK = 0.000264;
  VLU = 0.000176;

  Print(CK_ng_mg, 0., .5, 1., 2., 6., 20.);
  Data(CK_ng_mg, -1, -1, -1, -1, -1, -1);
  Print(CS_ng_mg, 0., .5, 1., 2., 6., 20.);
  Data(CS_ng_mg, -1, -1, -1, -1, -1, -1);
  Print(CL_ng_mg, 0., .5, 1., 2., 6., 20.);
  Data(CL_ng_mg, -1, -1, -1, -1, -1, -1);
  Print(CLU_ng_mg, 0., .5, 1., 2., 6., 20.);
  Data(CLU_ng_mg, -1, -1, -1, -1, -1, -1);
  Print(CSE_ng_mg, 0., .5, 1., 2., 6., 20.);
  Data(CSE_ng_mg, -1, -1, -1, -1, -1, -1);
  }

Simulation { # Mouse C, *** 0. hour

  SC_Dose=100.0;

  BW = 0.0194;
  VSp = 0.000160; #kg
  VL = 0.000998;
  VK = 0.000360;
  VLU = 0.000172;

  Print(CK_ng_mg, 0., .5, 1., 2., 6., 20.);
  Data(CK_ng_mg, -1, -1, -1, -1, -1, -1);
  Print(CS_ng_mg, 0., .5, 1., 2., 6., 20.);
```

```
  Data(CS_ng_mg, -1, -1, -1, -1, -1, -1);
  Print(CL_ng_mg, 0., .5, 1., 2., 6., 20.);
  Data(CL_ng_mg, -1, -1, -1, -1, -1, -1);
  Print(CLU_ng_mg, 0., .5, 1., 2., 6., 20.);
  Data(CLU_ng_mg, -1, -1, -1, -1, -1, -1);
  Print(CSE_ng_mg, 0., .5, 1., 2., 6., 20.);
  Data(CSE_ng_mg, -1, -1, -1, -1, -1, -1);
  }

Simulation { # Mouse D,  0. hour

  SC_Dose=100.0;

  BW = 0.0188;
  VSp = 0.000086; #kg
  VL = 0.000980;
  VK = 0.000269;
  VLU = 0.000168;

  Print(CK_ng_mg, 0., .5, 1., 2., 6., 20.);
  Data(CK_ng_mg, -1, -1, -1, -1, -1, -1);
  Print(CS_ng_mg, 0., .5, 1., 2., 6., 20.);
  Data(CS_ng_mg, -1, -1, -1, -1, -1, -1);
  Print(CL_ng_mg, 0., .5, 1., 2., 6., 20.);
  Data(CL_ng_mg, -1, -1, -1, -1, -1, -1);
  Print(CLU_ng_mg, 0., .5, 1., 2., 6., 20.);
  Data(CLU_ng_mg, -1, -1, -1, -1, -1, -1);
  Print(CSE_ng_mg, 0., .5, 1., 2., 6., 20.);
  Data(CSE_ng_mg, -1, -1, -1, -1, -1, -1);
  }


Simulation { # Mouse A,  0.5 hour

  SC_Dose=100.0;

  BW = 0.0185;  #kg
  VSp = 0.000056; #kg
  VL = 0.000796;
  VK = 0.000265;
  VLU = 0.000167;

  Print(CK_ng_mg, 0., .5, 1., 2., 6., 20.);
  Data(CK_ng_mg, -1, 130., -1, -1, -1, -1);
  Print(CS_ng_mg, 0., .5, 1., 2., 6., 20.);
  Data(CS_ng_mg, -1, 16.2, -1, -1, -1, -1);
  Print(CL_ng_mg, 0., .5, 1., 2., 6., 20.);
  Data(CL_ng_mg, -1, 17.2, -1, -1, -1, -1);
  Print(CLU_ng_mg, 0., .5, 1., 2., 6., 20.);
  Data(CLU_ng_mg, -1, 61.4, -1, -1, -1, -1);
  Print(CSE_ng_mg, 0., .5, 1., 2., 6., 20.);
  Data(CSE_ng_mg, -1, -1, -1, -1, -1, -1);
  }

Simulation { # Mouse B,  0.5 hour

  SC_Dose=100.0;
```

```
  BW = 0.0182;
  VSp = 0.000071; #kg
  VL = 0.000834;
  VK = 0.000243;
  VLU = 0.000227;

  Print(CK_ng_mg, 0., .5, 1., 2., 6., 20.);
  Data(CK_ng_mg, -1, 117.0, -1, -1, -1, -1);
  Print(CS_ng_mg, 0., .5, 1., 2., 6., 20.);
  Data(CS_ng_mg, -1, 12.6, -1, -1, -1, -1);
  Print(CL_ng_mg, 0., .5, 1., 2., 6., 20.);
  Data(CL_ng_mg, -1, 13.8, -1, -1, -1, -1);
  Print(CLU_ng_mg, 0., .5, 1., 2., 6., 20.);
  Data(CLU_ng_mg, -1, 46.6, -1, -1, -1, -1);
  Print(CSE_ng_mg, 0., .5, 1., 2., 6., 20.);
  Data(CSE_ng_mg, -1, 65.9, -1, -1, -1, -1);
  }

Simulation { # Mouse C,  0.5 hour

  SC_Dose=100.0;

  BW = 0.0180;
  VSp = 0.000069; #kg
  VL = 0.001037;
  VK = 0.000282;
  VLU = 0.000156;

  Print(CK_ng_mg, 0., .5, 1., 2., 6., 20.);
  Data(CK_ng_mg, -1, 114, -1, -1, -1, -1);
  Print(CS_ng_mg, 0., .5, 1., 2., 6., 20.);
  Data(CS_ng_mg, -1, 15.0, -1, -1, -1, -1);
  Print(CL_ng_mg, 0., .5, 1., 2., 6., 20.);
  Data(CL_ng_mg, -1, 12.8, -1, -1, -1, -1);
  Print(CLU_ng_mg, 0., .5, 1., 2., 6., 20.);
  Data(CLU_ng_mg, -1, 45.7, -1, -1, -1, -1);
  Print(CSE_ng_mg, 0., .5, 1., 2., 6., 20.);
  Data(CSE_ng_mg, -1, 57.9, -1, -1, -1, -1);
  }

Simulation { # Mouse D,  0.5 hour

  SC_Dose=100.0;

  BW = 0.0184;
  VSp = 0.000068; #kg
  VL = 0.001009;
  VK = 0.000305;
  VLU = 0.000181;

  Print(CK_ng_mg, 0., .5, 1., 2., 6., 20.);
  Data(CK_ng_mg, -1, 84.1, -1, -1, -1, -1);
  Print(CS_ng_mg, 0., .5, 1., 2., 6., 20.);
  Data(CS_ng_mg, -1, 10.3, -1, -1, -1, -1);
  Print(CL_ng_mg, 0., .5, 1., 2., 6., 20.);
  Data(CL_ng_mg, -1, 12.0, -1, -1, -1, -1);
```

```
  Print(CLU_ng_mg, 0., .5, 1., 2., 6., 20.);
  Data(CLU_ng_mg, -1, 33.8, -1, -1, -1, -1);
  Print(CSE_ng_mg, 0., .5, 1., 2., 6., 20.);
  Data(CSE_ng_mg, -1, 43.8, -1, -1, -1, -1);
  }

Simulation { # Mouse A,  1.0 hour

  SC_Dose=100.0;

  BW = 0.0182;
  VSp = 0.000070; #kg
  VL = 0.001072;
  VK = 0.000266;
  VLU = 0.000167;

  Print(CK_ng_mg, 0., .5, 1., 2., 6., 20.);
  Data(CK_ng_mg, -1, -1, 96.2, -1, -1, -1);
  Print(CS_ng_mg, 0., .5, 1., 2., 6., 20.);
  Data(CS_ng_mg, -1, -1, -1, -1, -1, -1);
  Print(CL_ng_mg, 0., .5, 1., 2., 6., 20.);
  Data(CL_ng_mg, -1, -1, -1, -1, -1, -1);
  Print(CLU_ng_mg, 0., .5, 1., 2., 6., 20.);
  Data(CLU_ng_mg, -1, -1, 19.1, -1, -1, -1);
  Print(CSE_ng_mg, 0., .5, 1., 2., 6., 20.);
  Data(CSE_ng_mg, -1, -1, 32.1, -1, -1, -1);
  }

Simulation { # Mouse B,  1.0 hour

  SC_Dose=100.0;

  BW = 0.0179;
  VSp = 0.000076; #kg
  VL = 0.000903;
  VK = 0.000273;
  VLU = 0.000185;

  Print(CK_ng_mg, 0., .5, 1., 2., 6., 20.);
  Data(CK_ng_mg, -1, -1, 146.0, -1, -1, -1);
  Print(CS_ng_mg, 0., .5, 1., 2., 6., 20.);
  Data(CS_ng_mg, -1, -1, -1, -1, -1, -1);
  Print(CL_ng_mg, 0., .5, 1., 2., 6., 20.);
  Data(CL_ng_mg, -1, -1, 10.4, -1, -1, -1);
  Print(CLU_ng_mg, 0., .5, 1., 2., 6., 20.);
  Data(CLU_ng_mg, -1, -1, 31.1, -1, -1, -1);
  Print(CSE_ng_mg, 0., .5, 1., 2., 6., 20.);
  Data(CSE_ng_mg, -1, -1, 47.9, -1, -1, -1);
  }

Simulation { # Mouse C,  1.0 hour

  SC_Dose=100.0;

  BW = 0.0183;
  VSp = 0.000061; #kg
  VL = 0.000976;
```

```
  VK = 0.000303;
  VLU = 0.000176;

  Print(CK_ng_mg, 0., .5, 1., 2., 6., 20.);
  Data(CK_ng_mg, -1, -1, 107.0, -1, -1, -1);
  Print(CS_ng_mg, 0., .5, 1., 2., 6., 20.);
  Data(CS_ng_mg, -1, -1, -1, -1, -1, -1);
  Print(CL_ng_mg, 0., .5, 1., 2., 6., 20.);
  Data(CL_ng_mg, -1, -1, -1, -1, -1, -1);
  Print(CLU_ng_mg, 0., .5, 1., 2., 6., 20.);
  Data(CLU_ng_mg, -1, -1, 15.0, -1, -1, -1);
  Print(CSE_ng_mg, 0., .5, 1., 2., 6., 20.);
  Data(CSE_ng_mg, -1, -1, 28.3, -1, -1, -1);
  }

Simulation { # Mouse D,  1.0 hour

  SC_Dose=100.0;

  BW = 0.0180;
  VSp = 0.000078; #kg
  VL = 0.000902;
  VK = 0.000261;
  VLU = 0.000166;

  Print(CK_ng_mg, 0., .5, 1., 2., 6., 20.);
  Data(CK_ng_mg, -1, -1, 130.0, -1, -1, -1);
  Print(CS_ng_mg, 0., .5, 1., 2., 6., 20.);
  Data(CS_ng_mg, -1, -1, -1, -1, -1, -1);
  Print(CL_ng_mg, 0., .5, 1., 2., 6., 20.);
  Data(CL_ng_mg, -1, -1, -1, -1, -1, -1);
  Print(CLU_ng_mg, 0., .5, 1., 2., 6., 20.);
  Data(CLU_ng_mg, -1, -1, -1, -1, -1, -1);
  Print(CSE_ng_mg, 0., .5, 1., 2., 6., 20.);
  Data(CSE_ng_mg, -1, -1, 29.1, -1, -1, -1);
  }

Simulation { # Mouse A,  2.0 hour

  SC_Dose=100.0;

  BW = 0.0187;
  VSp = 0.000065; #kg
  VL = 0.000895;
  VK = 0.000250;
  VLU = 0.000157;

  Print(CK_ng_mg, 0., .5, 1., 2., 6., 20.);
  Data(CK_ng_mg, -1, -1, -1, 211.0, -1, -1);
  Print(CS_ng_mg, 0., .5, 1., 2., 6., 20.);
  Data(CS_ng_mg, -1, -1, -1, -1, -1, -1);
  Print(CL_ng_mg, 0., .5, 1., 2., 6., 20.);
  Data(CL_ng_mg, -1, -1, -1, -1, -1, -1);
  Print(CLU_ng_mg, 0., .5, 1., 2., 6., 20.);
  Data(CLU_ng_mg, -1, -1, -1, 10.0, -1, -1);
  Print(CSE_ng_mg, 0., .5, 1., 2., 6., 20.);
  Data(CSE_ng_mg, -1, -1, -1, 4.55, -1, -1);
```

```
  }

Simulation { # Mouse B,  2.0 hour

  SC_Dose=100.0;

  BW = 0.0188;
  VSp = 0.000084; #kg
  VL = 0.000924;
  VK = 0.000284;
  VLU = 0.000172;

  Print(CK_ng_mg, 0., .5, 1., 2., 6., 20.);
  Data(CK_ng_mg, -1, -1, -1, 179.0, -1, -1);
  Print(CS_ng_mg, 0., .5, 1., 2., 6., 20.);
  Data(CS_ng_mg, -1, -1, -1, -1, -1, -1);
  Print(CL_ng_mg, 0., .5, 1., 2., 6., 20.);
  Data(CL_ng_mg, -1, -1, -1, -1, -1, -1);
  Print(CLU_ng_mg, 0., .5, 1., 2., 6., 20.);
  Data(CLU_ng_mg, -1, -1, -1, -1, -1, -1);
  Print(CSE_ng_mg, 0., .5, 1., 2., 6., 20.);
  Data(CSE_ng_mg, -1, -1, -1, 5.73, -1, -1);
  }

Simulation { # Mouse C,  2.0 hour

  SC_Dose=100.0;

  BW = 0.0179;
  VSp = 0.000059; #kg
  VL = 0.000881;
  VK = 0.000236;
  VLU = 0.000160;

  Print(CK_ng_mg, 0., .5, 1., 2., 6., 20.);
  Data(CK_ng_mg, -1, -1, -1, 195.0, -1, -1);
  Print(CS_ng_mg, 0., .5, 1., 2., 6., 20.);
  Data(CS_ng_mg, -1, -1, -1, -1, -1, -1);
  Print(CL_ng_mg, 0., .5, 1., 2., 6., 20.);
  Data(CL_ng_mg, -1, -1, -1, -1, -1, -1);
  Print(CLU_ng_mg, 0., .5, 1., 2., 6., 20.);
  Data(CLU_ng_mg, -1, -1, -1, 15.5, -1, -1);
  Print(CSE_ng_mg, 0., .5, 1., 2., 6., 20.);
  Data(CSE_ng_mg, -1, -1, -1, 12.6, -1, -1);
  }

Simulation { # Mouse D,  2.0 hour

  SC_Dose=100.0;

  BW = 0.0178;
  VSp = 0.000070; #kg
  VL = 0.000839;
  VK = 0.000250;
  VLU = 0.000169;

  Print(CK_ng_mg, 0., .5, 1., 2., 6., 20.);
```

```
  Data(CK_ng_mg, -1, -1, -1, 164.0, -1, -1);
  Print(CS_ng_mg, 0., .5, 1., 2., 6., 20.);
  Data(CS_ng_mg, -1, -1, -1, -1, -1, -1);
  Print(CL_ng_mg, 0., .5, 1., 2., 6., 20.);
  Data(CL_ng_mg, -1, -1, -1, -1, -1, -1);
  Print(CLU_ng_mg, 0., .5, 1., 2., 6., 20.);
  Data(CLU_ng_mg, -1, -1, -1, 10.4, -1, -1);
  Print(CSE_ng_mg, 0., .5, 1., 2., 6., 20.);
  Data(CSE_ng_mg, -1, -1, -1, 4.86, -1, -1);
  }

Simulation { # Mouse A,  6.0 hour

  SC_Dose=100.0;

  BW = 0.0185;
  VSp = 0.000062; #kg
  VL = 0.000869;
  VK = 0.000257;
  VLU = 0.000159;

  Print(CK_ng_mg, 0., .5, 1., 2., 6., 20.);
  Data(CK_ng_mg, -1, -1, -1, 210.0, -1, -1);
  Print(CS_ng_mg, 0., .5, 1., 2., 6., 20.);
  Data(CS_ng_mg, -1, -1, -1, -1, -1, -1);
  Print(CL_ng_mg, 0., .5, 1., 2., 6., 20.);
  Data(CL_ng_mg, -1, -1, -1, -1, -1, -1);
  Print(CLU_ng_mg, 0., .5, 1., 2., 6., 20.);
  Data(CLU_ng_mg, -1, -1, -1, -1, -1, -1);
  Print(CSE_ng_mg, 0., .5, 1., 2., 6., 20.);
  Data(CSE_ng_mg, -1, -1, -1, -1, -1, -1);
  }

Simulation { # Mouse B,  6.0 hour

  SC_Dose=100.0;

  BW = 0.0189;
  VSp = 0.000068; #kg
  VL = 0.000860;
  VK = 0.000258;
  VLU = 0.000156;

  Print(CK_ng_mg, 0., .5, 1., 2., 6., 20.);
  Data(CK_ng_mg, -1, -1, -1, 174.0, -1, -1);
  Print(CS_ng_mg, 0., .5, 1., 2., 6., 20.);
  Data(CS_ng_mg, -1, -1, -1, -1, -1, -1);
  Print(CL_ng_mg, 0., .5, 1., 2., 6., 20.);
  Data(CL_ng_mg, -1, -1, -1, -1, -1, -1);
  Print(CLU_ng_mg, 0., .5, 1., 2., 6., 20.);
  Data(CLU_ng_mg, -1, -1, -1, -1, -1, -1);
  Print(CSE_ng_mg, 0., .5, 1., 2., 6., 20.);
  Data(CSE_ng_mg, -1, -1, -1, -1, -1, -1);
  }

Simulation { # Mouse C,  6.0 hour
```

```
  SC_Dose=100.0;

  BW = 0.0191;
  VSp = 0.000069; #kg
  VL = 0.000930;
  VK = 0.000250;
  VLU = 0.000168;

  Print(CK_ng_mg, 0., .5, 1., 2., 6., 20.);
  Data(CK_ng_mg, -1, -1, -1, -1, 158.0, -1);
  Print(CS_ng_mg, 0., .5, 1., 2., 6., 20.);
  Data(CS_ng_mg, -1, -1, -1, -1, -1, -1);
  Print(CL_ng_mg, 0., .5, 1., 2., 6., 20.);
  Data(CL_ng_mg, -1, -1, -1, -1, -1, -1);
  Print(CLU_ng_mg, 0., .5, 1., 2., 6., 20.);
  Data(CLU_ng_mg, -1, -1, -1, -1, 10.0, -1);
  Print(CSE_ng_mg, 0., .5, 1., 2., 6., 20.);
  Data(CSE_ng_mg, -1, -1, -1, -1, -1, -1);
  }

Simulation { # Mouse D,  6.0 hour

  SC_Dose=100.0;

  BW = 0.0189;
  VSp = 0.000061; #kg
  VL = 0.000845;
  VK = 0.000238;
  VLU = 0.000143;

  Print(CK_ng_mg, 0., .5, 1., 2., 6., 20.);
  Data(CK_ng_mg,-1, -1, -1, -1, 185.0, -1);
  Print(CS_ng_mg, 0., .5, 1., 2., 6., 20.);
  Data(CS_ng_mg, -1, -1, -1, -1, -1, -1);
  Print(CL_ng_mg, 0., .5, 1., 2., 6., 20.);
  Data(CL_ng_mg, -1, -1, -1, -1, -1, -1);
  Print(CLU_ng_mg, 0., .5, 1., 2., 6., 20.);
  Data(CLU_ng_mg, -1, -1, -1, -1, -1, -1);
  Print(CSE_ng_mg, 0., .5, 1., 2., 6., 20.);
  Data(CSE_ng_mg, -1, -1, -1, -1, -1, -1);
  }

Simulation { # Mouse A,  20.0 hour

  SC_Dose=100.0;

  BW = 0.0184;
  VSp = 0.000074; #kg
  VL = 0.001082;
  VK = 0.000251;
  VLU = 0.000178;

  Print(CK_ng_mg, 0., .5, 1., 2., 6., 20.);
  Data(CK_ng_mg, -1, -1, -1, -1, 115.0, -1);
  Print(CS_ng_mg, 0., .5, 1., 2., 6., 20.);
  Data(CS_ng_mg, -1, -1, -1, -1, -1, -1);
  Print(CL_ng_mg, 0., .5, 1., 2., 6., 20.);
```

```
  Data(CL_ng_mg, -1, -1, -1, -1, -1, -1);
  Print(CLU_ng_mg, 0., .5, 1., 2., 6., 20.);
  Data(CLU_ng_mg, -1, -1, -1, -1, -1, -1);
  Print(CSE_ng_mg, 0., .5, 1., 2., 6., 20.);
  Data(CSE_ng_mg, -1, -1, -1, -1, -1, -1);
  }

Simulation { # Mouse B,  20.0 hour

  SC_Dose=100.0;

  BW = 0.0180;
  VSp = 0.000074; #kg
  VL = 0.000878;
  VK = 0.000247;
  VLU = 0.000210;

  Print(CK_ng_mg, 0., .5, 1., 2., 6., 20.);
  Data(CK_ng_mg, -1, -1, -1, -1, 131.0, -1);
  Print(CS_ng_mg, 0., .5, 1., 2., 6., 20.);
  Data(CS_ng_mg, -1, -1, -1, -1, -1, -1);
  Print(CL_ng_mg, 0., .5, 1., 2., 6., 20.);
  Data(CL_ng_mg, -1, -1, -1, -1, -1, -1);
  Print(CLU_ng_mg, 0., .5, 1., 2., 6., 20.);
  Data(CLU_ng_mg, -1, -1, -1, -1, -1, -1);
  Print(CSE_ng_mg, 0., .5, 1., 2., 6., 20.);
  Data(CSE_ng_mg, -1, -1, -1, -1, -1, -1);
  }

Simulation { # Mouse C,  20.0 hour

  SC_Dose=100.0;

  BW = 0.0186;
  VSp = 0.000056; #kg
  VL = 0.001106;
  VK = 0.000289;
  VLU = 0.000172;

  Print(CK_ng_mg, 0., .5, 1., 2., 6., 20.);
  Data(CK_ng_mg, -1, -1, -1, -1, 116.0, -1);
  Print(CS_ng_mg, 0., .5, 1., 2., 6., 20.);
  Data(CS_ng_mg, -1, -1, -1, -1, -1, -1);
  Print(CL_ng_mg, 0., .5, 1., 2., 6., 20.);
  Data(CL_ng_mg, -1, -1, -1, -1, -1, -1);
  Print(CLU_ng_mg, 0., .5, 1., 2., 6., 20.);
  Data(CLU_ng_mg, -1, -1, -1, -1, -1, -1);
  Print(CSE_ng_mg, 0., .5, 1., 2., 6., 20.);
  Data(CSE_ng_mg, -1, -1, -1, -1, -1, -1);
  }

Simulation { # Mouse D, 20.0 hour

  SC_Dose=100.0;

  BW = 0.0178;
  VSp = 0.000071; #kg
```

```
  VL = 0.001014;
  VK = 0.000236;
  VLU = 0.000167;

  Print(CK_ng_mg, 0., .5, 1., 2., 6., 20.);
  Data(CK_ng_mg, -1, -1, -1, -1, 146.0, -1);
  Print(CS_ng_mg, 0., .5, 1., 2., 6., 20.);
  Data(CS_ng_mg, -1, -1, -1, -1, -1, -1);
  Print(CL_ng_mg, 0., .5, 1., 2., 6., 20.);
  Data(CL_ng_mg, -1, -1, -1, -1, -1, -1);
  Print(CLU_ng_mg, 0., .5, 1., 2., 6., 20.);
  Data(CLU_ng_mg, -1, -1, -1, -1, -1, -1);
  Print(CSE_ng_mg, 0., .5, 1., 2., 6., 20.);
  Data(CSE_ng_mg, -1, -1, -1, -1, -1, -1);
  }

Simulation { # Mouse A, 0. hour

  SC_Dose=250.0;

  BW = 0.0179;  #kg
  VSp = 0.000060; #kg
  VL = 0.000892;
  VK = 0.000238;
  VLU = 0.000150;

  Print(CK_ng_mg, 0., .5, 1., 2., 6., 20.);
  Data(CK_ng_mg, -1, -1, -1, -1, -1, -1);
  Print(CS_ng_mg, 0., .5, 1., 2., 6., 20.);
  Data(CS_ng_mg, -1, -1, -1, -1, -1, -1);
  Print(CL_ng_mg, 0., .5, 1., 2., 6., 20.);
  Data(CL_ng_mg, -1, -1, -1, -1, -1, -1);
  Print(CLU_ng_mg, 0., .5, 1., 2., 6., 20.);
  Data(CLU_ng_mg, -1, -1, -1, -1, -1, -1);
  Print(CSE_ng_mg, 0., .5, 1., 2., 6., 20.);
  Data(CSE_ng_mg, -1, -1, -1, -1, -1, -1);
  }

Simulation { # Mouse B, 0. hour

  SC_Dose=250.0;

  BW = 0.0189;
  VSp = 0.000074; #kg
  VL = 0.000985;
  VK = 0.000255;
  VLU = 0.000152;

  Print(CK_ng_mg, 0., .5, 1., 2., 6., 20.);
  Data(CK_ng_mg, -1, -1, -1, -1, -1, -1);
  Print(CS_ng_mg, 0., .5, 1., 2., 6., 20.);
  Data(CS_ng_mg, -1, -1, -1, -1, -1, -1);
  Print(CL_ng_mg, 0., .5, 1., 2., 6., 20.);
  Data(CL_ng_mg, -1, -1, -1, -1, -1, -1);
  Print(CLU_ng_mg, 0., .5, 1., 2., 6., 20.);
  Data(CLU_ng_mg, -1, -1, -1, -1, -1, -1);
  Print(CSE_ng_mg, 0., .5, 1., 2., 6., 20.);
```

```
  Data(CSE_ng_mg, -1, -1, -1, -1, -1, -1);
  }

Simulation { # Mouse C, 0. hour

  SC_Dose=250.0;

  BW = 0.0185;
  VSp = 0.000081; #kg
  VL = 0.000908;
  VK = 0.000248;
  VLU = 0.000149;

  Print(CK_ng_mg, 0., .5, 1., 2., 6., 20.);
  Data(CK_ng_mg, -1, -1, -1, -1, -1, -1);
  Print(CS_ng_mg, 0., .5, 1., 2., 6., 20.);
  Data(CS_ng_mg, -1, -1, -1, -1, -1, -1);
  Print(CL_ng_mg, 0., .5, 1., 2., 6., 20.);
  Data(CL_ng_mg, -1, -1, -1, -1, -1, -1);
  Print(CLU_ng_mg, 0., .5, 1., 2., 6., 20.);
  Data(CLU_ng_mg, -1, -1, -1, -1, -1, -1);
  Print(CSE_ng_mg, 0., .5, 1., 2., 6., 20.);
  Data(CSE_ng_mg, -1, -1, -1, -1, -1, -1);
  }

Simulation { # Mouse D, 0. hour

  SC_Dose=250.0;

  BW = 0.0183;
  VSp = 0.000066; #kg
  VL = 0.000780;
  VK = 0.000261;
  VLU = 0.000132;

  Print(CK_ng_mg, 0., .5, 1., 2., 6., 20.);
  Data(CK_ng_mg, -1, -1, -1, -1, -1, -1);
  Print(CS_ng_mg, 0., .5, 1., 2., 6., 20.);
  Data(CS_ng_mg, -1, -1, -1, -1, -1, -1);
  Print(CL_ng_mg, 0., .5, 1., 2., 6., 20.);
  Data(CL_ng_mg, -1, -1, -1, -1, -1, -1);
  Print(CLU_ng_mg, 0., .5, 1., 2., 6., 20.);
  Data(CLU_ng_mg, -1, -1, -1, -1, -1, -1);
  Print(CSE_ng_mg, 0., .5, 1., 2., 6., 20.);
  Data(CSE_ng_mg, -1, -1, -1, -1, -1, -1);
  }

Simulation { # Mouse A, 0.5 hour

  SC_Dose=250.0;

  BW = 0.0106;
  VSp = 0.000057; #kg
  VL = 0.000974;
  VK = 0.000248;
  VLU = 0.000133;
```

```
  Print(CK_ng_mg, 0.5);
  Data(CK_ng_mg, 221.0);
  Print(CS_ng_mg, 0.5);
  Data(CS_ng_mg, 27.0);
  Print(CL_ng_mg, 0.5);
  Data(CL_ng_mg, 24.8);
  Print(CLU_ng_mg, 0.5);
  Data(CLU_ng_mg, 91.8);
  Print(CSE_ng_mg, 0.5);
  Data(CSE_ng_mg, 178.0);
}

Simulation { # Mouse B, 0.5 hour

  SC_Dose=250.0;

  BW = 0.0205;
  VSp = 0.000091; #kg
  VL = 0.00001012;
  VK = 0.000294;
  VLU = 0.000184;

  Print(CK_ng_mg, 0.5);
  Data(CK_ng_mg, 210.0);
  Print(CS_ng_mg, 0.5);
  Data(CS_ng_mg, 21.8);
  Print(CL_ng_mg, 0.5);
  Data(CL_ng_mg, 27.6);
  Print(CLU_ng_mg, 0.5);
  Data(CLU_ng_mg, 103.0);
  Print(CSE_ng_mg, 0.5);
  Data(CSE_ng_mg, 147.0);
}

Simulation { # Mouse C, 0.5 hour

  SC_Dose=250.0;

  BW = 0.0189;
  VSp = 0.000064; #kg
  VL = 0.000895;
  VK = 0.000234;
  VLU = 0.000141;

  Print(CK_ng_mg, 0.5);
  Data(CK_ng_mg, 223.0);
  Print(CS_ng_mg, 0.5);
  Data(CS_ng_mg, 32.5);
  Print(CL_ng_mg, 0.5);
  Data(CL_ng_mg, 26.1);
  Print(CLU_ng_mg, 0.5);
  Data(CLU_ng_mg, 96.0);
  Print(CSE_ng_mg, 0.5);
  Data(CSE_ng_mg, 180.0);
}

 Simulation { # Mouse D, 0.5 hour
```

```
  SC_Dose=250.0;

  BW = 0.0181;
  VSp = 0.000062; #kg
  VL = 0.000985;
  VK = 0.000257;
  VLU = 0.000142;

  Print(CK_ng_mg, 0.5);
  Data(CK_ng_mg, -1);
  Print(CS_ng_mg, 0.5);
  Data(CS_ng_mg, -1);
  Print(CL_ng_mg, 0.5);
  Data(CL_ng_mg, -1);
  Print(CLU_ng_mg, 0.5);
  Data(CLU_ng_mg, 20.7);
  Print(CSE_ng_mg, 0.5);
  Data(CSE_ng_mg, 26.8);
}

Simulation { # Mouse A, 1.0 hour

  SC_Dose=250.0;

  BW = 0.0197;
  VSp = 0.000069; #kg
  VL = 0.001050;
  VK = 0.0002677;
  VLU = 0.000156;

  Print(CK_ng_mg, 1.0);
  Data(CK_ng_mg, 313.0);
  Print(CS_ng_mg, 1.0);
  Data(CS_ng_mg, 18.2);
  Print(CL_ng_mg, 1.0);
  Data(CL_ng_mg, 22.4);
  Print(CLU_ng_mg, 1.0);
  Data(CLU_ng_mg, 45.4);
  Print(CSE_ng_mg, 1.0);
  Data(CSE_ng_mg, 131.0);
}

Simulation { # Mouse B, 1.0 hour

  SC_Dose=250.0;

  BW = 0.0191;
  VSp = 0.000071; #kg
  VL = 0.000970;
  VK = 0.000274;
  VLU = 0.000179;

  Print(CK_ng_mg, 1.0);
  Data(CK_ng_mg, 244.0);
  Print(CS_ng_mg, 1.0);
  Data(CS_ng_mg, 14.2);
```

```
  Print(CL_ng_mg, 1.0);
  Data(CL_ng_mg, 16.7);
  Print(CLU_ng_mg, 1.0);
  Data(CLU_ng_mg, 51.5);
  Print(CSE_ng_mg, 1.0);
  Data(CSE_ng_mg, 61.5);
}

Simulation { # Mouse C, 1.0 hour

  SC_Dose=250.0;

  BW = 0.0181;
  VSp = 0.000065; #kg
  VL = 0.000907;
  VK = 0.000258;
  VLU = 0.000163;

  Print(CK_ng_mg, 1.0);
  Data(CK_ng_mg, 183.0);
  Print(CS_ng_mg, 1.0);
  Data(CS_ng_mg, 14.0);
  Print(CL_ng_mg, 1.0);
  Data(CL_ng_mg, 14.7);
  Print(CLU_ng_mg, 1.0);
  Data(CLU_ng_mg, 41.1);
  Print(CSE_ng_mg, 1.0);
  Data(CSE_ng_mg, 64.7);
}

Simulation { # Mouse D, 1.0 hour

  SC_Dose= 250.0;

  BW = 0.0188;
  VSp = 0.000077; #kg
  VL = 0.000851;
  VK = 0.000265;
  VLU = 0.000147;

  Print(CK_ng_mg, 1.0);
  Data(CK_ng_mg, 255.0);
  Print(CS_ng_mg, 1.0);
  Data(CS_ng_mg, 14.5);
  Print(CL_ng_mg, 1.0);
  Data(CL_ng_mg, 22.6);
  Print(CLU_ng_mg, 1.0);
  Data(CLU_ng_mg, 61.7);
  Print(CSE_ng_mg, 1.0);
  Data(CSE_ng_mg, 90.1);
}

Simulation { # Mouse A, 2.0 hour

  SC_Dose=250.0;

  BW = 0.0195;
```

```
  VSp = 0.000062; #kg
  VL = 0.000998;
  VK = 0.000267;
  VLU = 0.000193;

  Print(CK_ng_mg, 2.0);
  Data(CK_ng_mg, 352.0);
  Print(CS_ng_mg, 2.0);
  Data(CS_ng_mg, -1);
  Print(CL_ng_mg, 2.0);
  Data(CL_ng_mg, -1);
  Print(CLU_ng_mg, 2.0);
  Data(CLU_ng_mg, 14.3);
  Print(CSE_ng_mg, 2.0);
  Data(CSE_ng_mg, 8.0);
}

Simulation { # Mouse B, 2.0 hour

  SC_Dose=250.0;

  BW = 0.0201;
  VSp = 0.000077; #kg
  VL = 0.001083;
  VK = 0.000268;
  VLU = 0.000162;

  Print(CK_ng_mg, 2.0);
  Data(CK_ng_mg, 340.0);
  Print(CS_ng_mg, 2.0);
  Data(CS_ng_mg, -1);
  Print(CL_ng_mg, 2.0);
  Data(CL_ng_mg, -1);
  Print(CLU_ng_mg, 2.0);
  Data(CLU_ng_mg, -1);
  Print(CSE_ng_mg, 2.0);
  Data(CSE_ng_mg, 13.7);
}

Simulation { # Mouse C, 2.0 hour

  SC_Dose=250.0;

  BW = 0.0206;
  VSp = 0.000080; #kg
  VL = 0.001110;
  VK = 0.000280;
  VLU = 0.000163;

  Print(CK_ng_mg, 2.0);
  Data(CK_ng_mg, 334.0);
  Print(CS_ng_mg, 2.0);
  Data(CS_ng_mg, -1);
  Print(CL_ng_mg, 2.0);
  Data(CL_ng_mg, -1);
  Print(CLU_ng_mg, 2.0);
  Data(CLU_ng_mg, 11.1);
```

```
  Print(CSE_ng_mg, 2.0);
  Data(CSE_ng_mg, 15.6);
}

 Simulation { # Mouse D, 2.0 hour

  SC_Dose=250.0;

  BW = 0.0197;
  VSp = 0.000063; #kg
  VL = 0.000924;
  VK = 0.000247;
  VLU = 0.000174;

  Print(CK_ng_mg, 2.0);
  Data(CK_ng_mg, -1);
  Print(CS_ng_mg, 2.0);
  Data(CS_ng_mg, -1);
  Print(CL_ng_mg, 2.0);
  Data(CL_ng_mg, -1);
  Print(CLU_ng_mg, 2.0);
  Data(CLU_ng_mg, -1);
  Print(CSE_ng_mg, 2.0);
  Data(CSE_ng_mg, -1);
}

Simulation { # Mouse A, 6.0 hour

  SC_Dose=250.0;

  BW = 0.0186;
  VSp = 0.000069; #kg
  VL = 0.000900;
  VK = 0.000235;
  VLU = 0.000144;

  Print(CK_ng_mg, 6.0);
  Data(CK_ng_mg, 226.0);
  Print(CS_ng_mg, 6.0);
  Data(CS_ng_mg, -1);
  Print(CL_ng_mg, 6.0);
  Data(CL_ng_mg, -1);
  Print(CLU_ng_mg, 6.0);
  Data(CLU_ng_mg, -1);
  Print(CSE_ng_mg, 6.0);
  Data(CSE_ng_mg, -1);
}

Simulation { # Mouse B, 6.0 hour

  SC_Dose=250.0;

  BW = 0.0197;
  VSp = 0.000074; #kg
  VL = 0.000963;
  VK = 0.000271;
  VLU = 0.000154;
```

```
  Print(CK_ng_mg, 6.0);
  Data(CK_ng_mg, 212.0);
  Print(CS_ng_mg, 6.0);
  Data(CS_ng_mg, -1);
  Print(CL_ng_mg, 6.0);
  Data(CL_ng_mg, -1);
  Print(CLU_ng_mg, 6.0);
  Data(CLU_ng_mg, -1);
  Print(CSE_ng_mg, 6.0);
  Data(CSE_ng_mg, -1);
}

Simulation { # Mouse C, 6.0 hour

  SC_Dose=250.0;

  BW = 0.0183;
  VSp = 0.000064; #kg
  VL = 0.000929;
  VK = 0.000257;
  VLU = 0.000141;

  Print(CK_ng_mg, 6.0);
  Data(CK_ng_mg, 311.0);
  Print(CS_ng_mg, 6.0);
  Data(CS_ng_mg, -1);
  Print(CL_ng_mg, 6.0);
  Data(CL_ng_mg, -1);
  Print(CLU_ng_mg, 6.0);
  Data(CLU_ng_mg, 10.5);
  Print(CSE_ng_mg, 6.0);
  Data(CSE_ng_mg, -1);
}

Simulation { # Mouse D, 6.0 hour

  SC_Dose=250.0;

  BW = 0.0196;
  VSp = 0.000074; #kg
  VL = 0.000951;
  VK = 0.000273;
  VLU = 0.000186;

  Print(CK_ng_mg, 6.0);
  Data(CK_ng_mg, 220.0);
  Print(CS_ng_mg, 6.0);
  Data(CS_ng_mg, -1);
  Print(CL_ng_mg, 6.0);
  Data(CL_ng_mg, -1);
  Print(CLU_ng_mg, 6.0);
  Data(CLU_ng_mg, -1);
  Print(CSE_ng_mg, 6.0);
  Data(CSE_ng_mg, -1);
}
```

```
Simulation { # Mouse A, 20.0 hour

  SC_Dose=250.0;

  BW = 0.0182;
  VSp = 0.000063; #kg
  VL = 0.0010761;
  VK = 0.000274;
  VLU = 0.000165;

  Print(CK_ng_mg, 20.0);
  Data(CK_ng_mg, 146.0);
  Print(CS_ng_mg, 20.0);
  Data(CS_ng_mg, -1);
  Print(CL_ng_mg, 20.0);
  Data(CL_ng_mg, -1);
  Print(CLU_ng_mg, 20.0);
  Data(CLU_ng_mg, -1);
  Print(CSE_ng_mg, 20.0);
  Data(CSE_ng_mg, -1);
}

Simulation { # Mouse B, 20.0 hour

  SC_Dose=250.0;

  BW = 0.0183;
  VSp = 0.000081; #kg
  VL = 0.001096;
  VK = 0.000261;
  VLU = 0.000146;

  Print(CK_ng_mg, 20.0);
  Data(CK_ng_mg, 116.0);
  Print(CS_ng_mg, 20.0);
  Data(CS_ng_mg, -1);
  Print(CL_ng_mg, 20.0);
  Data(CL_ng_mg, -1);
  Print(CLU_ng_mg, 20.0);
  Data(CLU_ng_mg, -1);
  Print(CSE_ng_mg, 20.0);
  Data(CSE_ng_mg, -1);
}

Simulation { # Mouse C, 20.0 hour

  SC_Dose=250.0;

  BW = 0.0191;
  VSp = 0.000069; #kg
  VL = 0.001003;
  VK = 0.000266;
  VLU = 0.000148;

  Print(CK_ng_mg, 20.0);
  Data(CK_ng_mg, 116.0);
  Print(CS_ng_mg, 20.0);
```

```
  Data(CS_ng_mg, -1);
  Print(CL_ng_mg, 20.0);
  Data(CL_ng_mg, -1);
  Print(CLU_ng_mg, 20.0);
  Data(CLU_ng_mg, -1);
  Print(CSE_ng_mg, 20.0);
  Data(CSE_ng_mg, -1);
}

Simulation { # Mouse D, 20.0 hour

  SC_Dose=250.0;

  BW = 0.0180;
  VSp = 0.000078; #kg
  VL = 0.001058;
  VK = 0.000249;
  VLU = 0.000152;

  Print(CK_ng_mg, 20.0);
  Data(CK_ng_mg, 220.0);
  Print(CS_ng_mg, 20.0);
  Data(CS_ng_mg, -1);
  Print(CL_ng_mg, 20.0);
  Data(CL_ng_mg, -1);
  Print(CLU_ng_mg, 20.0);
  Data(CLU_ng_mg, -1);
  Print(CSE_ng_mg, 20.0);
  Data(CSE_ng_mg, -1);
   }
 }
}
End.
```

Appendix XII: MCMC Posterior Parameter Predictions (Experimental Max Fit)

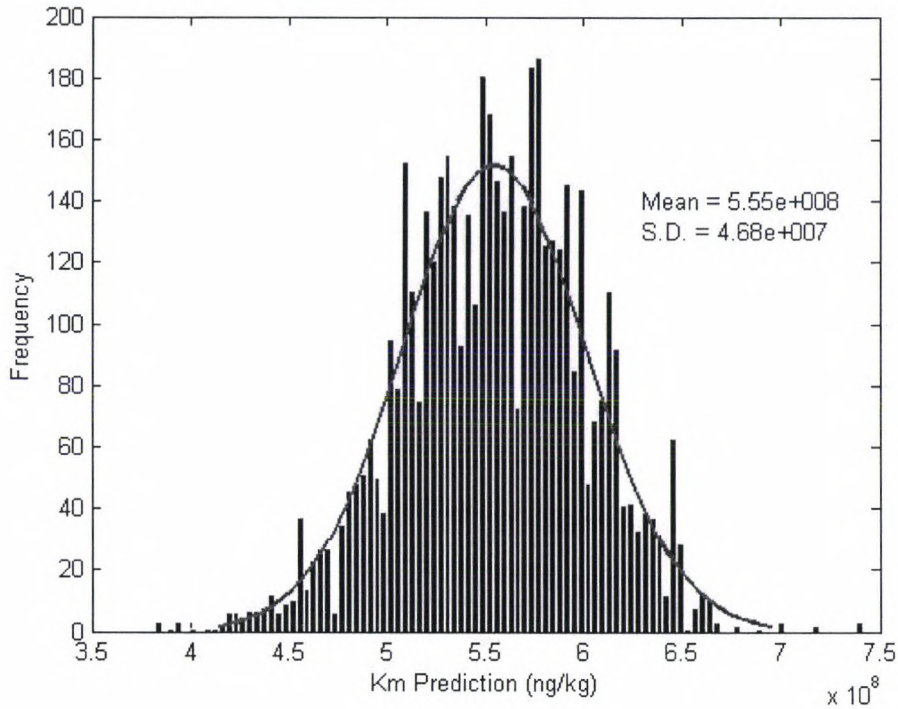

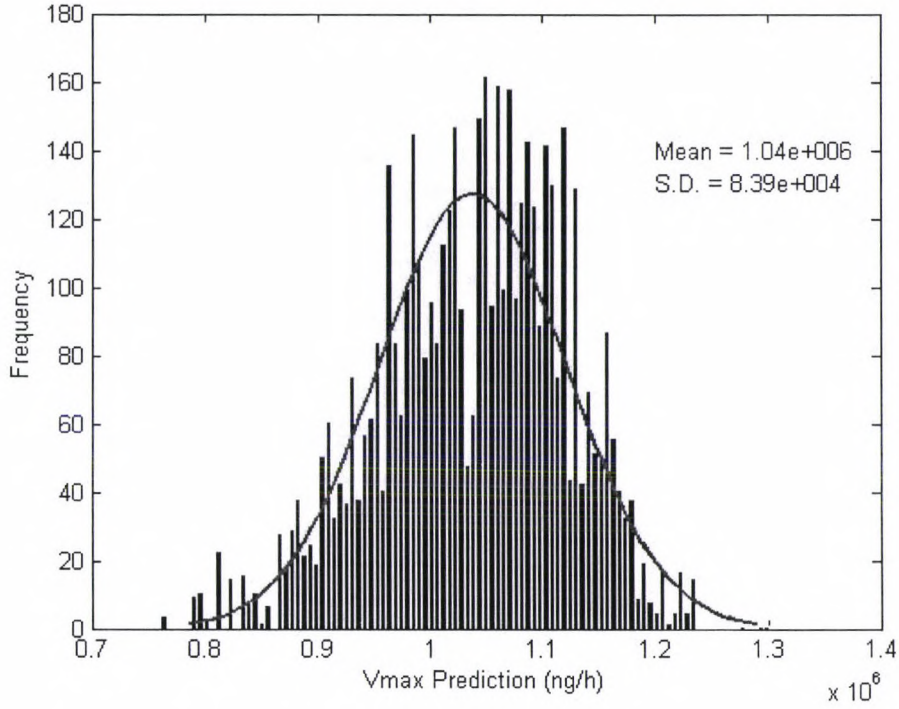
Mean = 1.04e+006
S.D. = 8.39e+004
Frequency
Vmax Prediction (ng/h)
x 10^6

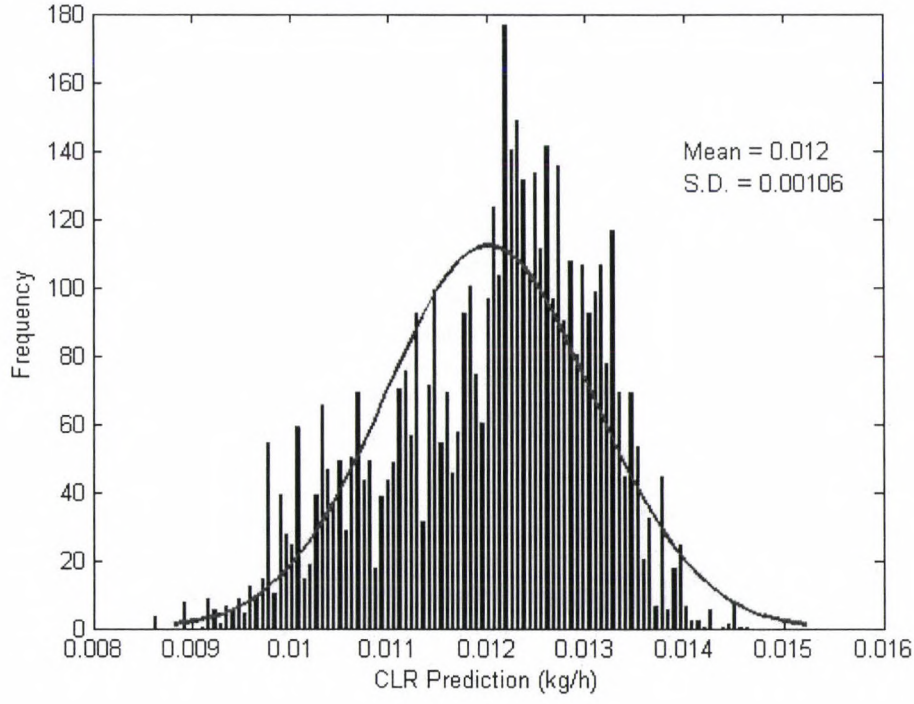
Mean = 0.012
S.D. = 0.00106
Frequency
CLR Prediction (kg/h)

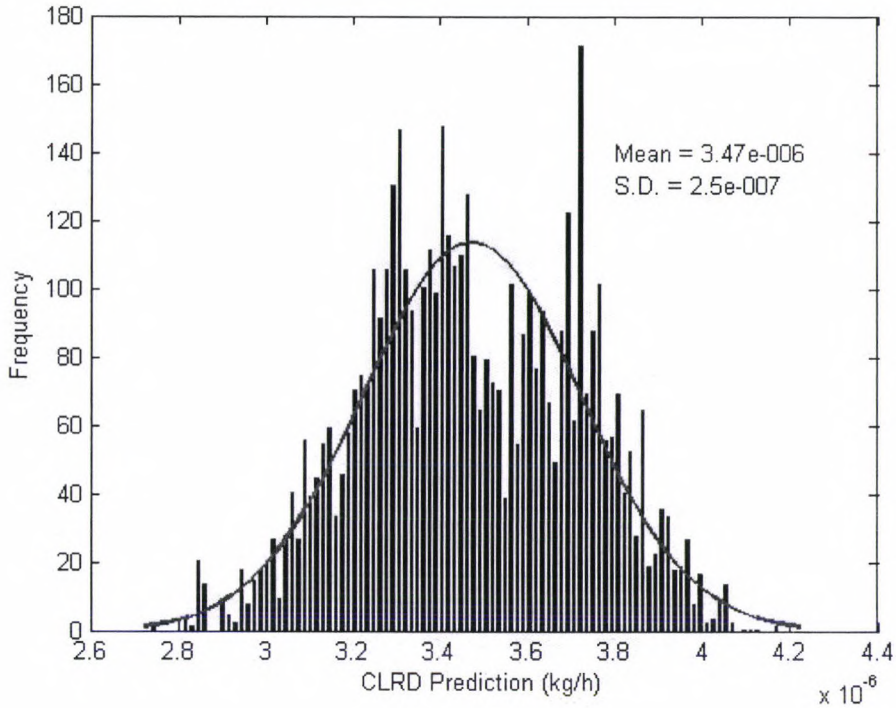
Mean = 3.47e-006
S.D. = 2.5e-007
Frequency
CLRD Prediction (kg/h)
x 10^-6

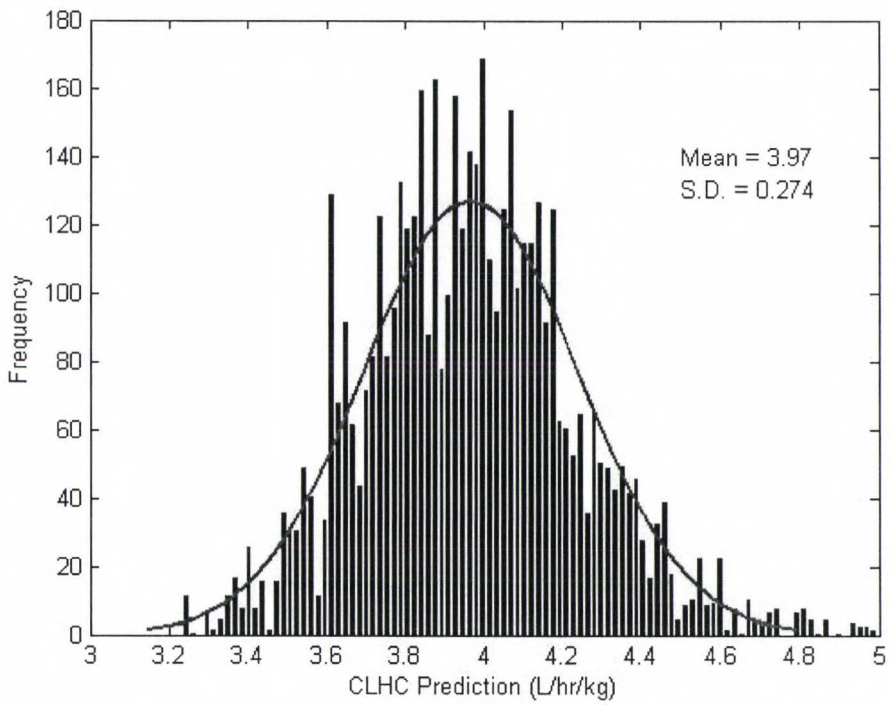
Mean = 3.97
S.D. = 0.274
Frequency
CLHC Prediction (L/hr/kg)

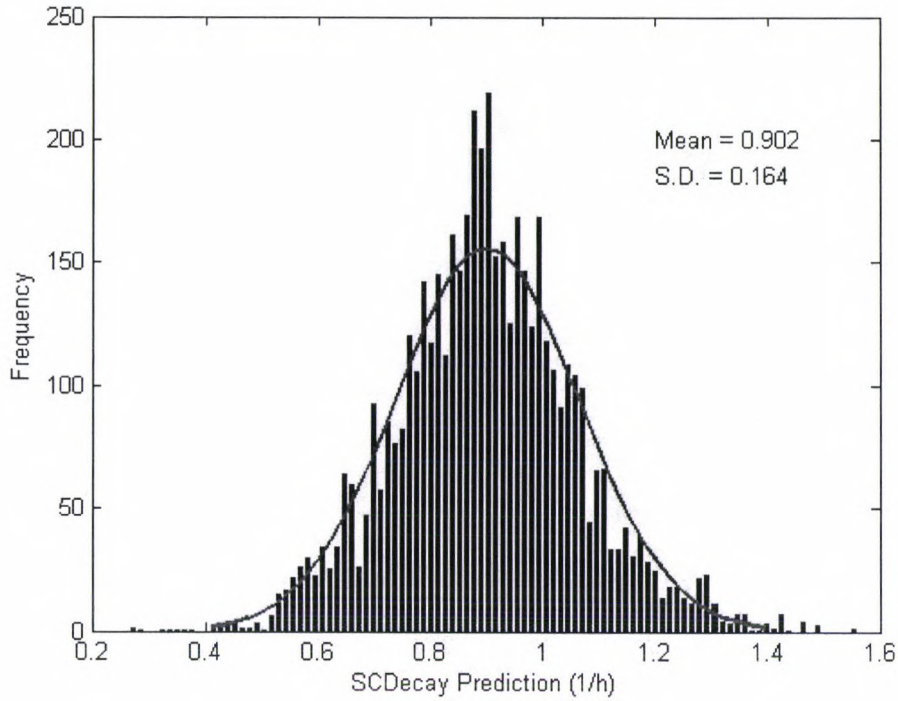
250
200
150
100
50
0
Frequency
Mean = 0.902
S.D. = 0.164
0.2
0.4
0.6
0.8
1
1.2
1.4
1.6
SCDecay Prediction (1/h)

Appendix XIII: MCMC Posterior Parameter Predictions (extrapolated max fit)

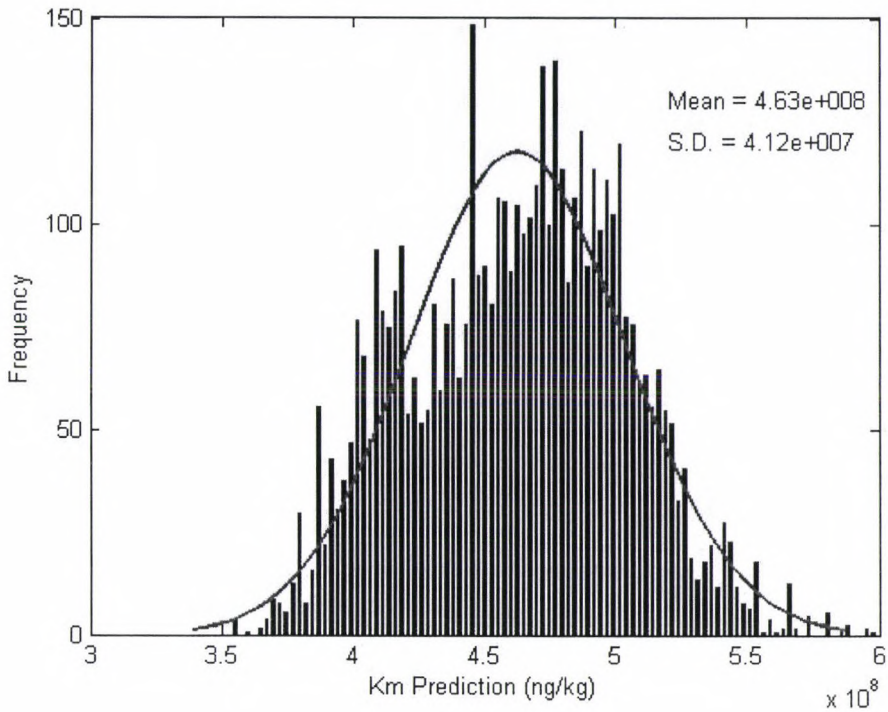

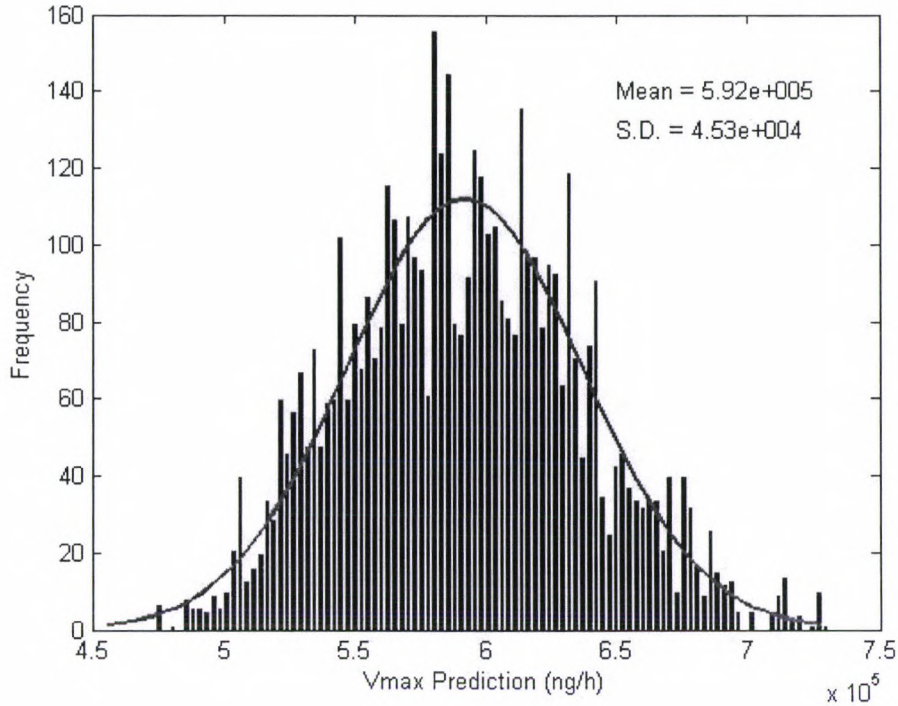
Mean = 5.92e+005
S.D. = 4.53e+004
Frequency
Vmax Prediction (ng/h)
x 10^5

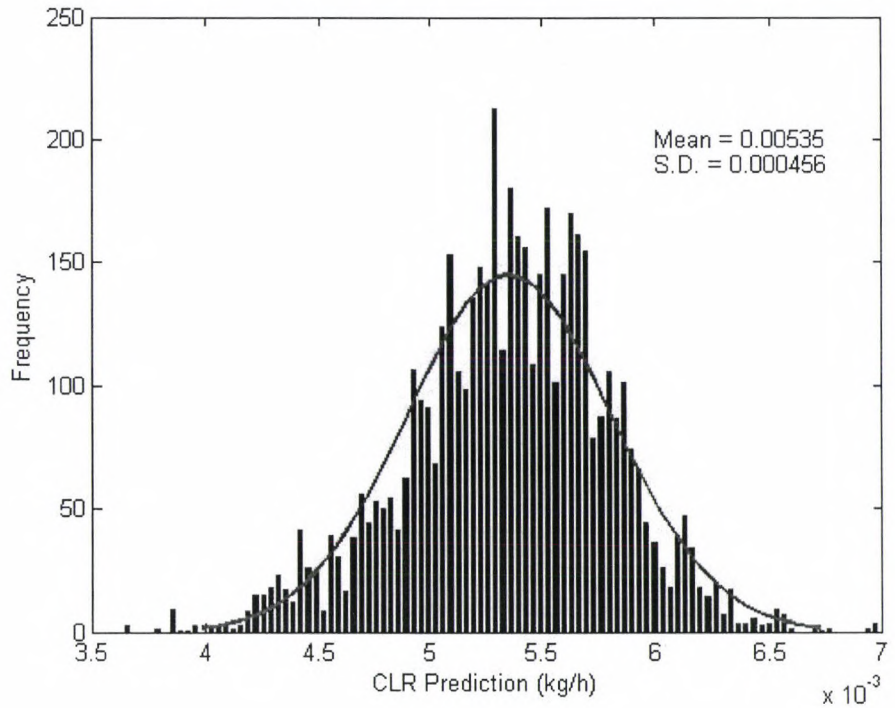
Mean = 0.00535
S.D. = 0.000456
Frequency
CLR Prediction (kg/h)
x 10^-3

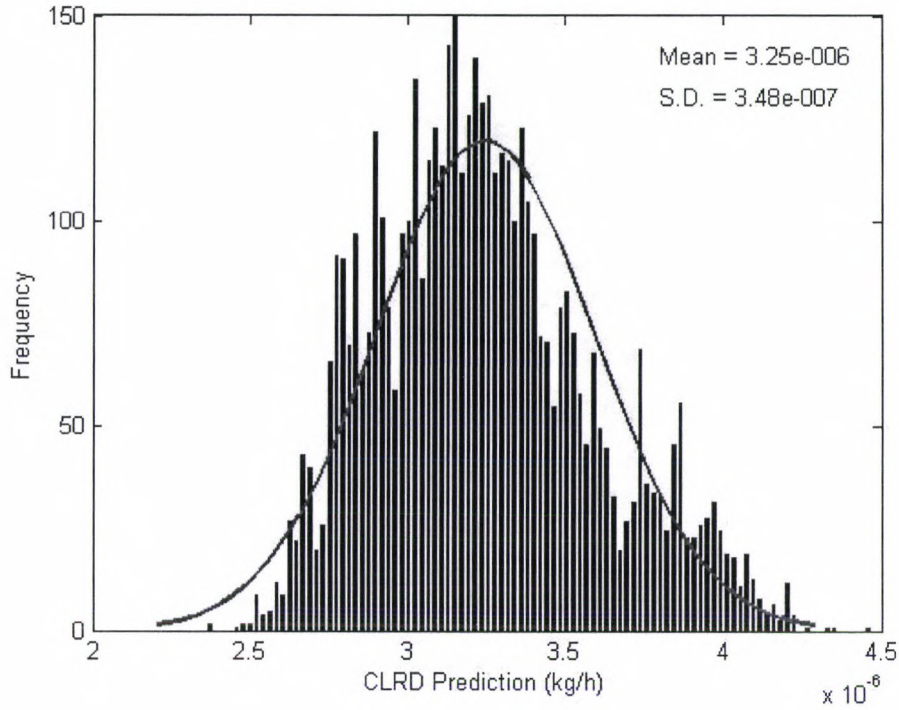
Mean = 3.25e-006
S.D. = 3.48e-007
Frequency
CLRD Prediction (kg/h)
x 10^-6

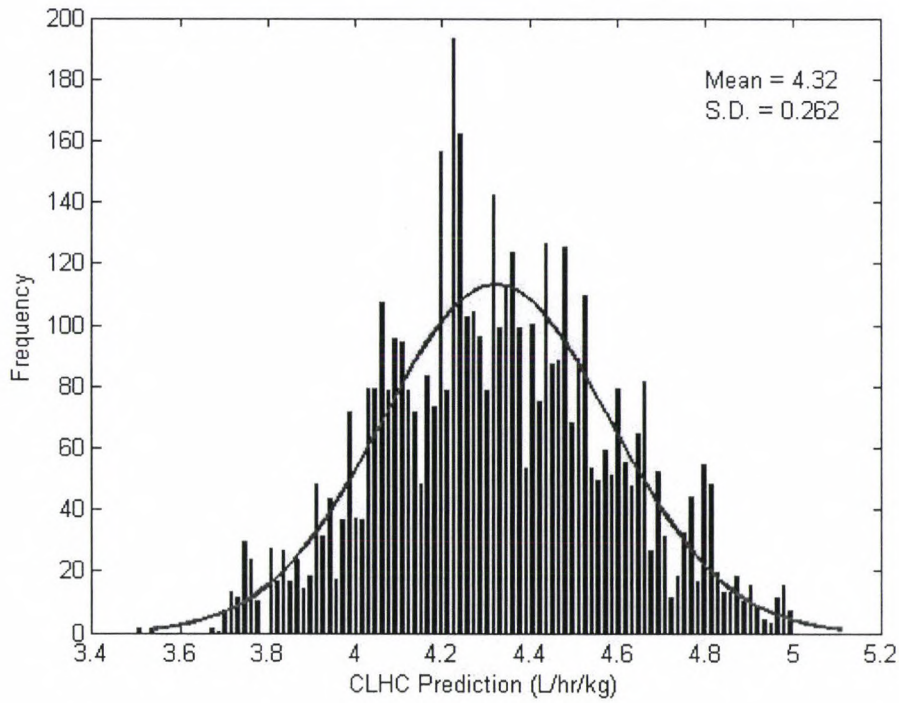
Mean = 4.32
S.D. = 0.262
Frequency
CLHC Prediction (L/hr/kg)

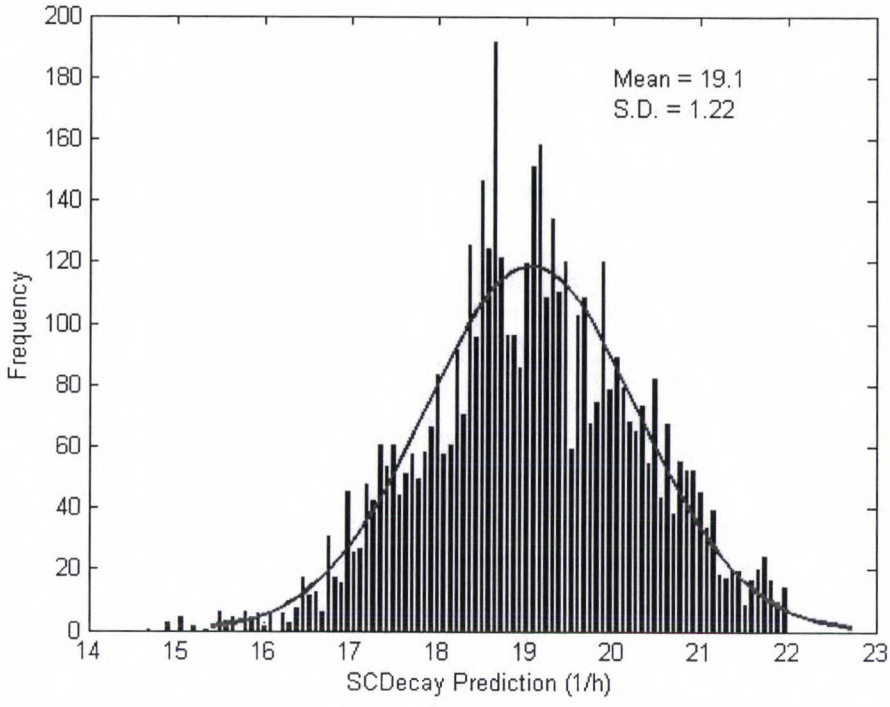
Mean = 19.1
S.D. = 1.22
Frequency
SCDecay Prediction (1/h)
0
20
40
60
80
100
120
140
160
180
200
14
15
16
17
18
19
20
21
22
23

Appendix XIV: Forward simulation results using MCMC posterior predicted parameter means (fit to experimental maximum) for a 100 mg/kg dose.

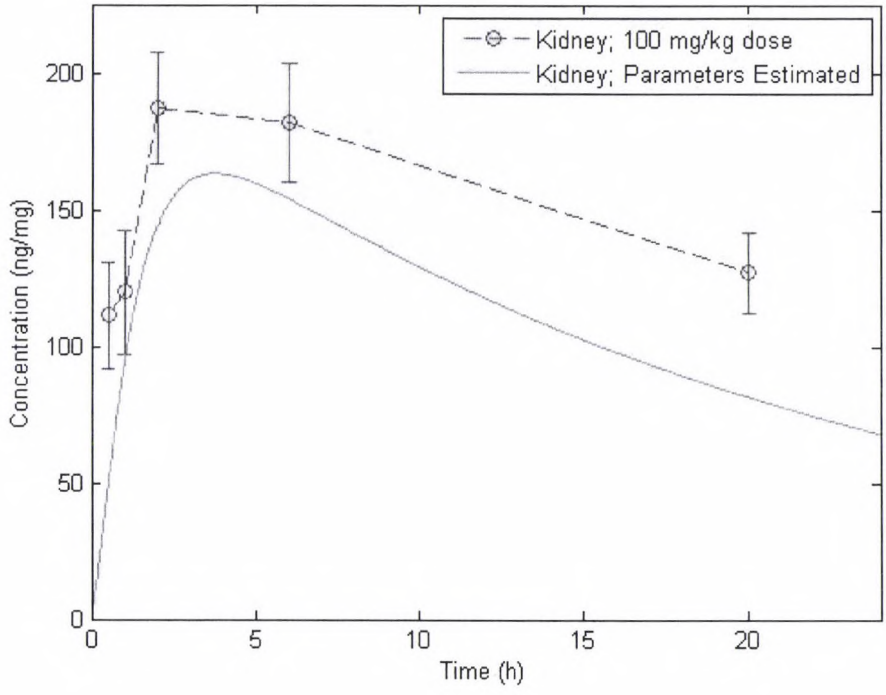

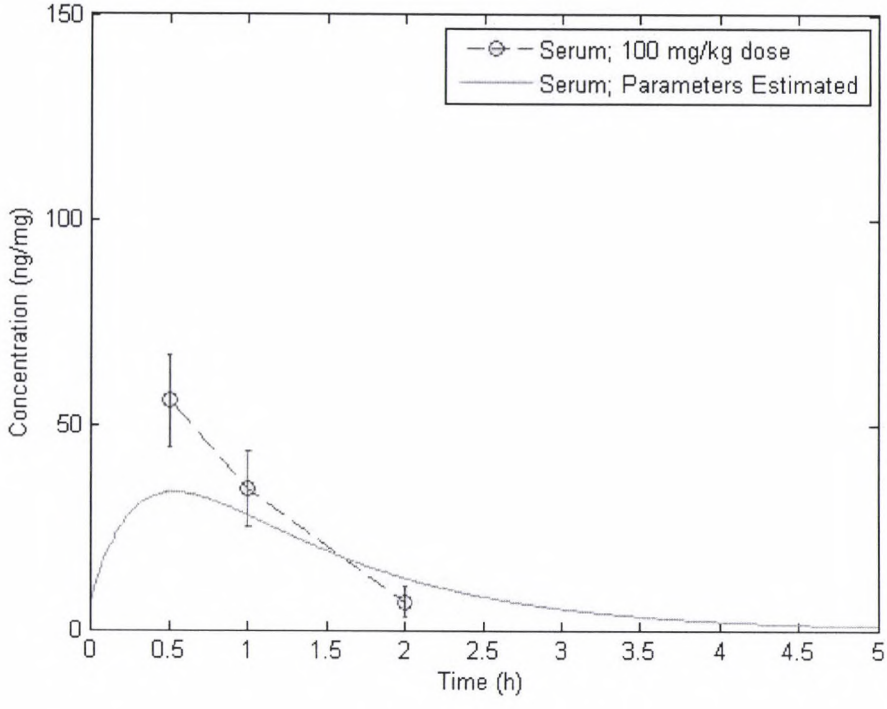
Serum; 100 mg/kg dose
Serum; Parameters Estimated
Concentration (ng/mg)
Time (h)
0
50
100
150
0
0.5
1
1.5
2
2.5
3
3.5
4
4.5
5

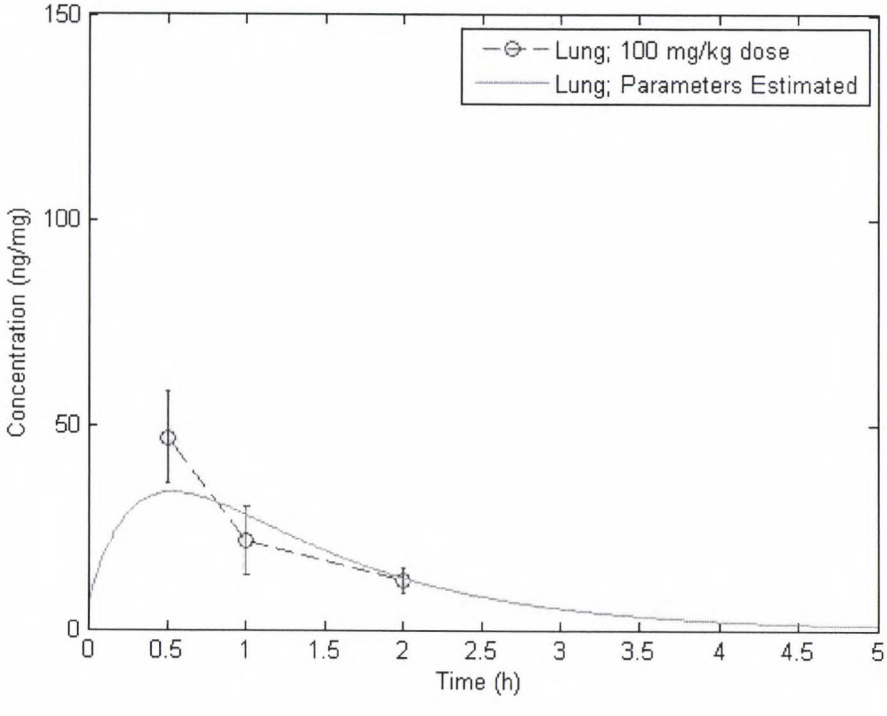
Lung; 100 mg/kg dose
Lung; Parameters Estimated
Concentration (ng/mg)
Time (h)
0
50
100
150
0
0.5
1
1.5
2
2.5
3
3.5
4
4.5
5

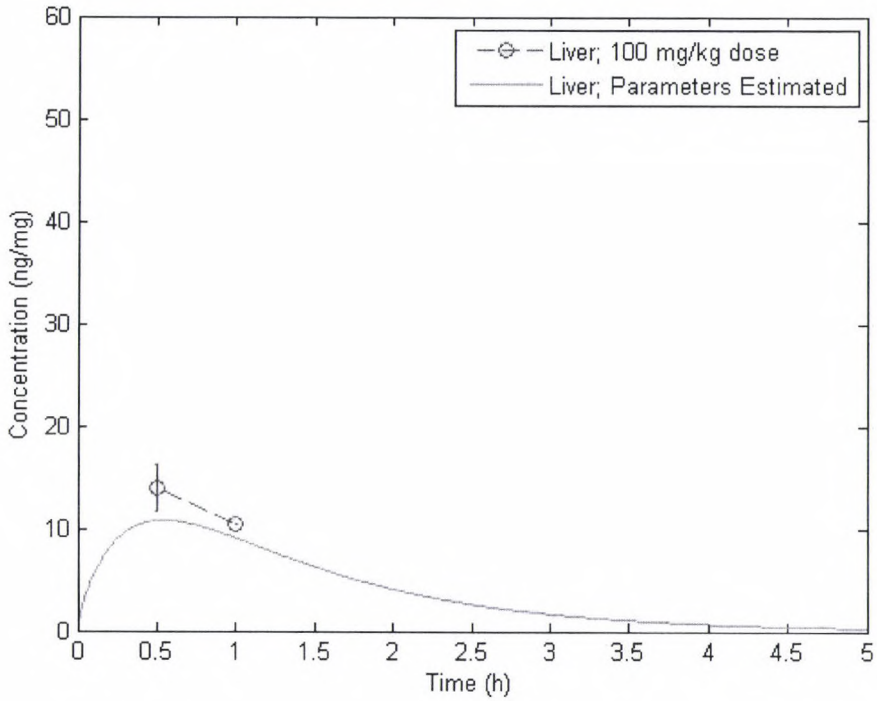
Liver; 100 mg/kg dose
Liver; Parameters Estimated
Concentration (ng/mg)
Time (h)
0
10
20
30
40
50
60
0
0.5
1
1.5
2
2.5
3
3.5
4
4.5
5

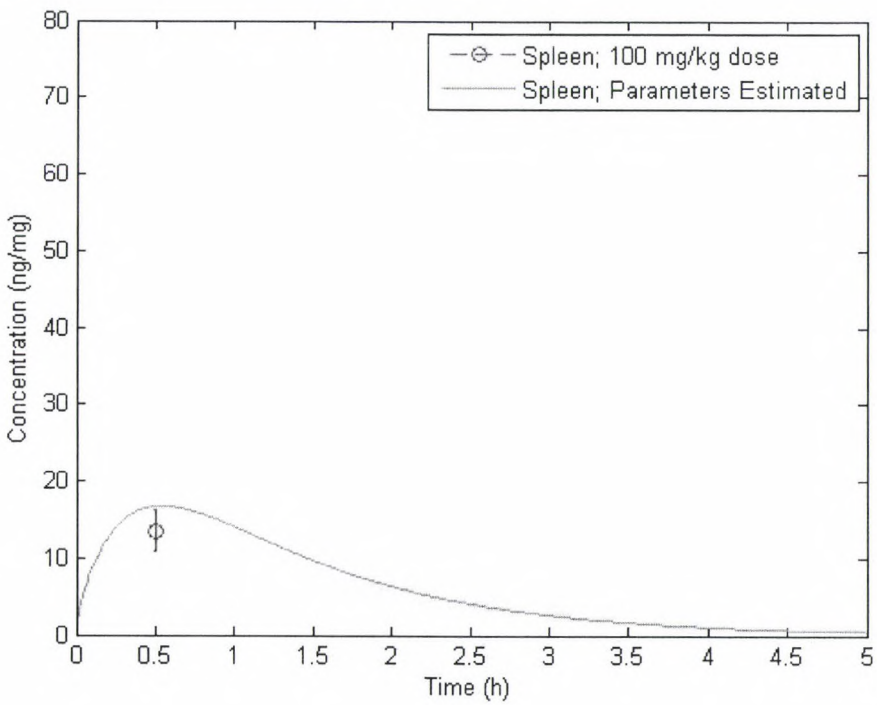
Spleen; 100 mg/kg dose
Spleen; Parameters Estimated
Concentration (ng/mg)
Time (h)
0
10
20
30
40
50
60
70
80
0
0.5
1
1.5
2
2.5
3
3.5
4
4.5
5

Appendix XV: Forward simulation results using MCMC posterior predicted parameter means (fit to experimental maximum) for a 250 mg/kg dose.

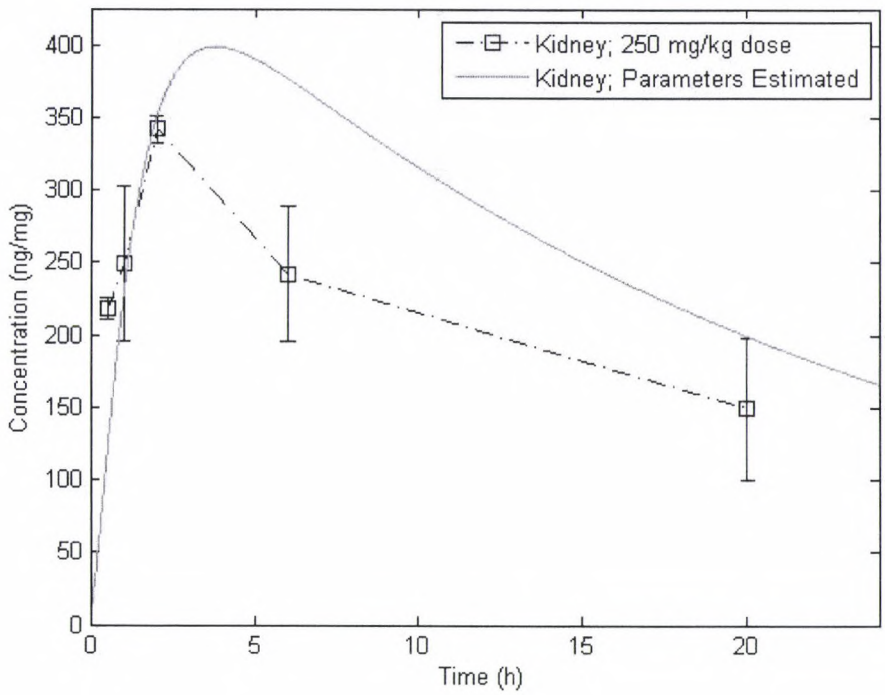

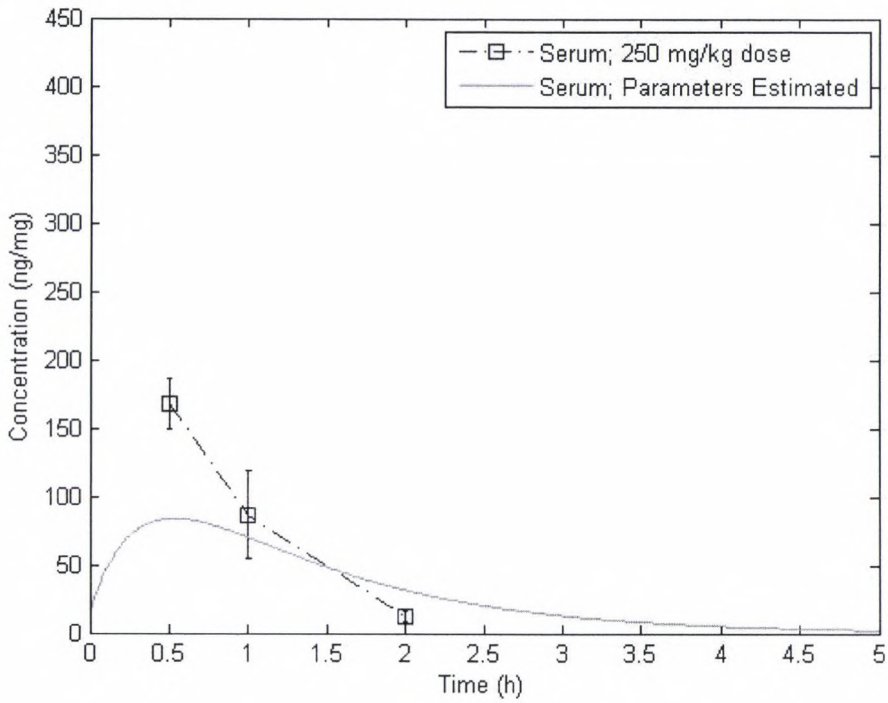
Serum; 250 mg/kg dose
Serum; Parameters Estimated
Concentration (ng/mg)
Time (h)
0
50
100
150
200
250
300
350
400
450
0
0.5
1
1.5
2
2.5
3
3.5
4
4.5
5

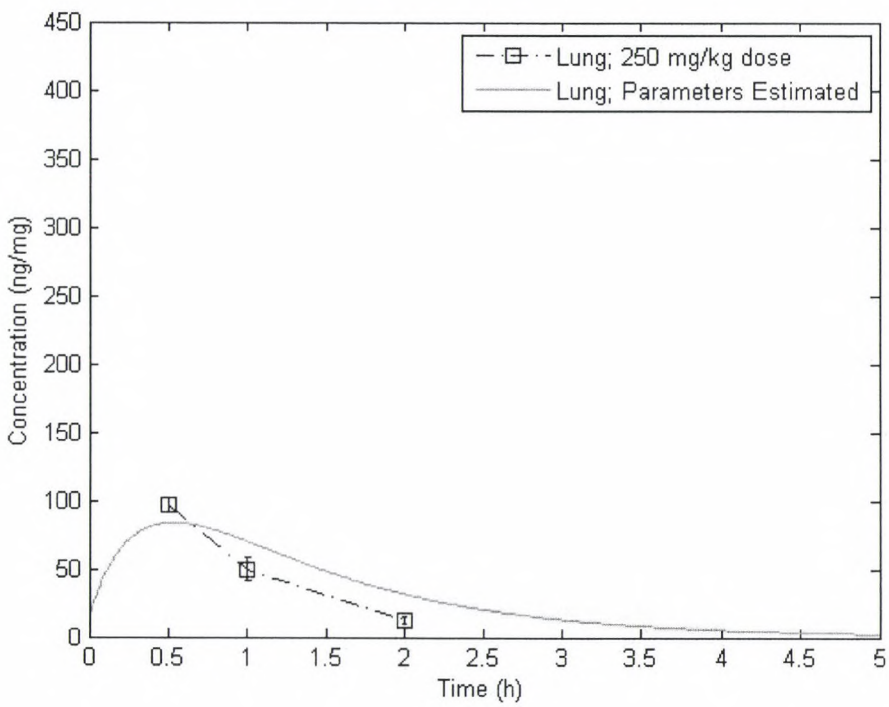
Lung; 250 mg/kg dose
Lung; Parameters Estimated
Concentration (ng/mg)
Time (h)
0
50
100
150
200
250
300
350
400
450
0
0.5
1
1.5
2
2.5
3
3.5
4
4.5
5

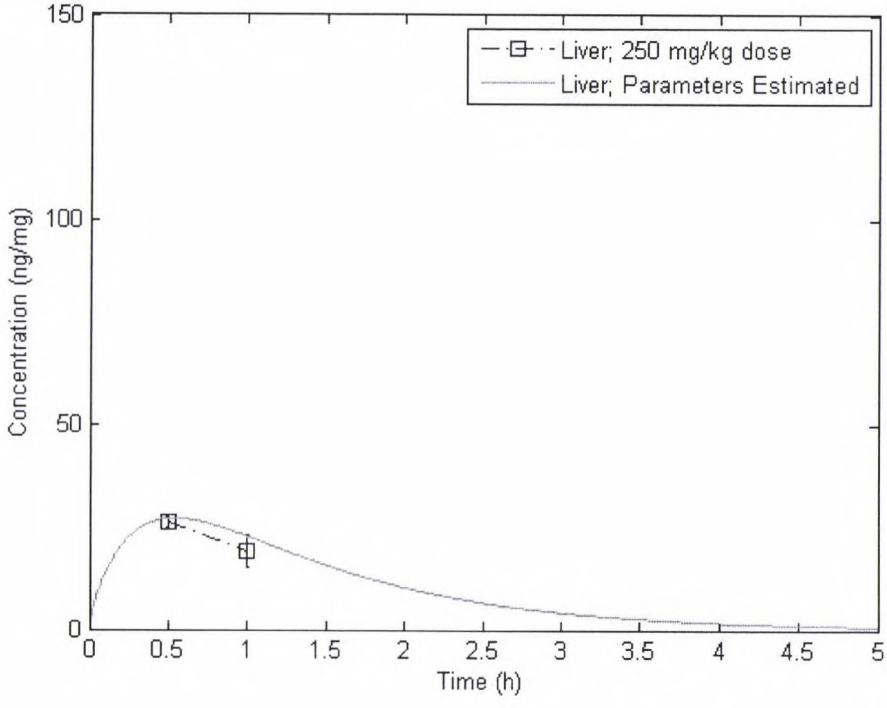
Liver; 250 mg/kg dose
Liver; Parameters Estimated
Concentration (ng/mg)
Time (h)
0
50
100
150
0
0.5
1
1.5
2
2.5
3
3.5
4
4.5
5

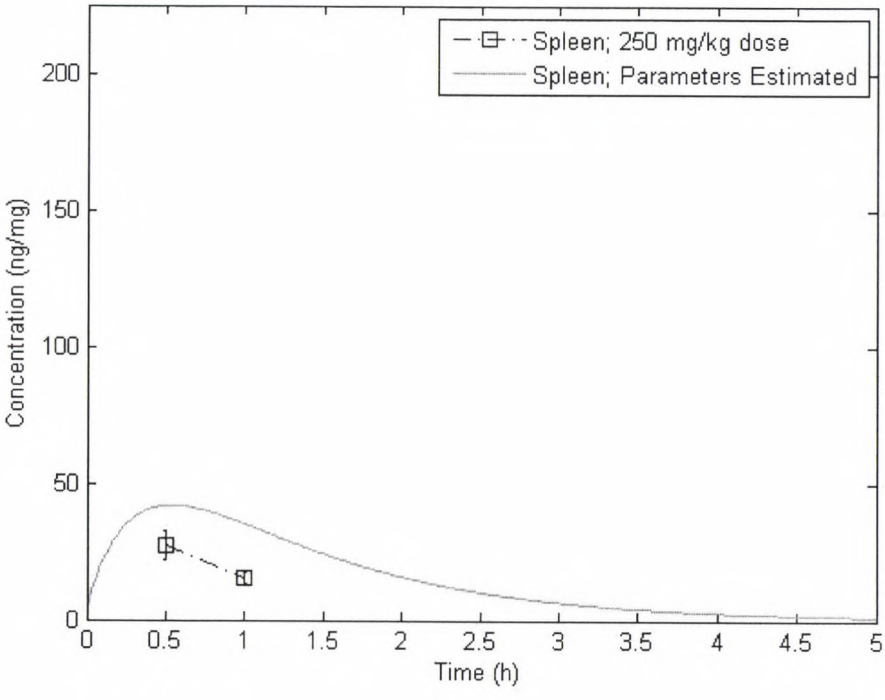
Spleen; 250 mg/kg dose
Spleen; Parameters Estimated
Concentration (ng/mg)
Time (h)
0
50
100
150
200
0
0.5
1
1.5
2
2.5
3
3.5
4
4.5
5

Appendix XVI: Forward simulation results using MCMC posterior predicted parameter means (fit to extrapolated maximum) for a 100 mg/kg dose.

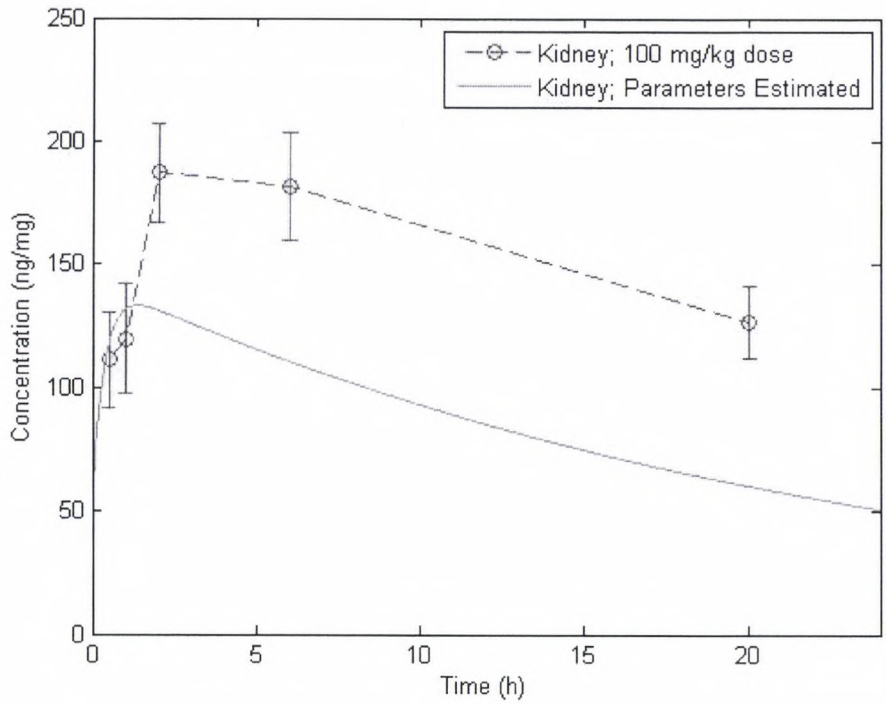

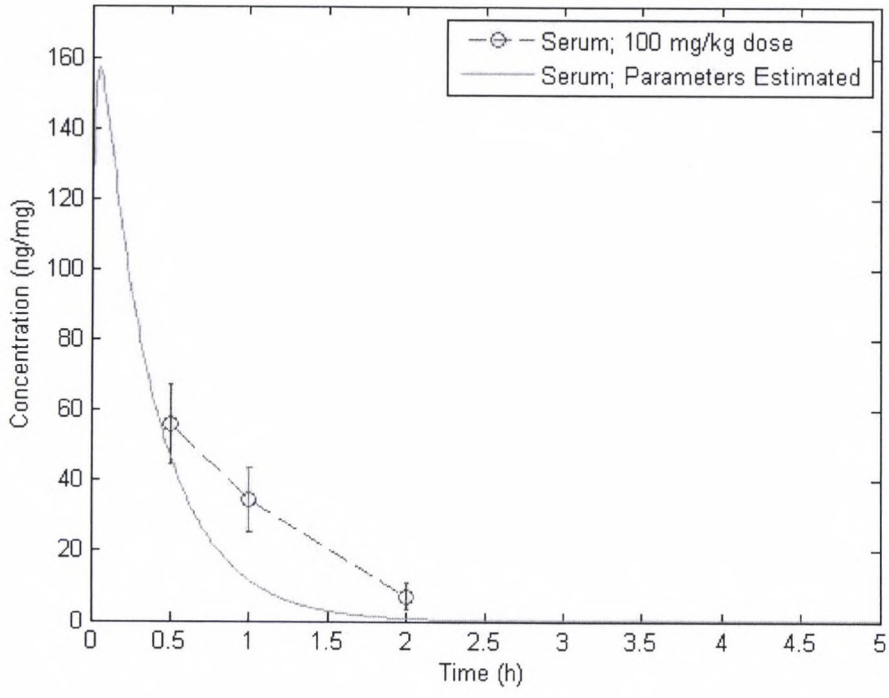
Serum; 100 mg/kg dose
Serum; Parameters Estimated
Concentration (ng/mg)
Time (h)
0
20
40
60
80
100
120
140
160
0
0.5
1
1.5
2
2.5
3
3.5
4
4.5
5

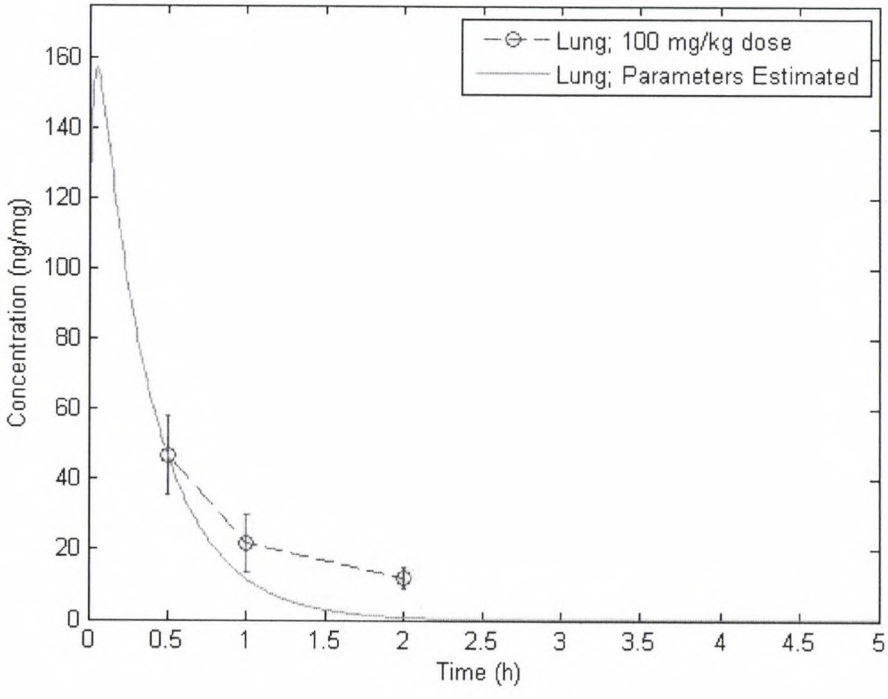
Lung; 100 mg/kg dose
Lung; Parameters Estimated
Concentration (ng/mg)
Time (h)
0
20
40
60
80
100
120
140
160
0
0.5
1
1.5
2
2.5
3
3.5
4
4.5
5

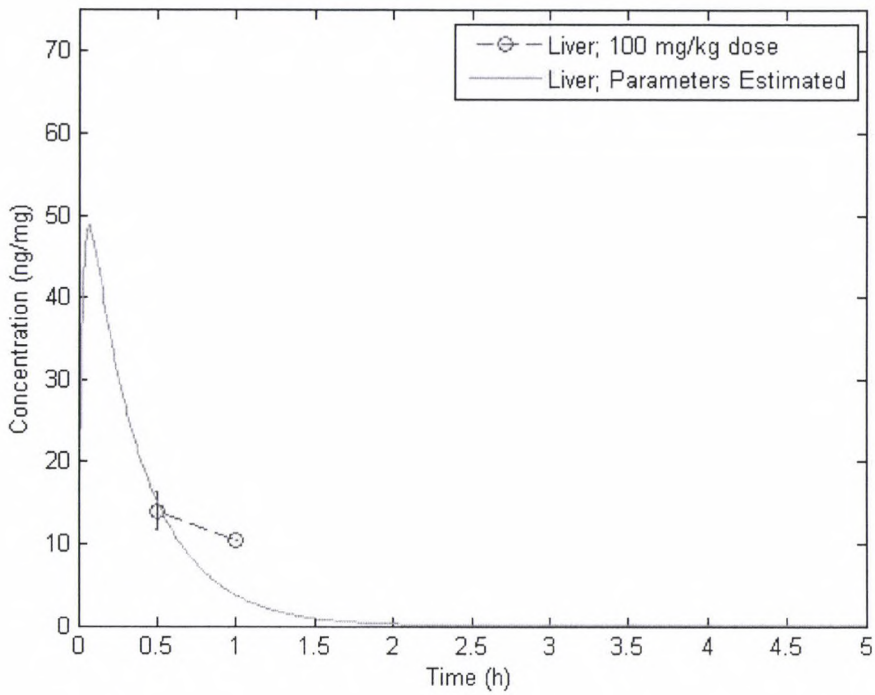
Liver; 100 mg/kg dose
Liver; Parameters Estimated
Concentration (ng/mg)
Time (h)
0
10
20
30
40
50
60
70
0
0.5
1
1.5
2
2.5
3
3.5
4
4.5
5

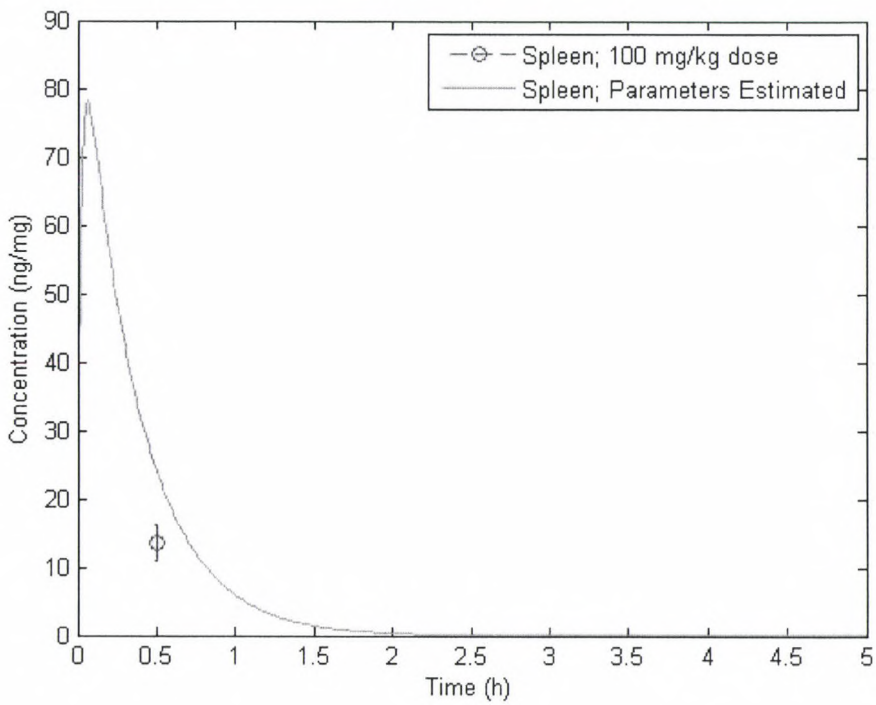
Spleen; 100 mg/kg dose
Spleen; Parameters Estimated
Concentration (ng/mg)
Time (h)
0
10
20
30
40
50
60
70
80
90
0
0.5
1
1.5
2
2.5
3
3.5
4
4.5
5

Appendix XVII: Forward simulation results using MCMC posterior predicted parameter means (fit to extrapolated maximum) for a 250 mg/kg dose.

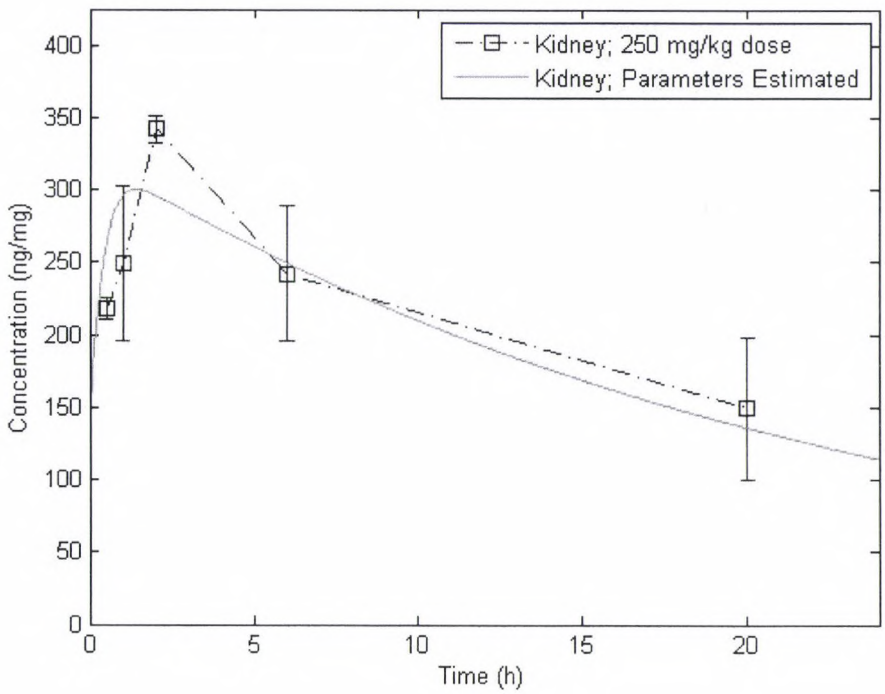

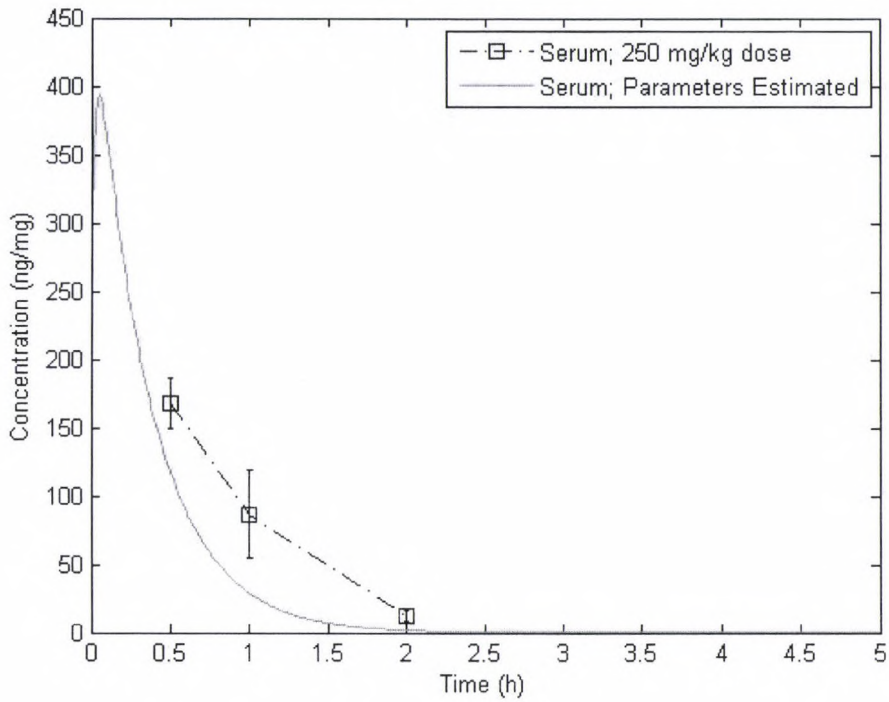
Serum; 250 mg/kg dose
Serum; Parameters Estimated
Concentration (ng/mg)
Time (h)
0
50
100
150
200
250
300
350
400
450
0
0.5
1
1.5
2
2.5
3
3.5
4
4.5
5

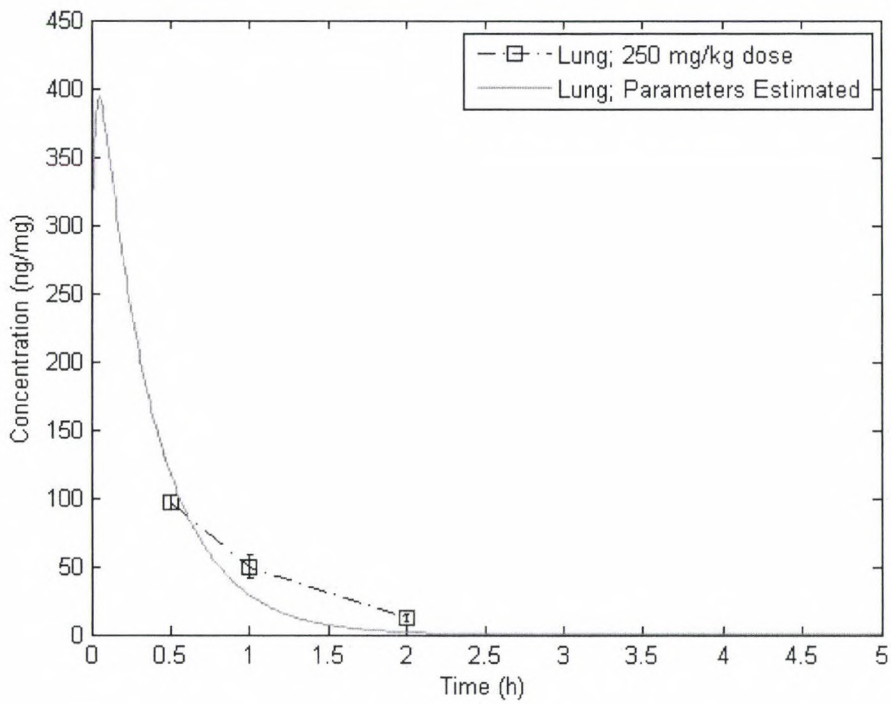
Lung; 250 mg/kg dose
Lung; Parameters Estimated
Concentration (ng/mg)
Time (h)
0
50
100
150
200
250
300
350
400
450
0
0.5
1
1.5
2
2.5
3
3.5
4
4.5
5

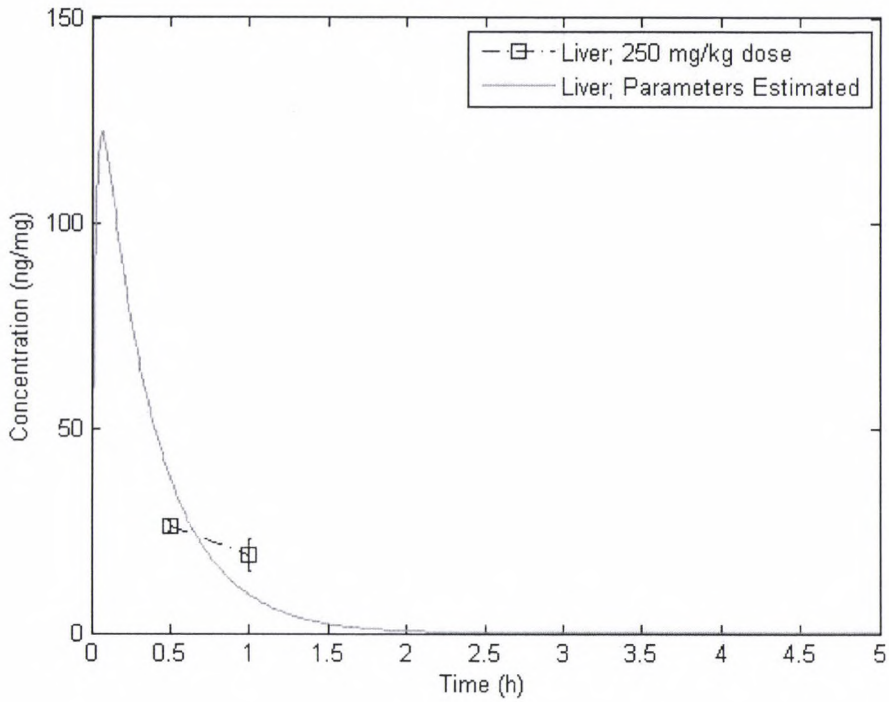
Liver; 250 mg/kg dose
Liver; Parameters Estimated
Concentration (ng/mg)
Time (h)
0
50
100
150
0
0.5
1
1.5
2
2.5
3
3.5
4
4.5
5

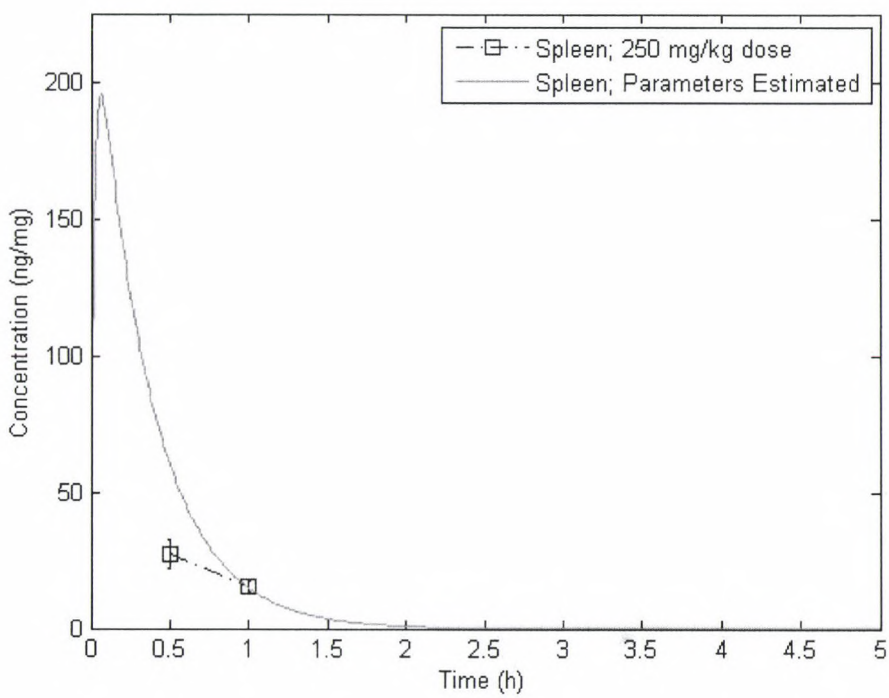
Spleen; 250 mg/kg dose
Spleen; Parameters Estimated
Concentration (ng/mg)
Time (h)
0
50
100
150
200
0
0.5
1
1.5
2
2.5
3
3.5
4
4.5
5

Appendix XVIII: Sample MATLAB m-file to randomize the MCMC output

```
CLHC=data(4000:5001,2);
Vmax=data(4000:5001,3);
Km=data(4000:5001,4);
CLR=data(4000:5001,5);
CLRD=data(4000:5001,6);
SC_Decay=data(4000:5001,7);
NPTS=numel(CLHC);
s_CLHC=CLHC(randperm(NPTS));
s_Vmax=Vmax(randperm(NPTS));
s_Km=Km(randperm(NPTS));
s_CLR=CLR(randperm(NPTS));
s_CLRD=CLRD(randperm(NPTS));
s_SC_Decay=SC_Decay(randperm(NPTS));

counter=(1:NPTS);
r_counter=transpose(counter);
s_vals=[r_counter s_CLHC s_Vmax s_Km s_CLR s_CLRD s_SC_Decay];

dlmwrite('c:\MCSim\Capreo\random.csv',s_vals)
```

Appendix XIX: Sample Set Points Simulation File

```
# capreo5_SC.sim

SimType(SetPoints)

SetPoints("capreo5_MC250.out", "randomMCMC_b.txt", 1000,
          CLHC, Vmax, Km, CLR, CLRD, SC_Decay);

# Partition Coefficients
  BP  = 1.; # Blood:plasma.
  PLU = 2.; # Lung:blood.
  PBR = 1.; # Brain:blood.
  PF  = 1.; # Fat:blood.
  PH  = 1.; # Heart:blood.
  PM  = 1.; # Muscle:blood.
  PB  = 1.; # Bone:blood.
  PSK = 1.; # Skin:blood.
  PKS = 1.; # Shallow kidney:blood.
  PS  = 1.; # Spleen:blood.
  PG  = 1.; # Gut:blood.
  PL  = 1.; # Liver:blood.
  PCR = 1.; # Carcass:blood.


Simulation { # 100 mg/kg

  SC_Dose=250.;

  PrintStep(CLU_ng_mg, 0, 24, 0.01);  # Lung.
  PrintStep(CSE_ng_mg, 0, 24, 0.01);  # Serum.
  PrintStep(CK_ng_mg,  0, 24, 0.01);  # Kidney.
  PrintStep(CS_ng_mg,  0, 24, 0.01);  # Spleen.
  PrintStep(CL_ng_mg,  0, 24, 0.01);  # Liver.

}

End.
```

Appendix XX: Sample MATLAB M-file for plotting maximum and minimum model prediction possibilities (250 mg/kg dose version)

```
clc
close all

A = data(1:1000,8:2408);
B = min(A);
C = max(A);
figure(1)
plot((0:0.01:24),B,'k')
hold on
plot((0:0.01:24),C,'--k')
hold on
t2= [.5,1.0,2.0];
c2= [96.93, 49.93, 12.7];
e2= [5.66, 8.93, 2.26];
errorbar(t2, c2, e2, '-.bs')
xlabel('Time (h)'),
ylabel('Concentration (ng/mg)')
legend('Lung Prediction Minimum', 'Lung Prediction Maximum','Lung
Experimental; 250 mg/kg dose')
axis([0 5. 0 450]);

D = data(1:1000,2409:4809);
E = min(D);
F = max(D);
figure(2)
plot((0:0.01:24),E,'k')
hold on
plot((0:0.01:24),F,'--k')
hold on
t2= [.5,1.0,2.0];
c2= [168.33,86.83,12.43];
e2= [18.50,32.11,3.96];
errorbar(t2, c2, e2, '-.bs')
xlabel('Time (h)'),
ylabel('Concentration (ng/mg)')
legend('Serum      Prediction      Minimum','Serum      Prediction
Maximum','Serum Experimental; 250 mg/kg dose')
axis([0 5. 0 450]);

G = data(1:1000,4810:7210);
H = min(G);
I = max(G);
figure(3)
plot((0:0.01:24),H,'k')
hold on
plot((0:0.01:24),I,'--k')
```

```
hold on
t2= [.5,1.0,2.0,6.0,20.0];
c2= [218.00,248.75,342.00,242.25,149.50];
e2= [7.00,53.27,9.17,46.19,49.08];
errorbar(t2, c2, e2, '-.bs')
xlabel('Time (h)'),
ylabel('Concentration (ng/mg)')
legend('Kidney Prediction Minimum', 'Kidney Prediction
Maximum','Kidney Experimental; 250 mg/kg dose')
axis([0 24. 0 425]);

J = data(1:1000,7211:9611);
K = min(J);
L = max(J);
figure(4)
plot((0:0.01:24),K,'k')
hold on
plot((0:0.01:24),L,'--k')
hold on
t2= [.5,1.0];
c2= [27.10,15.23];
e2= [5.35,1.99];
errorbar(t2, c2, e2, '-.bs')
xlabel('Time (h)'),
ylabel('Concentration (ng/mg)')
legend('Spleen Prediction Minimum', 'Spleen Prediction Maximum',
'Spleen Experimental; 250 mg/kg dose')
axis([0 5.0 0 225.]);


M = data(1:1000,7211:9611);
N = min(M);
P = max(M);
figure(5)
plot((0:0.01:24),N,'k')
hold on
plot((0:0.01:24),P,'--k')
hold on
t2= [.5,1.0];
c2= [26.17,19.10];
e2= [1.40,4.01];
errorbar(t2, c2, e2, '-.bs')
xlabel('Time (h)'),
ylabel('Concentration (ng/mg)')
legend('Liver Prediction Minimum','Liver Prediction Maximum',
'Liver Experimental; 250 mg/kg dose')
axis([0 5.0 0 225]);
```

Appendix XXI: Set points simulation results for a 100 mg/kg dose: maximum and minimum model bounds (experimental maximum fit).

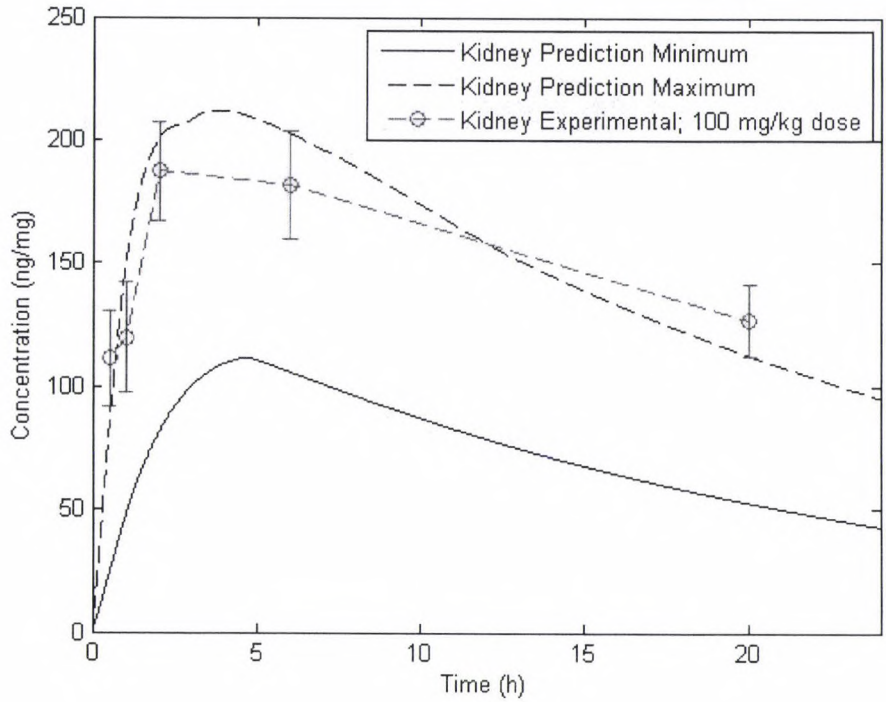

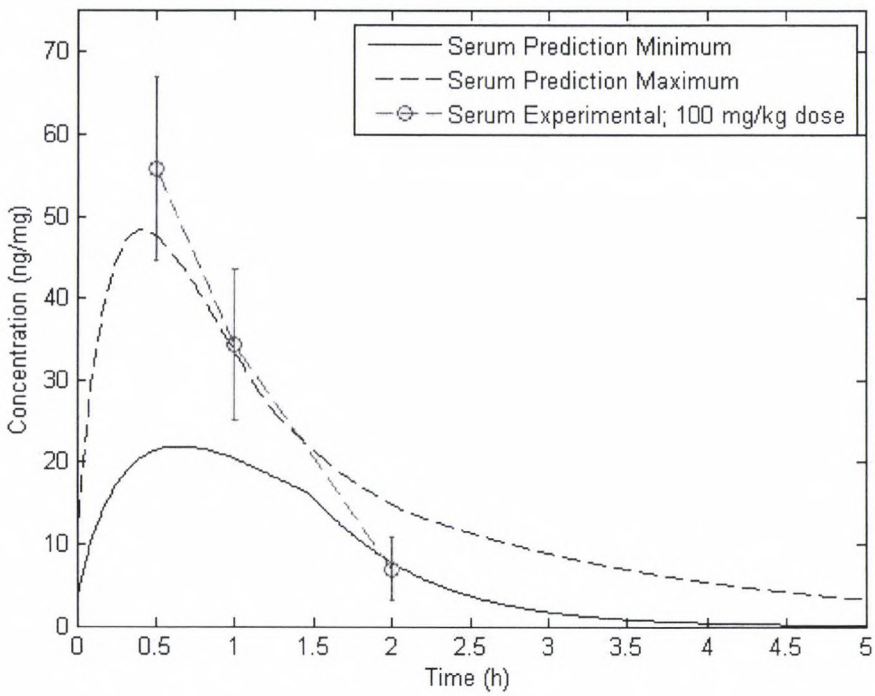
Serum Prediction Minimum
Serum Prediction Maximum
Serum Experimental; 100 mg/kg dose
Concentration (ng/mg)
Time (h)
0
10
20
30
40
50
60
70
0
0.5
1
1.5
2
2.5
3
3.5
4
4.5
5

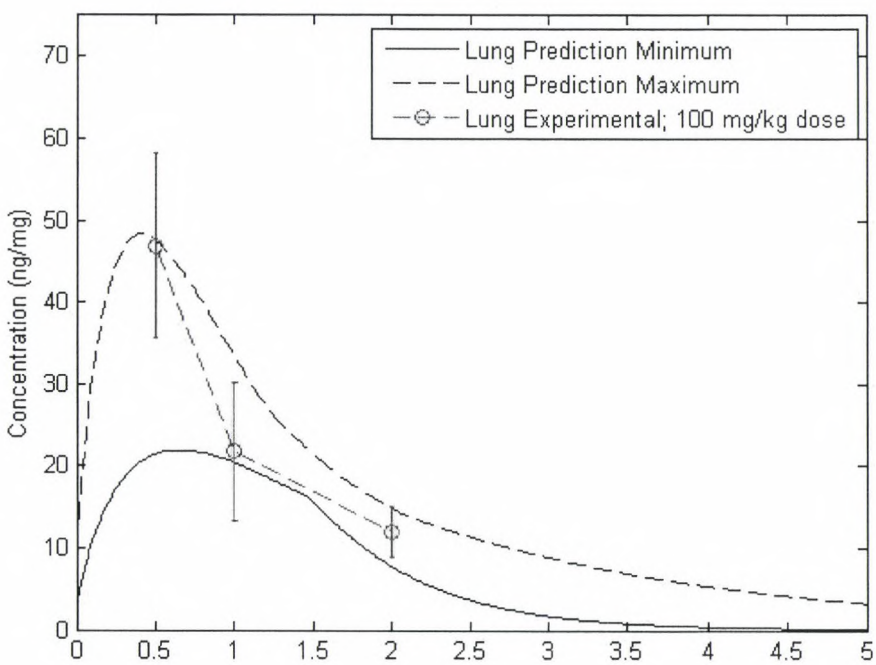
Lung Prediction Minimum
Lung Prediction Maximum
Lung Experimental; 100 mg/kg dose
Concentration (ng/mg)
0
10
20
30
40
50
60
70
0
0.5
1
1.5
2
2.5
3
3.5
4
4.5
5

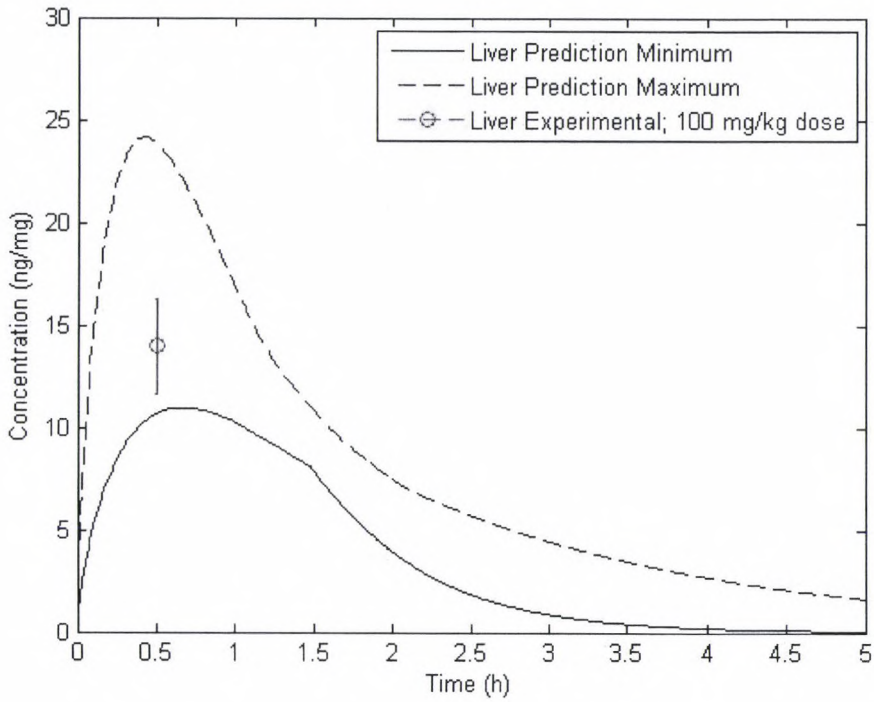
Liver Prediction Minimum
Liver Prediction Maximum
Liver Experimental; 100 mg/kg dose
Concentration (ng/mg)
Time (h)
0
5
10
15
20
25
30
0
0.5
1
1.5
2
2.5
3
3.5
4
4.5
5

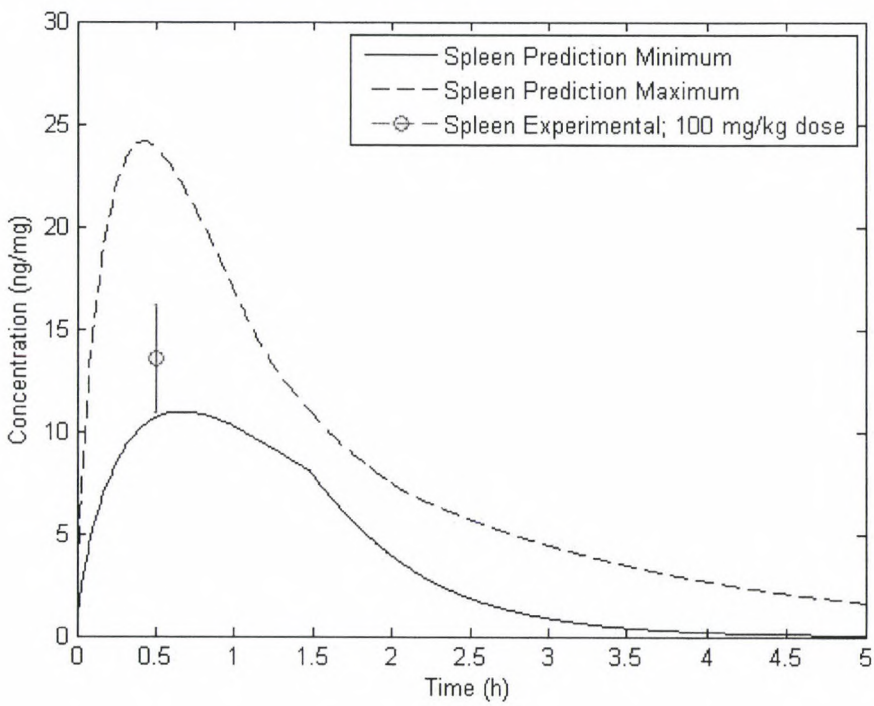
Spleen Prediction Minimum
Spleen Prediction Maximum
Spleen Experimental; 100 mg/kg dose
Concentration (ng/mg)
Time (h)
0
5
10
15
20
25
30
0
0.5
1
1.5
2
2.5
3
3.5
4
4.5
5

Appendix XXII: Set points simulation results for a 250 mg/kg dose, maximum and minimum model bounds (experimental maximum fit).

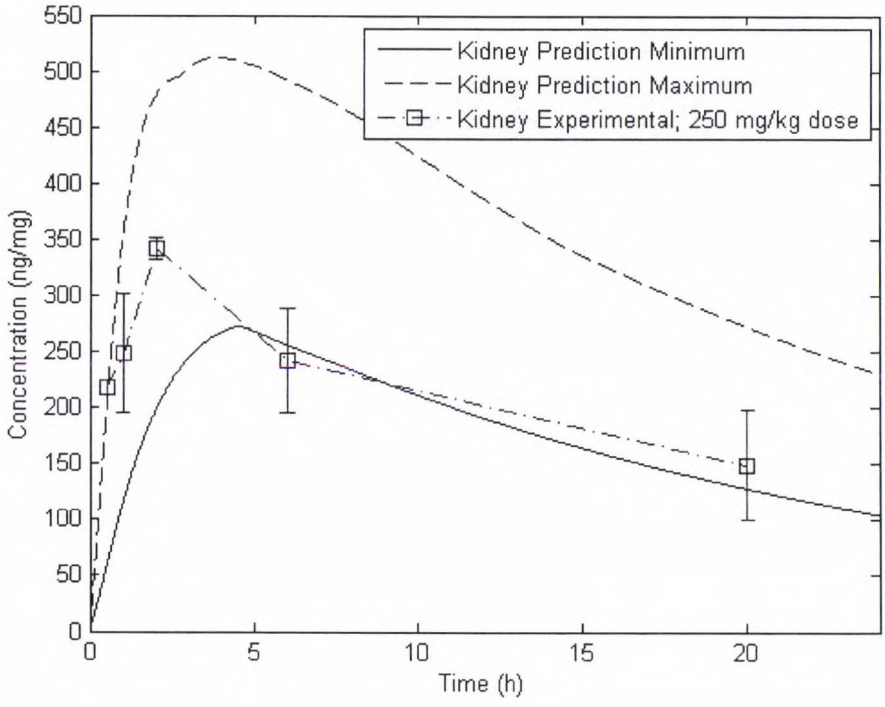

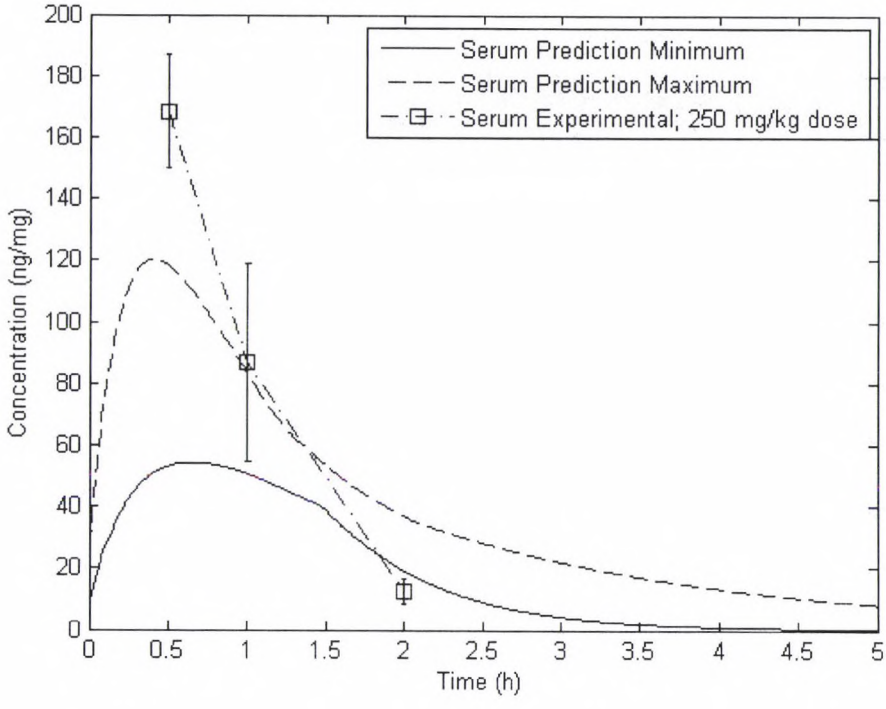
Serum Prediction Minimum
Serum Prediction Maximum
Serum Experimental; 250 mg/kg dose
Concentration (ng/mg)
Time (h)
0
20
40
60
80
100
120
140
160
180
200
0
0.5
1
1.5
2
2.5
3
3.5
4
4.5
5

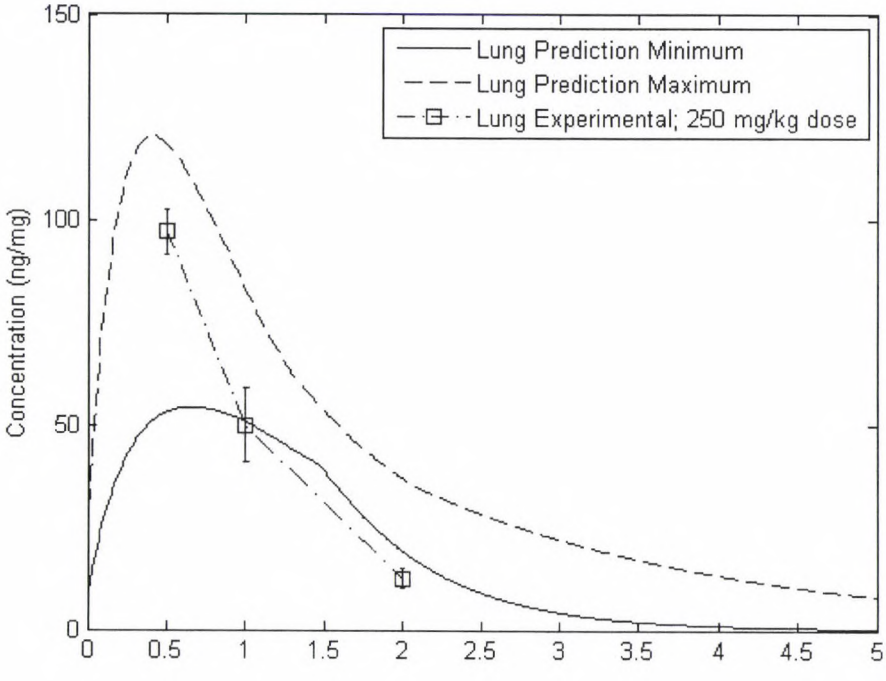
Lung Prediction Minimum
Lung Prediction Maximum
Lung Experimental; 250 mg/kg dose
Concentration (ng/mg)
0
50
100
150
0
0.5
1
1.5
2
2.5
3
3.5
4
4.5
5

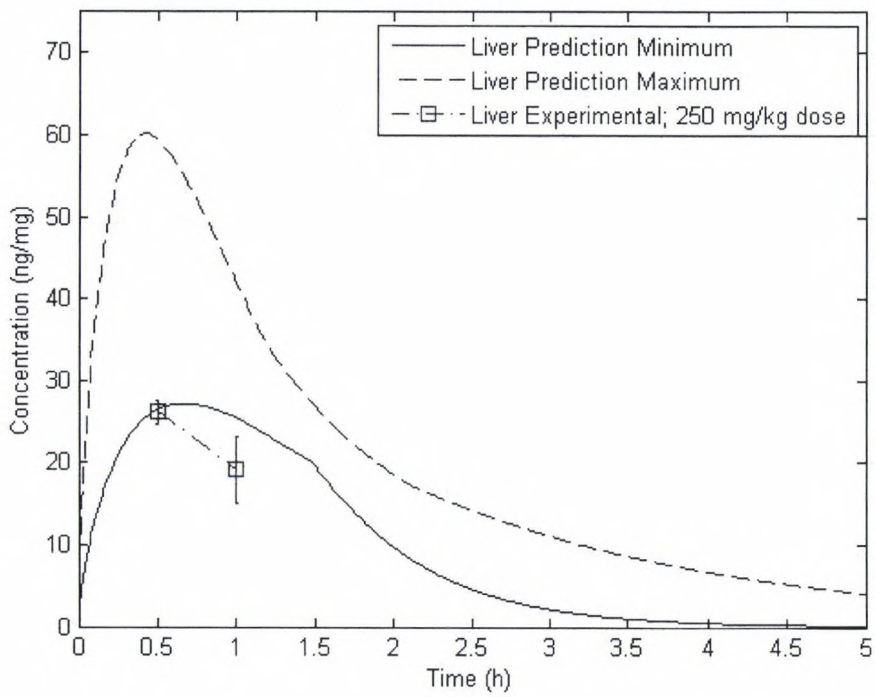
Liver Prediction Minimum
Liver Prediction Maximum
Liver Experimental; 250 mg/kg dose
Concentration (ng/mg)
Time (h)
0
10
20
30
40
50
60
70
0
0.5
1
1.5
2
2.5
3
3.5
4
4.5
5

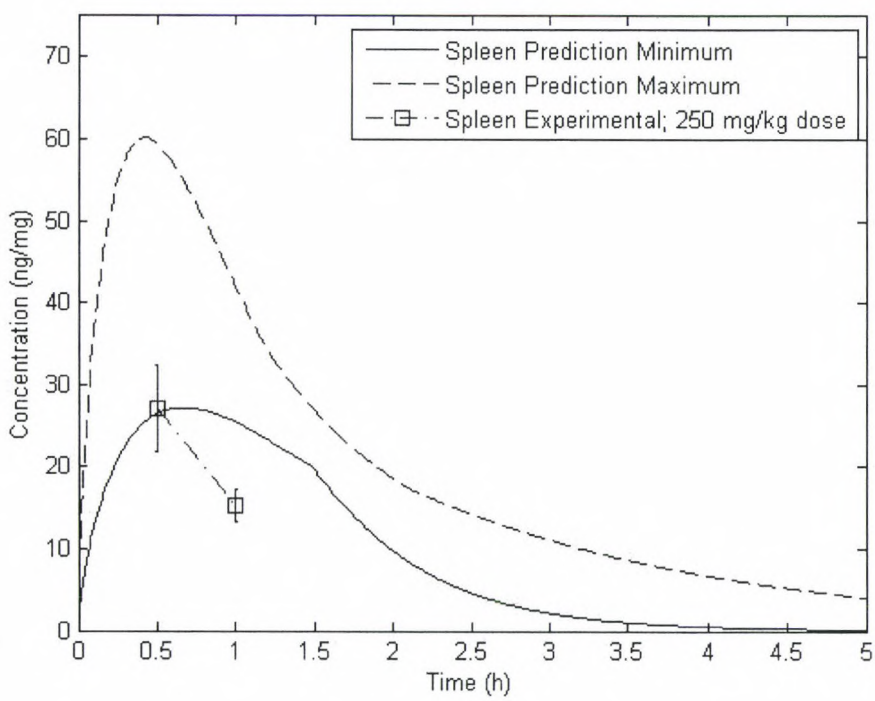
Spleen Prediction Minimum
Spleen Prediction Maximum
Spleen Experimental; 250 mg/kg dose
Concentration (ng/mg)
Time (h)
0
10
20
30
40
50
60
70
0
0.5
1
1.5
2
2.5
3
3.5
4
4.5
5

Appendix XXIII: Set points simulation results for a 100 mg/kg dose kidney maximum and minimum model bounds (extrapolated maximum fit).

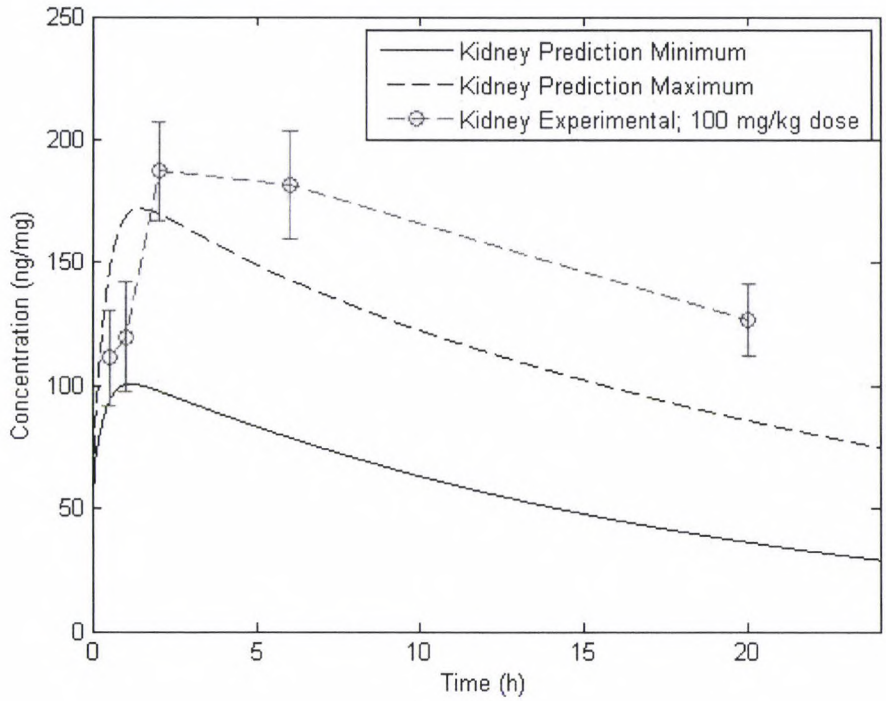

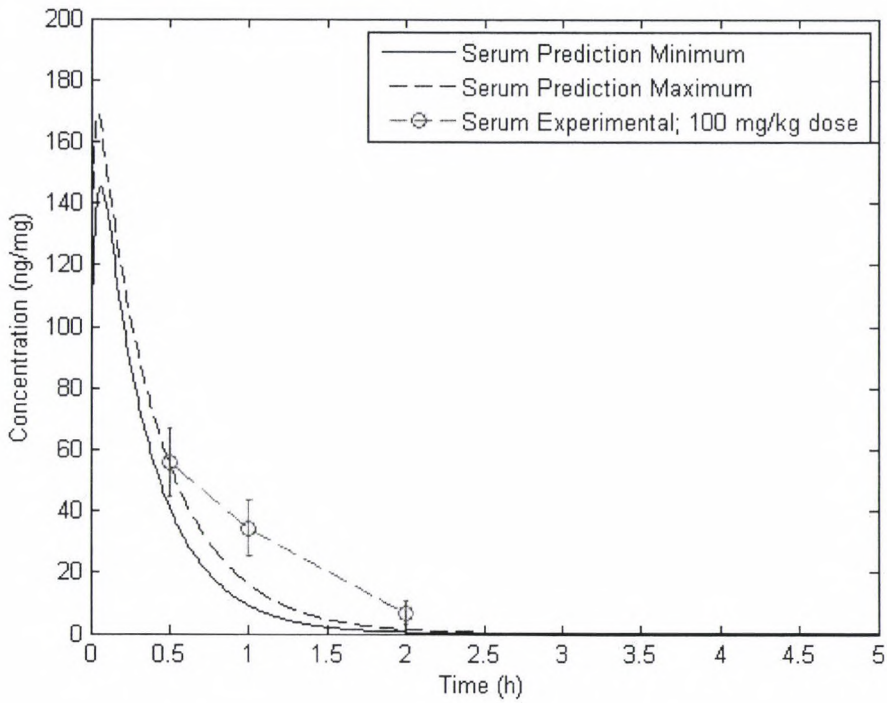
Serum Prediction Minimum
Serum Prediction Maximum
Serum Experimental; 100 mg/kg dose
Concentration (ng/mg)
Time (h)
0
20
40
60
80
100
120
140
160
180
200
0
0.5
1
1.5
2
2.5
3
3.5
4
4.5
5

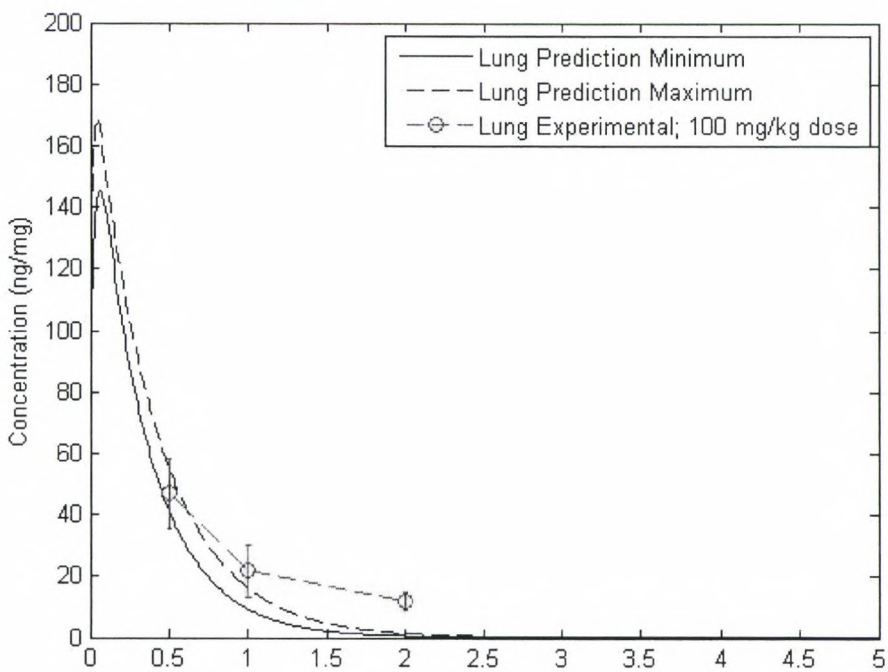
Lung Prediction Minimum
Lung Prediction Maximum
Lung Experimental; 100 mg/kg dose
Concentration (ng/mg)
0
20
40
60
80
100
120
140
160
180
200
0
0.5
1
1.5
2
2.5
3
3.5
4
4.5
5

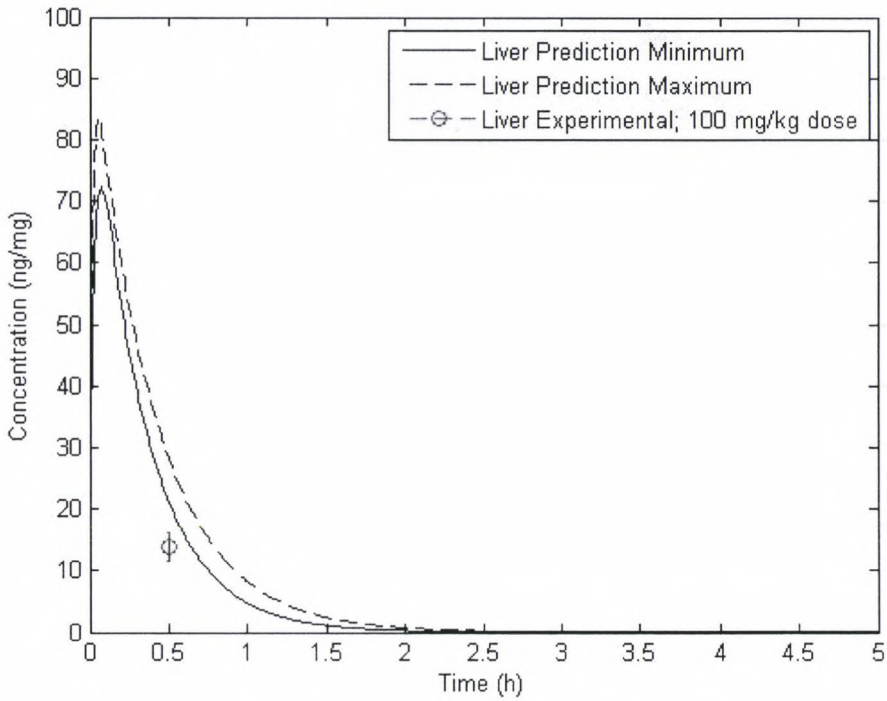
Liver Prediction Minimum
Liver Prediction Maximum
Liver Experimental; 100 mg/kg dose
Concentration (ng/mg)
Time (h)
0
10
20
30
40
50
60
70
80
90
100
0.5
1
1.5
2
2.5
3
3.5
4
4.5
5

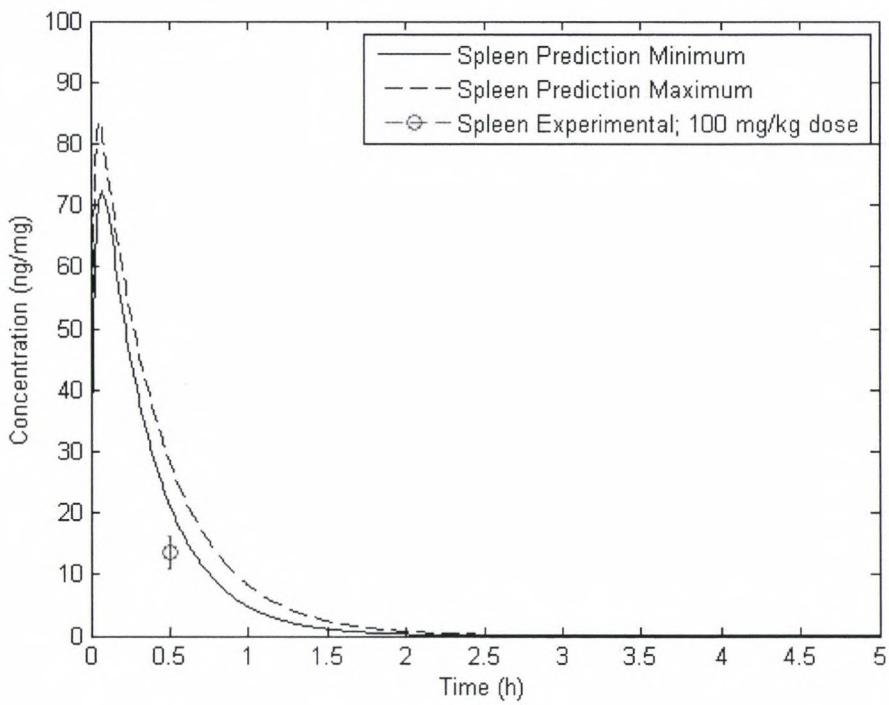
Spleen Prediction Minimum
Spleen Prediction Maximum
Spleen Experimental; 100 mg/kg dose
Concentration (ng/mg)
Time (h)
0
10
20
30
40
50
60
70
80
90
100
0.5
1
1.5
2
2.5
3
3.5
4
4.5
5

Appendix XXIV: Set points simulation results for a 250 mg/kg dose kidney maximum and minimum model bounds (extrapolated maximum fit).

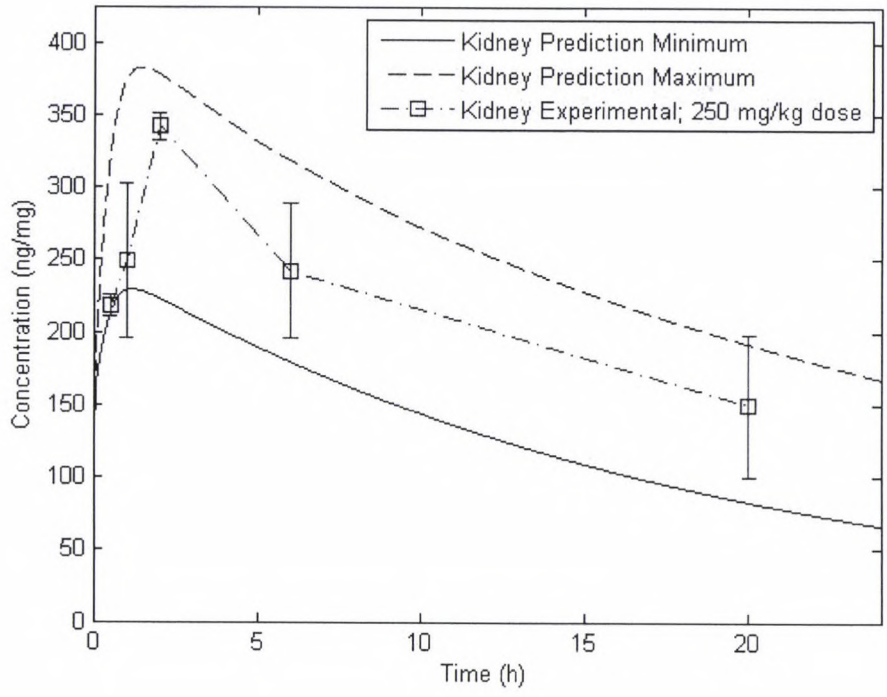

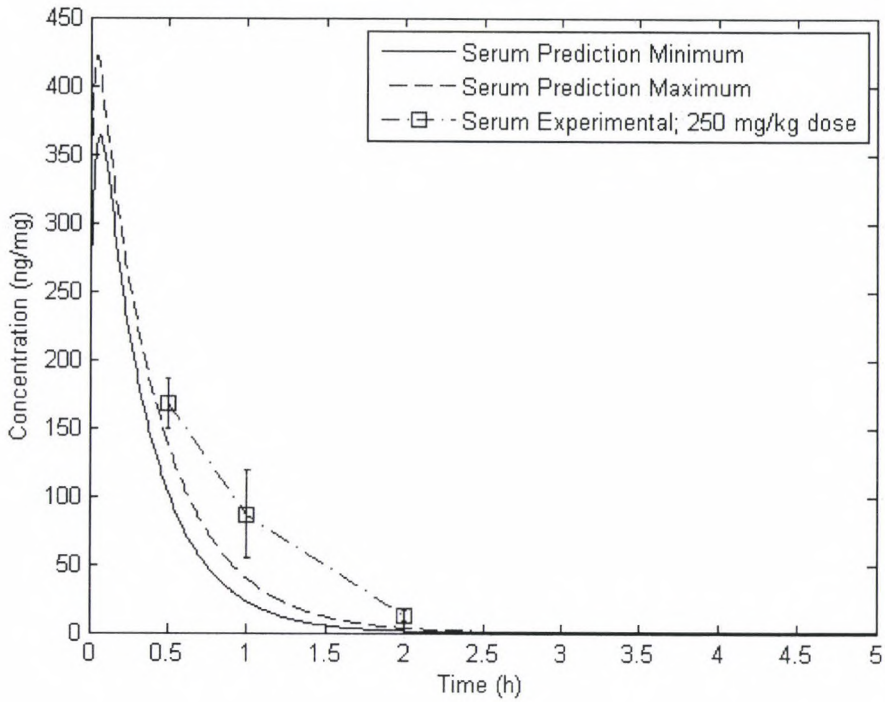
Serum Prediction Minimum
Serum Prediction Maximum
Serum Experimental; 250 mg/kg dose
Concentration (ng/mg)
Time (h)
0
50
100
150
200
250
300
350
400
450
0
0.5
1
1.5
2
2.5
3
3.5
4
4.5
5

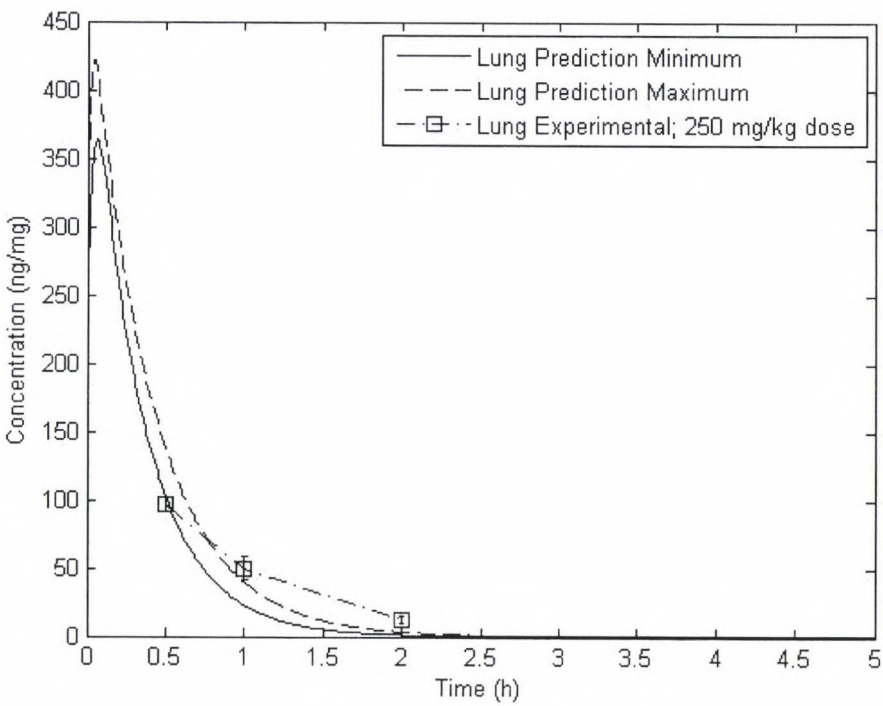
Lung Prediction Minimum
Lung Prediction Maximum
Lung Experimental; 250 mg/kg dose
Concentration (ng/mg)
Time (h)
0
50
100
150
200
250
300
350
400
450
0
0.5
1
1.5
2
2.5
3
3.5
4
4.5
5

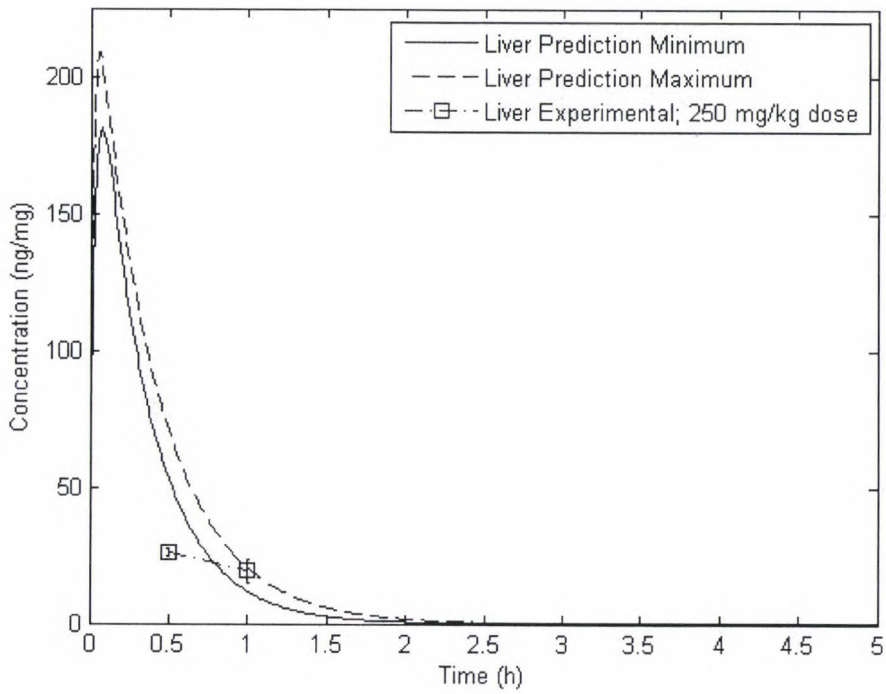
Liver Prediction Minimum
Liver Prediction Maximum
Liver Experimental; 250 mg/kg dose
Concentration (ng/mg)
Time (h)
0
50
100
150
200
0
0.5
1
1.5
2
2.5
3
3.5
4
4.5
5

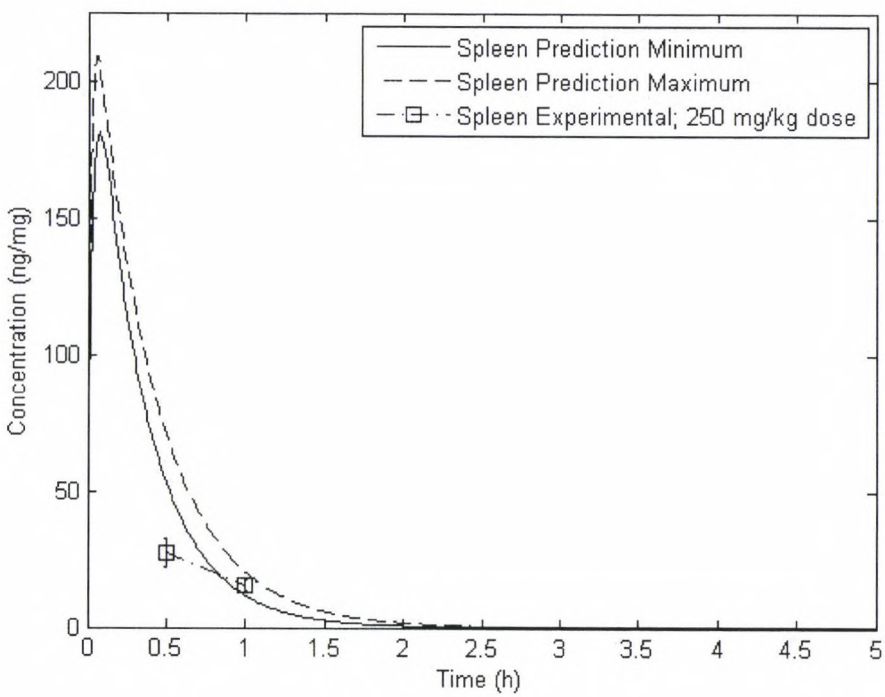
Spleen Prediction Minimum
Spleen Prediction Maximum
Spleen Experimental; 250 mg/kg dose
Concentration (ng/mg)
Time (h)
0
50
100
150
200
0
0.5
1
1.5
2
2.5
3
3.5
4
4.5
5

Appendix XXV: Human Physiology Model

```
# capreo5_human.model: PBPK model for capreomycin subcutaneous or IV
dose in human

# Written for MCSim

# Dimensions/Units:
# mass/kilogram (kg) /gram (g) /milligram (mg) /nanogram (ng).
# volume/liter (L) /milliliter (mL).
# time/hour (hr).

States = { # mass (ng).

  MSC,       # drug in subcutaneous layer.
  MIV,       # drug intravenously injected.
  MV,        # drug in venous blood.
  MLU,       # drug in lung.
  MA,        # drug in arterial blood.
  MBR,       # drug in brain.
  MF,        # drug in fat.
  MH,        # drug in heart.
  MM,        # drug in muscle.
  MB,        # drug in bone.
  MSK,       # drug in skin.
  MK,        # drug in kidney.
  MKE,       # drug eliminated from kidney.
  MKA,       # drug accumulating in kidney.
  MKS,       # drug in shallow kidney.
  MKD,       # drug in deep kidney.
  MKDE,      # drug leaving deep compartment.
  MS,        # drug in spleen.
  ML,        # drug in liver.
  MLE,       # drug eliminated from liver.
  MG,        # drug in gut.
  MCR,       # drug in carcass.

};


Outputs = { # Tissue/organ drug concentrations (ng drug/mg organ).

  CV_ng_mg,  CVP_ng_mg, CV,    # Venous blood, plasma.
  CLU_ng_mg, CLU,              # Lung.
  CA_ng_mg,  CA,               # Arterial blood.
  CSE_ng_mg, CSE,              # Total serum.
  CBR_ng_mg, CBR,              # Brain.
  CF_ng_mg,  CF,               # Fat.
  CH_ng_mg,  CH,               # Heart.
```

```
 CM_ng_mg,  CM,              # Muscle.
  CB_ng_mg,  CB,             # Bone.
  CSK_ng_mg, CSK,            # Skin.
  CK_ng_mg,  CK,             # Kidney.
  CKS_ng_mg, CKS,            # Shallow Kidney.
  CKD_ng_mg, CKD,            # Deep Kidney.
  CS_ng_mg,  CS,             # Spleen.
  CL_ng_mg,  CL,             # Liver.
  CG_ng_mg,  CG,             # Gut.
  CCR_ng_mg, CCR,            # Carcass.


# Mass balance checks (total accumulated, net input, balance error).
  ACC, NetIn, BalErr
};

# Anatomical/physiological parameters for humans
# Source: Brown, et al.
  BW  = 70.;       # Body weight (kg). Brown, pg 415.
  QC = 390.;       # Cardiac output (L/h). Brown, et al. Pg. 441.

# Exposure/dose
  SC_Dose   = 1.0;       # Subcutaneous dose (mg drug/kg body weight).
  SC_Decay  = 1.0;       # Decay rate of SC dose into blood (1/h).
  IV_Dose   = 1.0;       # Intravenous dose (mg/kg).
  IV_Decay  = 1.0;       # Decay rate of IV dose into blood (1/h).

# Fractional tissue weights. Brown, et al. Page 418, 435, 460.
  VLUC = 0.0076;         # Lung.
  VBRC = 0.02;           # Brain.
  VFC  = 0.2142;         # Fat.
  VHC  = 0.0047;         # Heart.
  VMC  = 0.400;          # Muscle.
  VBC  = 0.1429;         # Bone.
  VSKC = 0.0371;         # Skin.
  VKC  = 0.0044;         # Kidneys.
  VKSC = 0.0031;         # Shallow Kidney.
  VKDC = 0.0013;         # Deep Kidney.
  VSpC  = 0.0026;        # Spleen.
  VGC  = 0.0171;         # Gastrointestinal tract.
  VLC  = 0.0257;         # Liver.
  VVC  = 0.05214;        # Venous blood.
  VAC  = 0.02607;        # Arterial blood.
  VCRC = 1-(VLUC+VBRC+VFC+VHC+VMC+VBC+VSKC+VKC+VSpC+VGC+VLC+VVC+VAC);
      # Carcass (1 - all others).

# Fractional tissue flows (fraction of cardiac output). Davies. Brown,
et al. Page 442.
  QLUC = 1.0;            # Lung.
  QBRC = 0.12;           # Brain.
  QFC  = 0.05;           # Fat.
  QHC  = 0.04;           # Heart.
  QMC  = 0.13;           # Muscle.
  QBC  = 0.05;           # Bone.
  QSKC = 0.05;           # Skin.
  QKSC = 0.20;           # Shallow Kidney.
```

```
  QSC  = 0.01;          # Spleen.
  QGC  = 0.13;          # Gut.
  QLAC = 0.06;          # Hepatic artery.
  QCRC = 1-(QBRC+QFC+QHC+QMC+QBC+QSKC+QKSC+QSC+QGC+QLAC);          #
Carcass.
# Partition coefficients.
  BP  = 1.; # Blood:plasma.
  PLU = 2.;# Lung:blood.
  PBR = 1.; # Brain:blood.
  PF  = 1.; # Fat:blood.
  PH  = 1.; # Heart:blood.
  PM  = 1.; # Muscle:blood.
  PB  = 1.; # Bone:blood.
  PSK = 1.; # Skin:blood.
  PKS = 1.; # Shallow kidney:blood.
  PS  = 1.; # Spleen:blood.
  PG  = 1.; # Gut:blood.
  PL  = 1.; # Liver:blood.
  PCR = 1.; # Carcass:blood.

# Clearance parameters.
  CLHC = 1.;       # Hepatic clearance (L/hr/kg).
  CLR  = 1.;       # Renal clearance.
  CLRD = 1.;       # Deep renal tissue clearance.

# Michaelis Menten kidney accumulation parameters.
  Vmax = 1.;       # Max velocity.
  Km = 1.;         # MM constant.

# Scaled/calculated parameters.
  CLH; SCR; IVR;
  VLU; VBR; VF; VH; VM; VB; VSK; VKS; VKD; VK; VSp; VG; VL; VV; VA;
VCR;
  QLU; QBR; QF; QH; QM; QB; QSK; QKS; QS; QG; QLA; QL; QCR;

# Variance of predicted parameters.

  V_CLHC; V_Vmax; V_Km; V_CLR; V_CLRD; V_SC_Decay;

Initialize {

# Dose.
  SCR = (SC_Dose*BW*(1.E6));       # Total dose (ng).
  MSC = SCR;                       # Initial drug mass in SubCu layer.
  IVR = 1.E6*IV_Dose*BW;
  MIV = IVR;

# Compartment weight (kg).
  VTC = VLUC+VBRC+VFC+VHC+VMC+VBC+VSKC+VKC+VGC+VLC+VVC+VAC+VCRC;
  VLU = VLUC*BW/VTC;     # Lung.
  VBR = VBRC*BW/VTC;     # Brain.
  VF  = VFC*BW/VTC;      # Fat.
  VH  = VHC*BW/VTC;      # Heart.
  VM  = VMC*BW/VTC;      # Muscle.
  VB  = VBC*BW/VTC;      # Bone.
  VSK = VSKC*BW/VTC;     # Skin.
  VKD = VKDC*BW/VTC;     # Deep Kidney.
```

```
  VKS = VKSC*BW/VTC;     # Shallow Kidney.
  VK  = VKC*BW/VTC;      # Kidney.
  VSp  = VSpC*BW/VTC;    # Spleen.
  VG  = VGC*BW/VTC;      # Gut
  VL  = VLC*BW/VTC;      # Liver.
  VV  = VVC*BW/VTC;      # Venous blood.
  VA  = VAC*BW/VTC;      # Arterial blood.
  VCR = VCRC*BW/VTC;     # Carcass.

# Flow rates (L/hr).

  QTC = QBRC+QFC+QHC+QMC+QBC+QSKC+QKSC+QSC+QLAC+QGC+QCRC;
  QLU = QLUC*QC/QTC;           # Lung.
  QBR = QBRC*QC/QTC;           # Brain.
  QF  = QFC*QC/QTC;            # Fat.
  QH  = QHC*QC/QTC;            # Heart.
  QM  = QMC*QC/QTC;            # Muscle.
  QB  = QBC*QC/QTC;            # Bone.
  QSK = QSKC*QC/QTC;           # Skin.
  QKS = QKSC*QC/QTC;           # Shallow kidney.
  QS  = QSC*QC/QTC;            # Spleen.
  QG  = QGC*QC/QTC;            # Gut.
  QLA = QLAC*QC/QTC;           # Hepatic artery.
  QL  = QS+QG+QLA;             # Total liver flow.
  QCR = QCRC*QC/QTC;           # Carcass.

# Clearance (L/hr).
  CLH = CLHC*BW;
}

Dynamics {

# Subcutaneous dose (ng/h).

  dt(MSC) = -MSC*SC_Decay;                # Drug moving from SC to
blood.

# Intravenous dose.

  dt(MIV) = -MIV*IV_Decay;

# Drug Tissue/organ concentrations (ng/kg).
  CV  = MV/VV;                                # Venous blood.
  CA  = MA/VA;                                # Arterial blood.
  CLU = MLU/VLU;   CVLU = CLU/PLU;            # Lung.
  CBR = MBR/VBR;   CVBR = CBR/PBR;            # Brain.
  CF  = MF/VF;     CVF  = CF/PF;              # Fat.
  CH  = MH/VH;     CVH  = CH/PH;              # Heart.
  CM  = MM/VM;     CVM  = CM/PM;              # Muscle.
  CB  = MB/VB;     CVB  = CB/PB;              # Bone.
  CSK = MSK/VSK;   CVSK = CSK/PSK;            # Skin.
  CKS = MKS/VKS;   CVKS = CKS/PKS;            # Shallow kidney.
  CKD = MKD/VKD;   CVKD = CKD;                # Deep kidney.
  CK  = MK/VK;     CVK  = CK/PKS;             # Kidney.
  CS  = MS/VSp;    CVS  = CS/PS;              # Spleen.
  CG  = MG/VG;     CVG  = CG/PG;              # Gut.
  CL  = ML/VL;     CVL  = CL/PL;              # Liver.
```

```
  CCR = MCR/VCR;   CVCR = CCR/PCR;        # Carcass.

# Tissue/organ dynamics (ng/h).
# Venous blood
  dt(MV) =  QBR*CVBR + QF*CVF + QH*CVH + QM*CVM + QB*CVB + QSK*CVSK
            + QKS*CVKS  +  QL*CVL  +  QCR*CVCR  -  dt(MSC)-  dt(MIV)  -
QLU*CV;

# Lung
  dt(MLU) = QLU*(CV - CVLU);

# Arterial blood.
  dt(MA)  = QLU*(CVLU - CA);

# Brain.
  dt(MBR) = QBR*(CA - CVBR);

# Fat.
  dt(MF) = QF*(CA - CVF);

# Heart.
  dt(MH) = QH*(CA - CVH);

# Muscle.
  dt(MM) = QM*(CA - CVM);

# Bone.
  dt(MB) = QB*(CA - CVB);

# Skin.
  dt(MSK) = QSK*(CA - CVSK);

# Kidney.
  dt(MKE) = CLR*CVKS;
  dt(MKA) = (Vmax*CVKS)/(Km+CVKS);
  dt(MKDE)= CLRD*CVKD;
  dt(MKS) = QKS*(CA - CVKS)-dt(MKA)- dt(MKE)+dt(MKDE);
  dt(MKD) = dt(MKA)-dt(MKDE);
  dt(MK)  = dt(MKS) + dt(MKD);

# Spleen.
  dt(MS) = QS*(CA - CVS);

# Gut.
   dt(MG) = QG*(CA - CVG);

# Liver.
  dt(MLE) = CLH*CVL;
  dt(ML)  = QLA*CA + QS*CVS + QG*CVG - QL*CVL - dt(MLE);

# Rest of body.
  dt(MCR) = QCR*(CA - CVCR);

# Mass balance calculations.
 ACC = MA + MV + MLU + MBR + MF + MH + MM + MB + MSK + MK
         + MS + MG + ML + MCR + MSC + MIV;
```

```
 NetIn = IVR + SCR - (MLE + MKE);
}

CalcOutputs {
# Tissue/organ drug concentrations (ng/mg).
  CV_ng_mg   = CV/(1.E6);                    # Venous blood.
  CVP_ng_mg  = (CV/BP)/(1.E6);               # Plasma.
  CLU_ng_mg  = CLU/(1.E6);                   # Lung.
  CA_ng_mg   = CA/(1.E6);                    # Arterial blood.
  CSE_ng_mg  = (CA+CV)/(1.E6);               # Total Serum.
  CBR_ng_mg  = CBR/(1.E6);                   # Brain.
  CF_ng_mg   = CF/(1.E6);                    # Fat.
  CH_ng_mg   = CH/(1.E6);                    # Heart.
  CM_ng_mg   = CM/(1.E6);                    # Muscle.
  CB_ng_mg   = CB/(1.E6);                    # Bone.
  CSK_ng_mg  = CSK/(1.E6);                   # Skin.
  CK_ng_mg   = CK/(1.E6);                    # Kidney.
  CS_ng_mg   = CS/(1.E6);                    # Spleen.
  CL_ng_mg   = CL/(1.E6);                    # Liver.
  CG_ng_mg   = CG/(1.E6);                    # Gut.
  CCR_ng_mg  = CCR/(1.E6);

# Mass balance error.
 BalErr = NetIn - ACC;
}
```